ABSTRACT

Title of Thesis: HYDRAULIC COMPATIBILITY OF GEOTEXTILES WITH RECYCLED MATERIALS

Emre Odabasi, Master of Science, 2018

Thesis directed by: Professor Ahmet H. Aydilek, Department of Civil and Environmental Engineering

Large amounts of natural aggregate and manufactured materials are needed every year to support highway construction and rehabilitation in the United States. It is important that new construction materials be developed to improve the performance of highway systems, while at the same time providing cost-effective and sustainable technologies. Use of recycled materials instead of earthen materials is one way to improve sustainability of highway infrastructure. Similar benefits exist when sustainability is infused into designing modern landfill covers. Since geotextile filters and separators are used in such construction schemes, hydraulic compatibility of recycled materials with geotextile filters and long-term performance of these geotextiles are essential. A series of long-term filtration (LTF) tests were performed to evaluate the hydraulic compatibility of several woven and nonwoven geotextiles with four recycled materials commonly used in construction (recycled concrete aggregate, recycled asphalt pavement, foundry sand and recycled asphalt shingle). Upon completion of the LTF tests, grain size analyses, permittivity tests, image analyses, and piping measurements were conducted to investigate the clogging and retention behavior of the geotextiles. The results indicated that majority of the recycled materials tested were compatible with the nonwoven and woven geotextiles. Excessive piping was not observed even under relatively high hydraulic gradients. Permittivity and percent open area (POA) were the main parameters that influence the clogging and retention performance of nonwoven and woven geotextiles, respectively. The success of the existing criteria in predicting the filtration performance was inconsistent, suggesting that a detailed parametric study was needed to propose new filter criteria for these materials.

HYDRAULIC COMPATIBILITY OF GEOTEXTILES WITH RECYCLED MATERIALS

by

Emre Odabasi

Thesis submitted to the Faculty of the Graduate School of the

University of Maryland, College Park, in partial fulfillment

of the requirements for the degree of

Master of Science

2018

Advisory Committee:

Dr. Ahmet H. Aydilek, Chair

Dr. Charles W. Schwartz

Dr. Natasha Andrade

Acknowledgements

I am forever indebted to my advisor Professor Ahmet H. Aydilek for his great support and help on all stages of my research and on my coursework. I would also like to thank my committee members Dr. Charles W. Schwartz and Dr. Natasha Andrade for their time and guidance. The funding for this study was provided by the Turkish General Directorate of State Hydraulic Works (DSI). This support is gratefully acknowledged.

Table of Contents

List of Tables

List of Figures

Chapter 1

Introduction

The American Society for Testing Materials (ASTM) D35 defines geotextiles as "permeable textiles used with geotechnical materials as an integral part of a man-made project, structure or system". The global geotextile market is expected to reach $8.18 Billion by 2024 with the annual growth rate of 10.4% from 2016 to 2024 (Grand View Research, 2016). The main increase in use of geotextiles in geotechnical and environmental construction is due to their cost-effectiveness, ease of transport and installation, consistent material properties, as well as reduction in the use of earthen granular filters (Palmeira, 2008; Vieira et al. 2010). Conventional filtration method involves using granular materials (i.e., gravels and sands) in roadways, retaining walls and landfills; however, a properly selected geotextile can be a more practical and economical alternative to traditional granular filters due to its excellent, and often superior, hydraulic properties such as permeability/permittivity, and pore size distribution.

One of the common use of geotextiles in highway construction is at the interface of subgrade and the granular base course (Das and Shin, 1998). A geotextile placed at this location fulfills a combination of separation and filtration functions (Figure 1.1). Accordingly, the major function of a geotextile filter when used in highway systems is to minimize movement of fine particles from the subgrade and to prevent development of excessive pore water pressures at the soil-geotextile filter interface.

Similarly, geotextiles are used in landfills and have become an important part of the design of landfill final covers. Geotextiles are used as filters in landfill cover systems to prevent adjacent fine-grained soils from clogging geonet/aggregate drainage layers placed above the geomembrane or low permeability compacted clays (Figure 1.1).

The filtration mechanism at the soil-geotextile interface is a complex process involving many parameters and depends on the physical compatibility between the geotextile and soil. The fundamental purpose of a geotextile filter is to minimize the excessive migration of soil particles through the filter (i.e., piping), while not causing excessive clogging inside the geotextile, which may, otherwise, adversely affect the flow of water in a downward or an upward direction. The three processes that impede the flow in geotextiles are blinding, clogging and caking. Blinding is a typical phenomenon observed for woven filters and occurs when the subgrade particles block the openings at the bottom surface of the geotextile. Clogging occurs when particles become trapped within the geotextile structure. Caking refers to particle deposition at the top surface of a geotextile (mostly nonwoven), and it occurs when fines either filter down to the bottom of the base course or when fines are deposited after migrating through the geotextile (Metcalfe, 1993). Figure 1.2 illustrates the blinding, clogging, and caking phenomena at the aggregate/geotextile/subgrade interface.

Among these three mechanisms that influence particle movement in porous media, clogging is the main one affecting the durability of geotextile filters used in filtration systems. A geotextile filter can be considered as a filtering zone that develops over time, and the reason for clogging can be due to physical, biological, or chemical factors or a combination of them (Koerner et al., 1988; Rollin and Lombard, 1988). Accumulation of fine soil fraction within the voids between the geotextile fibers in roadways and landfill covers causes the physical clogging, which often accounts for the largest reduction in the effective porosity and hydraulic conductivity of a geotextile (Giroud 1996, Palmeira and Gardoni 2000, Fannin 2010). Water has been identified as one of the main parameters affecting the behavior and the long-term performance of pavement systems (Bilodeau and Dore, 2012 and Richter, 2006). The pore water pressure generated at the subgrade and the base course interface leads to undesirable phenomena, such as erosion and subsequent migration of fine soil fraction into the base course (Trani and Indraratna, 2010, Christopher et al. 2006).

Studies related to analysis of physical clogging of geotextiles have been reported by Bell et al. (1982), Floss et al. (1990), Nishida and Nishigata (1994), Palmeira and Cunha (1993) and Tsai and Holtz (1998). Brorsson and Ericksson (1986) exhumed nine different geotextiles after 5 and 10 years of service and no migration of subgrade fines into the base material was reported. Bonaparte et al. (1988) also reported similar observations from a field investigation of nonwoven geotextiles exhumed from seven existing roads. Tsai et al. (1993) reported the results of a test road with geotextile separators in State of Washington, and their observations indicated that needle-punched nonwoven geotextiles allowed unrestricted drainage of subgrade while others exhibited clogging.

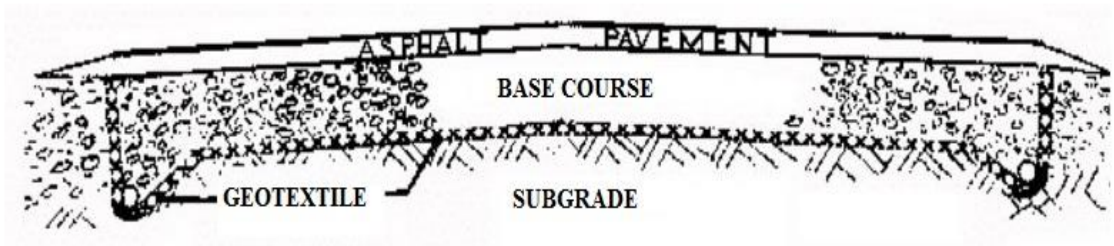

(a)

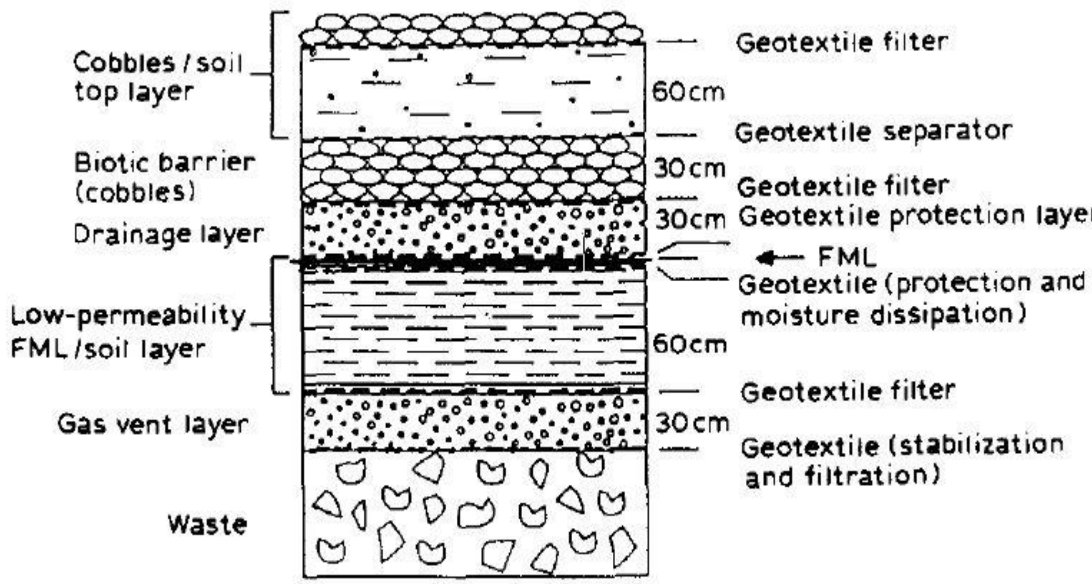

(b)

Figure 1.1 Illustration of geotextile use in (a) highway between base course and subgrade and (b) in landfill covers (adapted from "US Environmental Protection Agency (1989). Technical guidance document: final covers on hazardous waste landfills and surface Impoundments. EPA-530/SW-89-047")

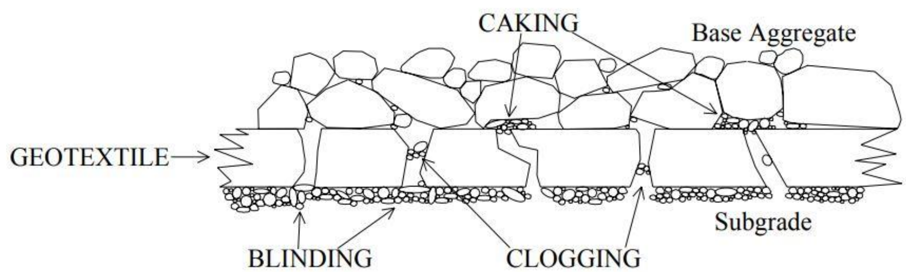

Figure 1.2 Illustration of blinding, clogging and caking (after Metcalfe et al., 1994)

Bell et al. (1981) and Glynn and Cochrane (1987) reported that intermixing of softened clay subgrade and base course aggregate resulted in reduction in design depth of a subbase layer, and reduced drainability. Palmeira et al. (2015) conducted large-scale tests on armored slopes where geotextile and granular filters were employed. The results showed that presence of geotextile reduced the values of maximum pore pressure in the base soil as well as improving draining conditions at the slope face while effectively retaining the soil. Franks et al. (2013, 2014) investigated removing suspended solids from runoff through geotextile filtration by using sand column tests. The results indicated that geotextile filter performed better than sand in terms of removing total suspended soils and extending the overall lifespan. Field removal of suspended solids by the same nonwoven geotextile was also verified via long-term pilot tests (Franks et al. 2015).

Fatahi et al. (2011) investigated the impact of a nonwoven geotextile on filtration behavior of railway ballast and indicated that introducing the geotextile layer has significantly reduced the thickness of the granular layer as well as reduced the base loss per volume. Similarly, Meshram et al. (2013) evaluated incorporating coir textile filters over poor subgrade soils and reported a reduction in thickness of the subbase layer due to a geotextile-induced control of intrusion of subgrade fines into the overlying soil. Sañudo-Fontaneda et al. (2018) conducted a set of laboratory experiments to investigate the effects of geotextile filters in highway filter drains. The results showed that presence of a geotextile influenced the hydraulic performance by increasing peak attenuation as well as trapping applied pollutants without clogging the geotextile filter. Bourgès-Gastaud et al. (2014) conducted filtration tests on nonwoven geotextiles for dewatering high-clay content sludges. The results showed that the geotextile was successful in retaining a very high percentage of the solids. Veylon et al. (2016) evaluated the long-term performance of two types of geotextiles that were used for 18 years in drainage trenches to stabilize the slopes in the French Alps. The results from the study showed that geotextiles performed well in terms of mechanical and filtration properties; however; formation of calcite crust on the downstream face of the geotextiles caused a decrease in the hydraulic properties.

Christopher and Valero (1999) measured the permeability of a woven monofilament polypropylene geotextile filter installed in 1969 in Florida. Furthermore, Christopher (1983) conducted a similar study at the site in 1979 and the results showed that permeability remained unchanged from the time of installation in 1969. Both studies indicated that the POA (i.e., percent open area) remained unchanged, except for a small decrease (~%10). Similarly, a study was conducted by Saathoff (1988) to evaluate long-term filtration performance of 81 geotextiles used in shore protection, inland waterway construction, railroad track laying applications, and road construction. The geotextiles investigated consisted of 52 nonwoven and 29 woven fabrics that had been in service between 1 and 14 years. The ratio of virgin geotextile hydraulic conductivity to hydraulic conductivity of the soil-contaminated geotextile averaged about 20 for nonwoven geotextiles and about 300 for woven geotextiles. The ratio of hydraulic conductivity of the soil-contaminated geotextile to that of the filtered soil was greater than 5 for the woven fabrics and greater than 2 for the nonwoven fabrics. The ratio of virgin geotextile hydraulic conductivity to that of soil was greater than 80 for the nonwoven geotextiles and greater than 170 for the woven geotextiles.

Currently, there is a growing interest in infusing sustainability into highway and landfill design by incorporating recycled materials (also called industrial by-products). Use of recycled materials in landfills and highways has several benefits, including reduction in solid waste disposal costs incurred by industry, reduction in landfill requirements, minimization of damage to natural resources caused by excavating earthen materials for construction, obtaining added value from waste materials, conservation of production energy, and ultimately providing sustainable construction and economic growth. Moreover, these efforts are in parallel with the objectives of Green Highways Partnership initiative developed by the United States Federal Highway Administration and co-sponsored by several States.

Although there have been numerous installations of geotextiles in filter systems, very few have been monitored to determine their long-term performance. Moreover, there is lack of information on use of recycled materials with geotextile filters when placed in highways and landfill systems. Thus, there is a need to define the hydraulic compatibility of geotextile filters with recycled materials.

To respond to this need, a battery of long-term filtration tests was performed on geotextiles interacting with four different recycled materials, namely RCA (Recycled Concrete Aggregate), RAP (Recycled Asphalt Pavement), FS (Foundry Sand), and RAS (Recycled Asphalt Shingle). Image analyses, post-test sieve analysis, and permittivity tests were conducted to verify the results obtained from filtration tests. Attempts were made to relate the observed filtration performance to geotextile pore structure parameters and applied hydraulic gradients. Applicability of existing filtration criteria to the tested recycled material-geotextile systems was investigated. Results of these tests were used to develop recommendations for long-term hydraulic compatibility of the recycled materials with geotextiles. The current study has focused on physical clogging of the geotextiles with recycled material fines. Biological or chemical clogging was not within the scope of this study.

Chapter 2

Materials and Methods

2.1. *Materials*

Four different recycled materials, recycled concrete aggregate (RCA), recycled asphalt pavement (RAP), foundry sand (FS), and recycled asphalt shingle (RAS) were subjected to long-term filtration tests. A representative sample of the stored material was obtained prior to every laboratory testing procedure by utilizing a mechanical splitter (ASTM C 702). Debris and foreign materials within the materials were removed by hand before sieving. Index properties of all recycled materials are summarized in Table 2.1. Figures 2.1 and 2.2 present the grain size distributions and standard Proctor compaction curves, respectively, for the materials tested.

The recycled concrete aggregates, RCA-1 and RCA-2, used in the study were obtained from two different sources. RCA-1 was collected from a material quarry near Centreville, Virginia. RCA-2 samples were obtained from Mandt Sandfill, located in Fitchburg, Wisconsin. RCA in these facilities consist of hydraulic cement concrete from many different origins including, but not limited to, concrete from demolished structures, curb and gutter, pipes, and washouts. All samples were collected within a week after being crushed and stockpiled.

Table 2.1 Physical properties of all materials tested

Material	Fines (%)	Sand (%)	Gravel (%)	C_c	C_u	PI	G_s	ω_{opt} (%)	$\gamma_{dry, max}$ pcf (kN/m^3)	k (cm/sec)
RCA-1	8.7	76.7	14.6	1.9	78.9	NP	2.73	15	122.4 (19.06)	3.4×10^{-3}
RCA-2	5.6	75.2	19.2	2.1	49.9	NP	2.62	10.5	126.8 (19.74)	4.8×10^{-3}
RAP	1.2	74.2	24.6	1.3	10.8	NP	2.55	6	124.6 (19.40)	3.6×10^{-3}
FS	7.1	92.6	0.3	0.9	2.0	NP	2.6	12	116.9 (18.20)	3.2×10^{-6}
RAS	0.2	78.8	21	1.4	7.5	NP	1.53	7	62 (9.65)	9.5×10^{-3}

Notes: C_c: coefficient of curvature, C_u: coefficient of uniformity, PI: plasticity index, NP: non-plastic, G_s: specific gravity, ω_{opt}: optimum moisture content, $\gamma_{dry, max}$: maximum dry unit weight, k: hydraulic conductivity

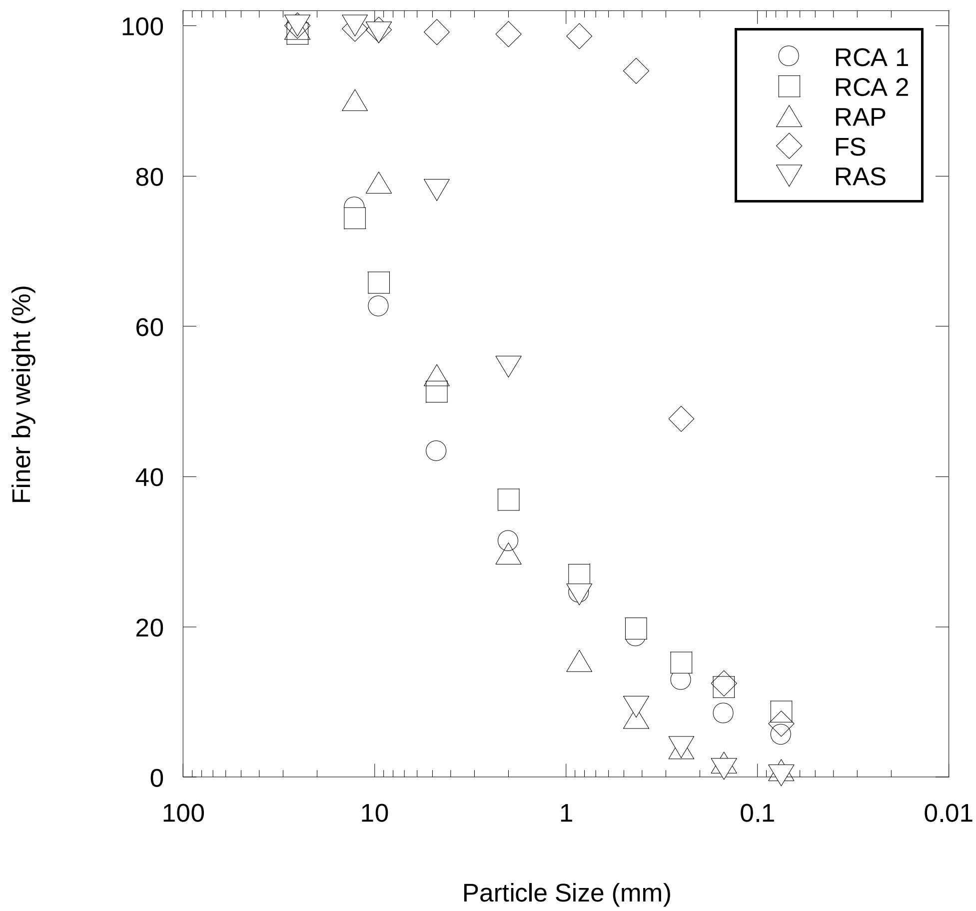

Figure 2.1 Grain size distributions of the materials tested

Both RCA samples had similar resemblance with angular, rough particle surfaces and contained a noticeable amount of attached (bonded to aggregate) and separated (unbonded to aggregate) mortar. RCA-2 had additional materials such as wood chips, glass, tiles, and plastic mixed with RCA, which contained approximately 0.6% of the bulk sample by mass while RCA-1 samples did not have such impurities. This could be due to the fact that the facility where these samples were obtained from has been producing RCA regularly for road construction for several years and had different quality control measures during production to eliminate these impurities. RCA-1 sample is classified as well-graded sand to silty sand (SW-SM) and RCA-2 sample as poorly graded gravel (GP) according to the Unified Soil Classification System (USCS), and A-1-a and A-1-a, respectively, per American Association of State Highway and Transportation Officials (AASHTO) Classification System. In general, both of the classifications and the properties of RCA tested in this study are within the range of RCA tested by others (Edil et al. 2012 and Goulias et al. 2015). The compaction curves for both RCA samples (Figure 2.2) suggest that both materials have similar maximum dry unit weight values ($\gamma_{dmax} \approx 19.3$ kN/m^3). RCA-2 has lower optimum moisture content (10.5%) with a flatter compaction curve in comparison to the RCA-1 material with a well-defined peak and higher optimum moisture content (15.2%), expected characteristics for poorly graded and well graded coarse material, respectively (Germaine and Germaine, 2009). The maximum dry unit weight for both RCAs are located close to the zero-air-void (ZAV) curves, indicating a higher degree of saturation around the maximum dry unit weight than what is typically observed for natural soils/aggregates.

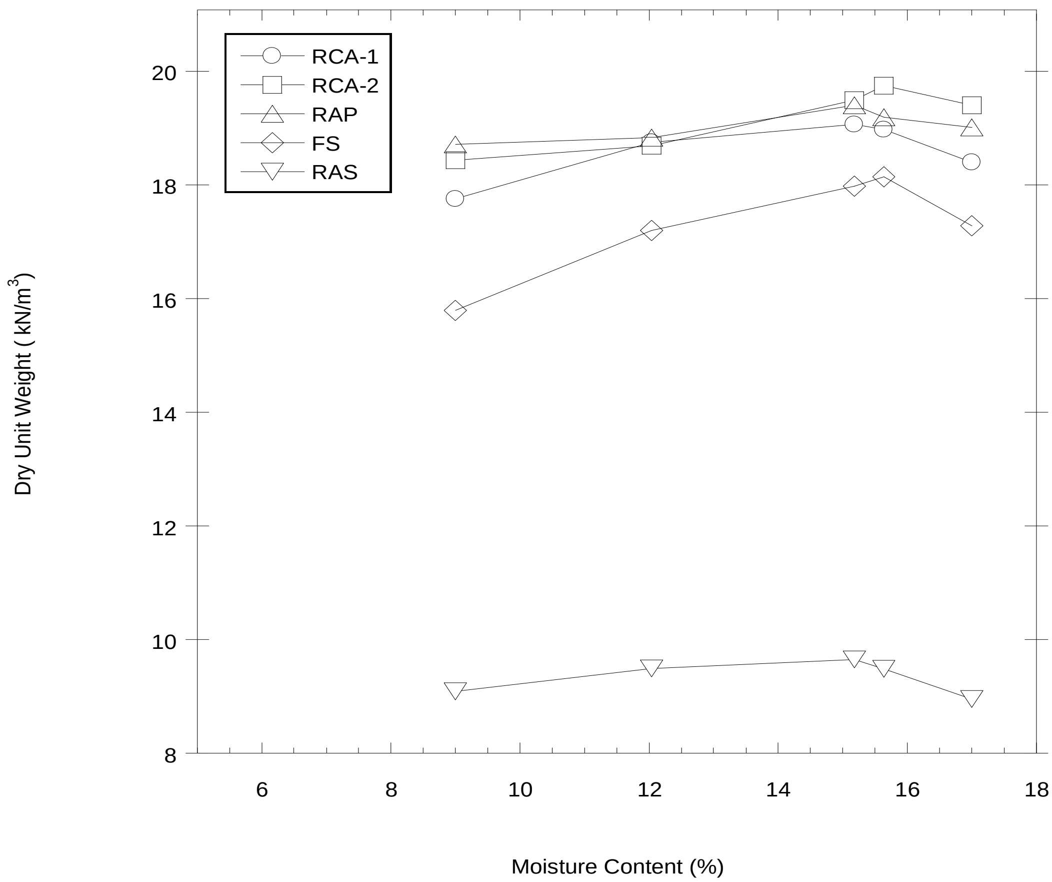

Figure 2.2 Moisture-dry unit weight relationship for recycled materials

Both samples have comparable fines content (7.7-8.7%). RCA-2 meets the requirements to be considered as granular base for highways in Maryland (Haider et al. 2014) while the fines content of RCA-1 is slightly above the limit of 8% set for Maryland highways but not very far from the fines content observed in granular bases in other States (Goulias et al. 2015).

The recycled asphalt pavement (RAP) materials were obtained from an unidentified county road in Maryland and delivered to the UMD Laboratories by the local highway agency personnel. The material is classified as well-graded sand (SW) in accordance with USCS, and A-1-a according to AASHTO Classification System. The material is non-plastic and a very small amount of the particles (1.2%) passes through the U.S. No. 200 sieve (Figure 2.1). Maximum dry unit weight and the optimum moisture content of RAP per ASTM D 698 are 6% and 19.4 kN/m^3, respectively.

The foundry sand (FS) used in the study was obtained from a stockpile in Wisconsin. FS can be classified as poorly-graded silty sand (SP-SM) in accordance with USCS, and A-3(0) according to AASHTO Classification System. The foundry sand can have varying percentages of bentonite. Abichou et al. (1998a) reported that the bentonite content of most foundry sands is between 0 and 16%. Particle size analysis shows that 7.1% of the material passes through No. 200 US standard sieve and the particle shape is typically subangular to rounded (Figure 2.1). These data are consistent with the findings of Benson et al. (2011). The sand does not exhibit any plastic behavior per ASTM D 4318. Foundry sand are found to be plastic only when the bentonite content is above 6% Abichou et al. (2004). Maximum dry unit weight and the optimum moisture content of FS per ASTM D 698 are 11.8% and 18.20 kN/m^3, respectively.

The recycled asphalt shingle (RAS) used in the study was obtained an unidentified stockpile in Wisconsin. Visual inspection indicated that the RAS contained some wood chips. RAS is classified as poorly-graded sand (SP) and A-3(0) per USCS and AASHTO, respectively. RAS contains minor amounts of fines (0.2% by weight) and is non-plastic (Table 2.1). The low specific gravity of the RAS (G_s=1.53) is attributed to the presence of asphalt binder and cellulose fibers, which are typically present in RAS at 18–40% by weight (Krivit 2007; Townsend et al. 2007). Maximum dry unit weight and the optimum moisture content of RAS are 6.9 % and 9.65 kN/m^3, respectively.

In order to check the hydraulic compatibility of geotextiles with the four recycled materials, three woven and two nonwoven geotextiles were employed in testing. A third nonwoven (NW3) geotextile, a fabric that is commonly used as part of geocomposites, was also subjected to filtration tests with the recycled materials by placing double layer of the geotextile in the column to simulate the vertical flow through the geocomposite. All geotextiles were selected considering their hydraulic properties such as permittivity (ψ), apparent opening size (AOS) and percent open area (POA). Strength parameters of geotextiles were not taken into consideration since the scope of the study was focused on filtration behavior. Manufacturer's reported physical and hydraulic properties are provided in Table 2.2. Permittivities and the apparent opening sizes of the nonwoven geotextiles ranged from 0.8 s^{-1} to 2.0

s^{-1}, and 0.15 to 0.30 mm, respectively. For the woven textiles, percent open areas and apparent opening sizes ranged from 3% to 10%, and 0.15 to 0.60mm, respectively.

2.2. *Methods*

2.2.1. Long Term Filtration (LTF) Test

Long-term filtration tests were conducted on a combination of recycled materials and geotextiles. Table 2.3 shows the test matrix for all geotextile-recycled materials combinations. Due to very low hydraulic conductivity values which caused difficulty in taking the flow rate readings, the tests with foundry sand and W3, NW2 and NW3 were not performed.

The apparatus is composed of a rigid-wall permeameter, inflow and outflow constant head devices, manometer boards, water circulation system, and the connecting hoses (Figure 2.3). ASTM D5101 procedures were followed when performing the tests except the tests were continued under the applied hydraulic gradient until the steady-state flow conditions were obtained. The 24-hour test period recommended in ASTM D5101 is usually enough to reach a steady-state hydraulic conditions when natural soils are tested; however, this test period may lead to misleading results when difficult soils were tested (Fischer, 1994). Following the recommendations of Fischer (1994), Aydilek and Edil (2003), Kutay and Aydilek (2005), and Abbaspour et al. (2018) , the geotextile-recycled material combinations were subjected to filtration tests until steady-state flow was obtained. The system was considered to be at steady-state flow condition if the change in last four consecutive permeability ratios (K_R) were lower or equal to 25% of the average of those readings by monitoring outflow discharge and the permeability of the system and the soil, as described in ASTM D5101. Hydraulic gradients of 1, 2.5, and 5 were imposed by adjusting the inflow device. All samples were compacted in the columns of 152.5-mm in diameter and 100-mm in height using sliding tamper per ASTM D2434 to 95% of their corresponding maximum dry density obtained by standard Proctor compaction (ASTM D698).

Table 2.2 Minimum average roll values (MARV) for properties of the geosynthetics tested.

Geotextile				**NW1**	**NW2**	**NW3**	**W1**	**W2**	**W3**
Structure				**NW, NP, PP**	**NW, NP, PP**	**NW, NP, PP**	**W, MF, PP**	**W, MF, PP**	**W, MF, FB, PP**
Property		Test Method	Units	**(MD/XD)**	**(MD/XD)**	**(MD/XD)**	**(MD/XD)**	**(MD/XD)**	**(MD/XD)**
Index Properties	Mass/Unit Area	ASTM D 5261	g/m^2	115	407	136	141	232	234
	Thickness	ASTM D 5199	mm	1.30	3.60	1.40	0.60	0.80	0.78
Mechanical Properties	Grab Tensile Strength	ASTM D 4632	N	356/356	1335/1335	445/445	1624/890	1780/1491	1669/1669
	Grab Tensile Elongation	ASTM D 4632	%	50/50	50/50	50/50	24/10	20/15	15/8
	Wide Width Tensile Strength (Ultimate)	ASTM D 4595	kN/m	NA	NA	NA	35/25	40/39	NA
	Wide Width Elongation	ASTM D 4595	%	NA	NA	NA	NA	NA	NA
	Trapezoidal Tear	ASTM D 4533	N	134/134	512/512	200/200	512/334	645/556	534/534
	Puncture	ASTM D 6241	N	79	3560	200	3004	5563	5340
Hydraulic Properties	Percent Open Area (POA)	COE-02215	%	NP	NP	NP	10	8	3
	Permittivity	ASTM D 4491	sec^{-1}	2.1	0.8	2.0	2.1	1.5	0.2
	Water Flow Rate	ASTM D 4491	l/min/m^2	6315	2648	5704	5907	4685	611
	Apparent Opening Size (AOS)	ASTM D 4751	mm	0.3	0.15	0.212	0.425	0.6	0.3

Note: MD= machine direction, XD=cross-machine direction, NP= not applicable; NA: Not available, NW: nonwoven, NP: needle punched, PP: polypropylene, W: Woven, MF: monofilament, PP: polypropylene, FP: fibrillated yarn, NA: Not available

Table 2.3 Geotextile and recycled material combinations.

Recycled Material	Woven Geotextiles			Nonwoven Geotextiles			Nonwoven Duplicates	
	W1	W2	W3	NW1	NW2	NW3	NW1	NW2
RCA-1	x	x	x	x	x	x	x	x
RCA-2	x	x	x	x	x	x	x	x
RAP	x	x	x	x	x	x	x	x
FS	x	x	NP	x	NP	NP	NP	NP
RAS	x	x	X	x	x	x	x	x

NP: Test not performed, x: test performed

(a)

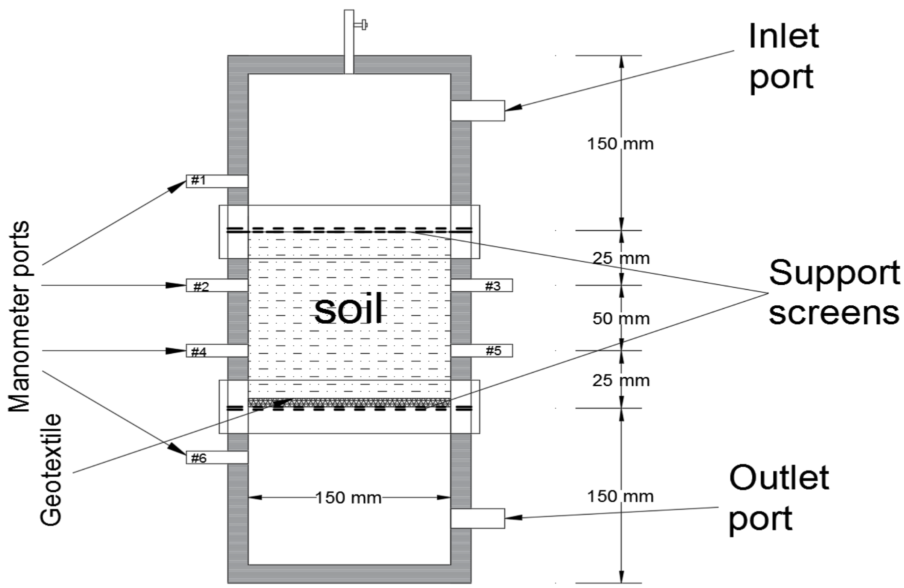

(b)

Figure 2.3 Overview of the LFT setup (a), schematic drawing of the rigid-wall permeameter (b)

In order to maintain consistency between compaction, permeability, and filtration tests and to avoid applying any type of correction factor in sample preparation, maximum particle size for all samples was limited to 19 mm. All samples were prepared and placed by the same operator. Samples were saturated by vacuuming the chamber and introducing water with slow discharge from the bottom of the chamber until the sample was submerged. After the saturation process was complete, all samples were rested in water-filled chambers for at least 24 hours before initiating the test. This sitting time was implemented to allow time for any possible entrapped air bubbles during saturation to dissolve back into the de-aired water. A 5-micron filter was used to filter suspended particles in tap water. A nano-membrane contactor system under vacuum pressure with the absolute depth of minimum 0.7 bars was used to de-air the water. The total dissolved oxygen in the outlet of the tank was measured to be 1.75- 2.20 ppm at 22 °C. Commercial chlorine tablets were added to the inflow reservoirs to control the algae growth during the tests. Manometer readings and discharge quantity, as well as the temperature of inflow and outflow, were recorded on a regular frequency, at least once every 24 hours. After termination of each test, chambers were drained from the bottom port. The soil sample was collected carefully in four layers, air-dried, and wash-sieved to determine any changes in its original grain size distribution. The surface of exhumed geotextiles was cleaned, brushed and air-dried for further evaluation. The deposited sediment in the bottom chamber after each test was collected and weighed to evaluate the retention capacity of geotextile and possibility of erosion occurrence within the soil sample. Hydraulic gradient was calculated as:

$$i = \frac{\Delta h}{L} \qquad (1)$$

where Δh is the head difference between manometer ports 1 and 6, in mm; L is the length of test specimen which is equal to 100 mm. Gradient ratio (GR) values of the system were calculated using the manometer readings as follows:

$$GR = \frac{\Delta h_{sf}/L_{sf}}{\Delta h_s/L_s} \qquad (2)$$

$$\Delta h_s = \frac{(M_2 - M_4) + (M_3 - M_5)}{2} \qquad (3)$$

$$\Delta h_{sf} = \frac{(M_4 - M_6) + (M_5 - M_6)}{2} \qquad (4)$$

where M_n is the manometer readings in mm; L_s is the distance between manometer ports 3 and 5, in mm; L_{sf} is the distance between manometer ports 5 and the bottom support screen (including the geotextile thickness), in mm.

Calculation of the hydraulic conductivity of the system with temperature correction is shown below,

$$k_{20} = \frac{Q}{(iAt) * 100} * \frac{\mu_T}{\mu_{20}} \qquad (5)$$

where k_{20} is system permeability at 20°C (m/s), i is hydraulic gradient of the system, Q is outflow discharge measured (cm^3), A is the cross sectional area of the specimen

(cm^2), t is the time for the measured quantity of flow (seconds), μ_T and μ_{20} are the water viscosities (Pa·s) at test temperature at 20°C, respectively.

However, GR values can be significantly influenced from any small changes in manometers, and permeability ratio (K_R), utilized by (A.H. Aydilek & Edil, 2002), Sabiri et al. (2017) and Abbaspour et al. (2018), was calculated due to the limitations of GR in defining the clogging conditions:

$$K_R = \frac{k_{soil}}{k_{system}} \quad (6)$$

where k_{soil} and k_{system} are the permeability in the soil and the whole system respectively. The k_{soil} is calculated using the pressure heads recorded at manometers placed at 25 mm and 75 mm above geotextile (i.e. port #2 – port #3 and port #4 – port #6) and k_{system} is determined using the applied hydraulic gradient on the system (Equation 5). However, flow discharge passing from the soil/geotextile system is assumed to be constant for any section of the specimen.

2.2.2. Falling Head Permeability Test

All soil samples were subjected to a series of falling-head tests. The specimens were compacted to 95% of maximum dry unit weight using the standard Proctor effort (ASTM D 698) in a PVC mold with an inner diameter of 152.5 mm and a height of 152.5 mm. The maximum hydraulic gradient of 2.0 was applied to avoid channeling along the sidewall, consolidation, washing of fine particles downstream and plugging of the effluent end of the specimen, which would increase or decrease the hydraulic conductivity (ASTM D 5856). The length (L) of the specimen was measured after completion of permeation.

2.2.3. Image Analysis

The permittivity of virgin and post-filtration geotextiles was determined following the procedures listed in ASTM D4491. Tests were initiated with an applied head of 10 mm, which would give a flow discharge similar to filtration tests. After 30 minutes, the applied head was increased in 10 mm increments to measure the permittivity of the samples at higher flow discharges. Upon termination of the filtration tests, permittivity tests and digital image analyses were performed on the geotextile samples in order to quantify the changes in their hydraulic performance and pore structures, respectively. Any soil remaining on the surface of the geotextile was removed by lightly brushing the geotextile. Extensive specimen preparation was necessary before imaging the nonwoven geotextile, as the three-dimensional structure of this geotextile causes difficulties in capturing pore structures from two-dimensional images, and planar and cross-sectional thin-sections need to be prepared to provide detailed information on clogging. The thin sections of the nonwoven geotextiles investigated in this study were prepared following the procedures employed in preparing thin sections of rock samples and the details of the procedure developed for geotextiles are summarized by (Aydilek et al. 2002).

Pore structure images of all geotextiles were captured using an optical light microscope. The microscope had a 45 mm x 25 mm workstation platform, and a 2.5 to 100X macro zoom lens coupled with an image-capturing software. A digital camera was attached to the microscope that sent the captured images to the software. Resolutions of 1298 by 968 pixels were used for all images. Magnification (objective) ratio was 2.5X and 2.5-5X, and the corresponding pixel size was approximately 6.97 mm and 3.25-6.9 mm for the planar and cross-sections, respectively. The specimens were illuminated from the bottom as suggested by (Jang, Frost, & Park, 1999) and (Aydilek et al., 2002).

Image J, a public domain, Java-based image processing program, which was developed at the National Institutes of Health and commonly used in various engineering applications (Schneider et al. 2012), was utilized to analyze the images. The threshold value for generating a binary image and differentiating the background from the image objects of interest was set to the mid-point of the pixel intensity values recorded at the two ends of the histogram and ranged from 158 to 225. In the binary image, the white pixels corresponded to pore openings, whereas the black pixels represent the fibers for the virgin samples and the fibers and the recycled material particles for the post-filtration test samples, respectively. The pore openings in each individual planar and cross-sectional images were counted, and the ratio of the number of openings to the whole image size was referred to as porosity (n). For pore size distribution (PSD) calculations, a range of geotextile opening diameters (i.e., comparable to the sieve sizes commonly used in (ASTM 4751) dry sieving test) was defined. Each opening diameter was compared to the diameter of a circle fitted to the pore, and percentage of geotextile pore sizes smaller than the defined opening diameters were calculated. The process was repeated for the images of all samples of a particular geotextile, and an average PSD was reported. The details of the PSD determination procedure are provided in (Aydilek et al., 2002).

Chapter 3

Results of Laboratory Study of Filtration by Woven Geotextiles

3.1. *Clogging Behavior*

3.1.1. Long-Term Filtration Test Results

Table 3.1 summarizes the results of the long term filtration tests performed using RCA-1, RCA-2, RAP, FS and RAS with the woven geotextiles (W1, W2, W3). Gradient ratio is defined as the ratio of hydraulic gradient through soil-geotextile system to hydraulic gradient through the soil alone (ASTM D5101). For successful applications, a gradient ratio of under 3 is suggested for compatible systems as a part of the U.S. Army Corps of Engineers' criterion (Haliburton and Wood 1982). Also, same limit can be used for the permeability ratio (i.e., $K_R < 3$) as an indication of acceptable filtration compatibility between soil and geotextile (Aydilek and Edil 2003, Kutay and Aydilek 2005, Koerner 2012). The time required for stabilization of flow under each hydraulic gradient ranged from 200 to 300 hours. This is consistent with the findings of Aydilek and Edil (2003), Narejo et al. (2013) and Abbaspour et al. (2018) who indicated a 24-hour procedure recommended in the ASTM D5101 is insufficient and long term testing is required.

A review of the data in Table 3.1 shows that W1 tested with RCA-2, RAP, FS and also W3 tested with RAP would be considered clogged based on the criterion that sets GR_{ASTM} of 1 as a limit, and only two of them (W1 with FS and W3 with RAP) would be considered clogged when U.S. Army Corps of Engineers limit of 3 used.

Table 3.1 Results of the long term filtration tests with woven geotextiles

Recycled Material	Geotextile	Piping Rate (g/m^2)	K_{system} (cm/sec)	K_{soil} (cm/sec)	$K_R = k_{soil}/k_{system}$	Gradient Ratio (G_R)
RCA-1	W1	1100				
	i=1.0		1.4×10^{-4}	1.0×10^{-4}	0.7	0.1
	i=2.5		1.8×10^{-4}	1.2×10^{-4}	0.7	0.1
	i=5.0		NA	NA	NA	NA
	W2	34				
	i=1.0		6.9×10^{-6}	3.5×10^{-6}	0.5	0.0
	i=2.5		8.7×10^{-6}	5.9×10^{-6}	0.7	0.2
	i=5.0		1.3×10^{-5}	7.8×10^{-6}	0.6	0.4
	W3	68				
	i=1.0		1.7×10^{-5}	9.4×10^{-6}	0.6	0.2
	i=2.5		2.3×10^{-5}	1.3×10^{-5}	0.6	0.3
	i=5.0		2.0×10^{-5}	1.2×10^{-5}	0.6	0.3
RCA-2	W1	2280				
	i=1.0		6.8×10^{-3}	6.7×10^{-3}	1.0	1.9
	i=2.5		1.2×10^{-3}	1.2×10^{-3}	1.0	2.0
	i=5.0		NA	NA	NA	NA
	W2	68				
	i=1.0		3.4×10^{-4}	1.9×10^{-4}	0.6	0.1
	i=2.5		2.3×10^{-4}	1.3×10^{-4}	0.6	0.1
	i=5.0		2.2×10^{-4}	1.2×10^{-4}	0.5	0.1
	W3	23				
	i=1.0		4.6×10^{-5}	2.7×10^{-5}	0.6	0.4
	i=2.5		2.0×10^{-5}	1.1×10^{-5}	0.6	0.2
	i=5.0		1.5×10^{-5}	8.1×10^{-6}	0.6	0.2
RAP	W1	840				
	i=1.0		1.2×10^{-2}	1.5×10^{-2}	1.2	2.6
	i=2.5		2.7×10^{-3}	3.0×10^{-3}	1.1	2.2
	i=5.0		NA	NA	NA	NA
	W2	215				
	i=1.0		2.6×10^{-3}	1.7×10^{-3}	0.7	0.6
	i=2.5		1.9×10^{-3}	1.3×10^{-3}	0.7	0.6
	i=5.0		1.5×10^{-3}	1.0×10^{-3}	0.7	0.7
	W3	96				
	i=1.0		2.2×10^{-2}	4.9×10^{-2}	2.2	6.1
	i=2.5		1.1×10^{-2}	4.0×10^{-2}	3.5	10.9
	i=5.0		5.7×10^{-3}	2.5×10^{-2}	4.4	15.1

NA: Test not performed.

Table 3.1. Results of the long-term filtration tests with woven geotextiles (continued)

Recycled Material	Geotextile	Piping Rate (g/m^2)	K_{system} (cm/sec)	K_{soil} (cm/sec)	$K_R = k_{soil}/k_{system}$	Gradient Ratio (G_R)
FS	W1	1120				
	i=1.0		1.6×10^{-6}	1.5×10^{-6}	0.9	1.6
	i=2.5		3.3×10^{-6}	7.8×10^{-6}	2.4	6.7
	i=5.0		NA	NA	NA	NA
	W2	215				
	i=1.0		3.7×10^{-7}	3.2×10^{-7}	0.9	0.02
	i=2.5		3.2×10^{-7}	2.2×10^{-7}	0.7	0.03
	i=5.0		3.7×10^{-7}	4.9×10^{-7}	1.3	0.03
	W3	NA				
	i=1.0		NA	NA	NA	NA
	i=2.5		NA	NA	NA	NA
	i=5.0		NA	NA	NA	NA
RAS	W1	140				
	i=1.0		7.8×10^{-4}	2.9×10^{-3}	3.9	0.2
	i=2.5		NA	NA	NA	NA
	i=5.0		NA	NA	NA	NA
	W2	14				
	i=1.0		3.5×10^{-3}	5.1×10^{-3}	1.5	1.3
	i=2.5		1.7×10^{-3}	2.9×10^{-3}	1.7	0.9
	i=5.0		4.6×10^{-4}	7.8×10^{-4}	1.7	0.2
	W3	12				
	i=1.0		1.5×10^{-3}	1.6×10^{-3}	1.0	0.5
	i=2.5		7.6×10^{-4}	8.8×10^{-4}	1.2	0.6
	i=5.0		5.5×10^{-4}	5.7×10^{-4}	1.0	0.4

NA: Test not performed.

For example, stabilized soil and system permeabilities of 1.2 x 10^{-3} cm/sec were measured for W1 with RCA-2, which indicates minimal impedance of flow through the system and development of a bridging network. However, the gradient ratio at the end of the test was 1.9, which clearly indicates clogging, according to the ASTM D5101 recommendations. Additionally, geotextile W3 with RAP had a stabilized soil permeability of 4.9 x 10^{-2} cm/sec under a hydraulic gradient of 1.0 with a corresponding system permeability of 2.2 x 10^{-2} cm/sec. The ratio of those two permeabilities (K_R) is 2.3 which is below the limit set for clogging; however, the gradient ratio is 6, which again indicates severe clogging. All geotextile-soil combinations indicated acceptable performance based on their K_R ratios except W1 with RAS (K_R= 3.9) and W3 with RAP (K_R= 4.4). Their performance also verified by the calculated Ψ_R and POA_R ratios (Table 3.2). The results show that gradient ratio is a good indicator of observing soil-geotextile compatibility. However, due to the problems that can occur during tests (i.e., clogging of manometer ports, increase in dissolved oxygen levels of inlet water, biological and chemical clogging) K_R, POA_R and Ψ_R are considered as better indicators of filtration performance of geotextiles tested with recycled materials.

Table 3.2 illustrates that most of the POA_R values are comparable with Ψ_R. The discordance monitored with W3 is attributed to its low POA and small apparent opening size (AOS). Majority of POA_R and Ψ_R are around 1, which suggests that the three geotextiles, in general, remained unclogged upon testing with the industrial by-products. The Ψ_R value measured for W1-RAS was 0.78, slightly lower than 1.0, verified by the high K_R value (3.7) for this combination.

Table 3.2 Summary of long term filtration tests

Recycled Materials	Permittivity Ratio, Ψ_R			POA ratio, POA_R			Permeability Ratio*, K_R			Gradient Ratio* G_R			Piping Rate, (g/m^2)		
	W1	**W2**	**W3**	**W1**	**W2**	**W3**	**W1**	**W2**	**W3**	**W1**	**W2**	**W3**	**W1**	**W2**	**W3**
RCA-1	0.96	0.95	0.98	0.9	0.7	0.8	0.7	0.6	0.6	0.1	0.4	0.3	1100	34	68
RCA-2	0.94	0.96	0.94	0.8	0.9	0.3	1.0	0.5	0.6	2.0	0.1	0.2	2280	68	23
RAP	0.93	0.88	0.99	0.9	1.0	0.8	1.1	0.7	4.4	2.2	0.7	15.1	840	215	96
FS	0.92	0.94	NA	0.9	0.9	NA	2.3	0.6	NA	6.7	0.0	NA	1120	215	NA
RAS	0.78	0.98	0.98	0.8	1.0	0.9	3.7	1.7	1.0	0.2	0.2	0.4	140	14	12

*Reported clogging values are the stabilized values at the end of testing. NA: Test not performed.

Temporal characteristics of system permeabilities and K_R are given in Figure 3.1, Figure 3.2 and Figure 3.3. A clogged geotextile results in a decrease in system permeability. Three different hydraulic gradients (i=1, i=2.5, i=5.0) applied except for W1 where only two were used (i=1.0 and i=2.5). The data in Figures 3.1-3.3 show that permeability ratio (K_R) values for RCA-1 and RCA-2 range between 0.54 and 1.03 which is an indicator of good compatibility. However, poor compatibility observed on W1-RAS, W1-FS and W3-RAP combinations. FS were not tested with W3 due to foundry sand's very low hydraulic permeability and W3's low permittivity due to geotextile structure.

A blocking/blinding pattern is observed for W1-RAS after 200 hours of testing. The system permeability decreases from 7.2 x 10^{-3} cm/s to 7.7 x 10^{-4} cm/s and is accompanied by an increase in K_R from 0.9 to 3.8. A comparable decrease in hydraulic conductivity is recorded for RAP tested with W3 after increasing the hydraulic gradient from 1.0 to 2.5. The permeability decreases from 2.2 x 10^{-2} cm/s to 5.7 x 10^{-3} cm/s and is accompanied by increase in K_R 2.2 to 4.4, and then stabilizes at ~4.4. Similar observations can be observed during testing of RAS with W2. The permeability decreases from 1.0 x 10^{-2} cm/s to 2.8 x 10^{-3} cm/s under an applied hydraulic gradient of 1, from 3.2 x 10^{-3} cm/s to 1.4 x 10^{-3} cm/s under a gradient of 2.5, and from 2.3 x 10^{-3} cm/s to 3.9 x 10^{-4} cm/s when the applied gradient is 5. The corresponding increases in K_R are as follows; from 0.7 to 2.5, from 1.3 to 1.8 and from 1.5 to 1.7, respectively.

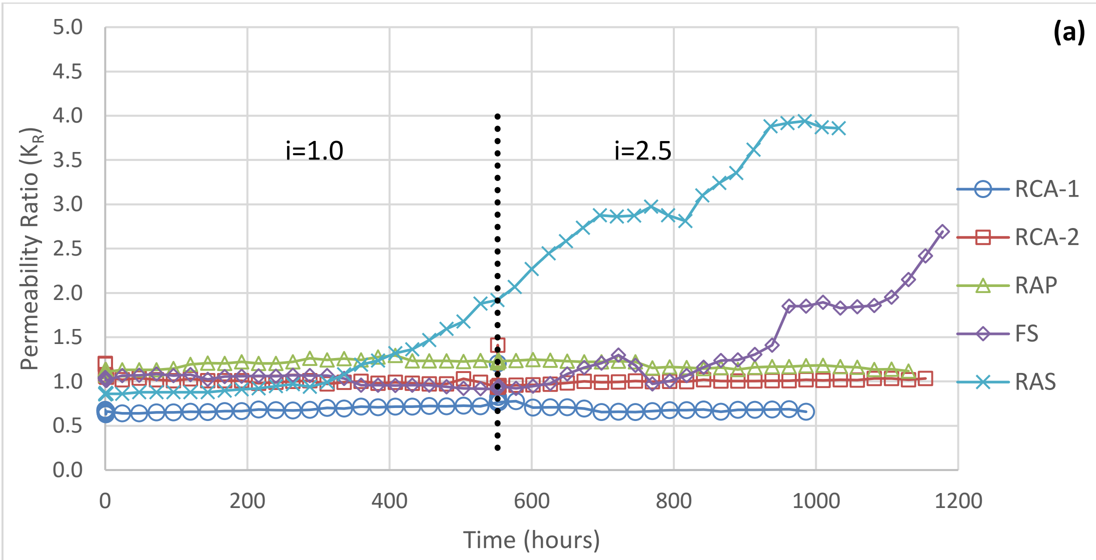

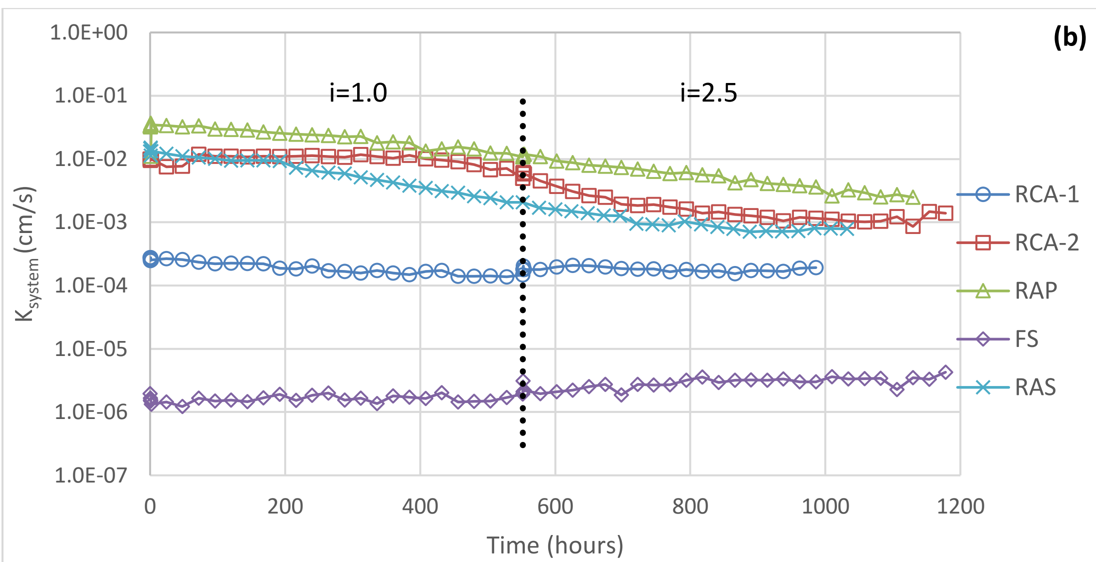

Figure 3.1 Permeability ratio versus time relationship for W1 (a), System Permeability versus time relationship for W1 (b)

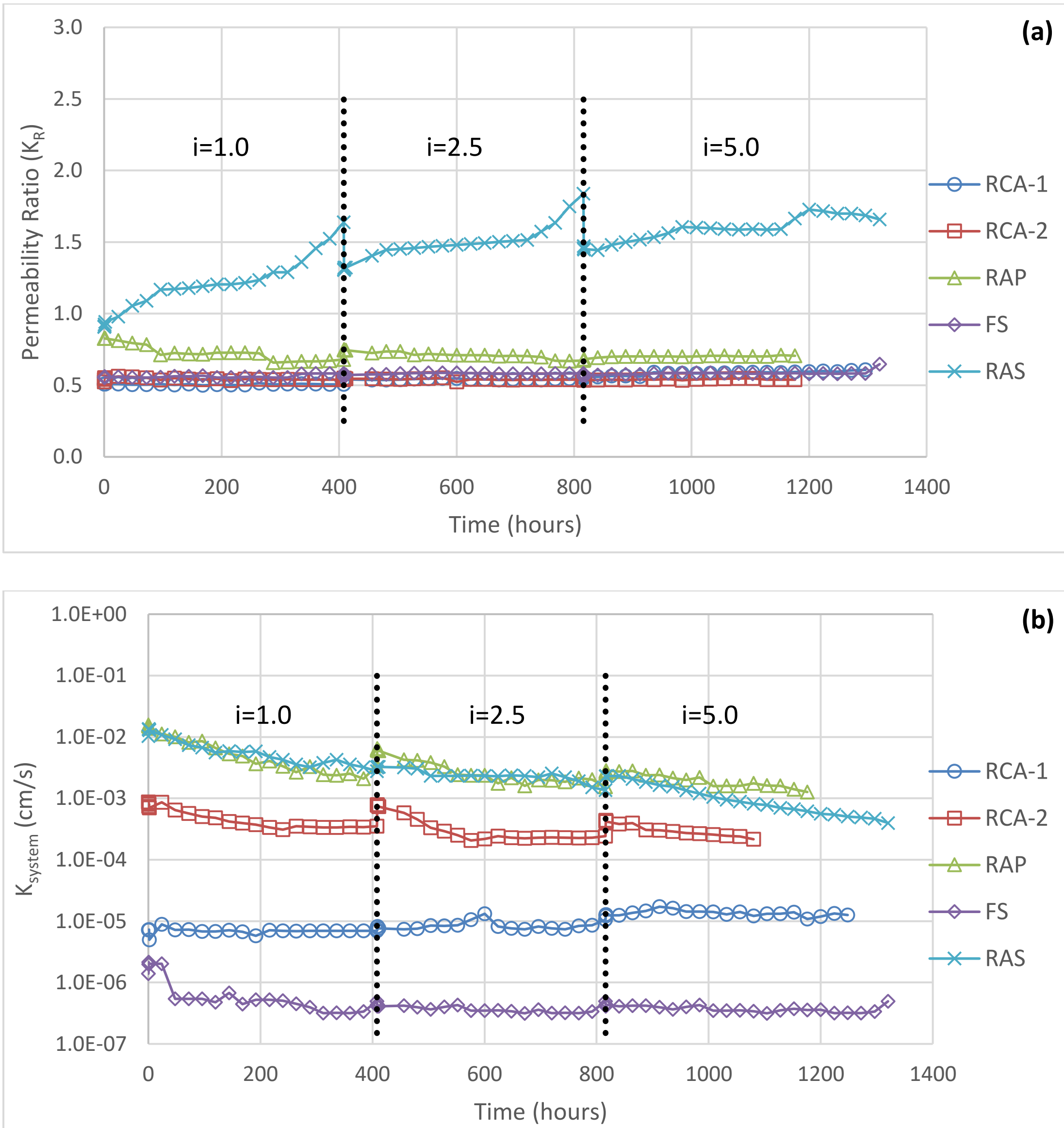

Figure 3.2 Permeability ratio versus time relationship for W2 (a), System Permeability versus time relationship for W2 (b)

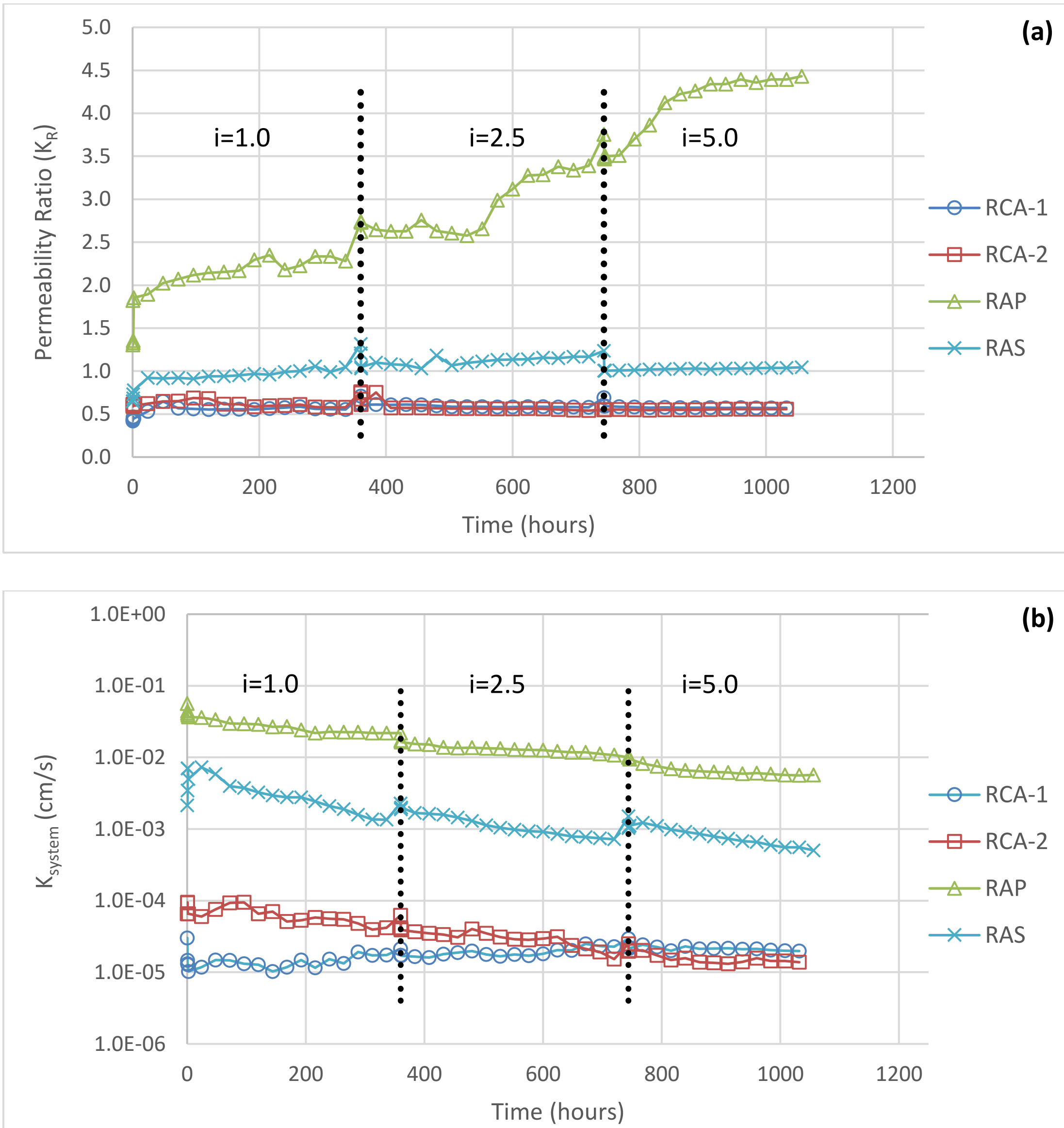

Figure 3.3 Permeability ratio versus time relationship for W3 (a), System Permeability versus time relationship for W3 (b)

A mixed behavior is observed for the foundry sand tested with W1 after increasing the hydraulic gradient from 1.0 to 2.5. The system permeability slightly increased from 1.3 x 10^{-6} cm/s to 3.3 x 10^{-6} cm/s, typically an indicative of continuous piping. The changes in permeability are accompanied by an initial increase in K_R from 0.9 to 2.7, which stabilizes at 2.4. Rollin et al. (1985) observed similar flow patterns during long term filtration tests and classified them into three groups as follows; normal, piping and mixed behavior. Normal behavior is defined as movement of soil particles through geotextile resulting in an increase in the density of the soil layer just above the geotextile and thus reducing permeability. A behavior where loss of soil particles (piping) followed by a filter cake formation at the soil geotextile interface is called mixed behavior.

Average material hydraulic conductivities (k_{soil}) for RCA-1, RCA-2, RAP, FS, and RAS are 3.5 x 10^{-5} cm/sec, 1.1 x 10^{-3} cm/sec, 1.7 x 10^{-2} cm/sec, 2.1 x 10^{-6} cm/sec, 2.1 x 10^{-3} cm/sec, respectively. These values are highly comparable with those reported by Locander (2009), Nokkaew et al. (2012), Shedivy et al. (2012), Rahman et al. (2014) and McCulloch et al. (2017). Abichou et al. (2000) reports a hydraulic conductivity range of 5.3 x 10^{-5}- 6.1 x 10^{-9} cm/sec for foundry sands with varying bentonite contents, which is in a good agreement with the findings of the current study. Soleimanbeigi et al. (2013) reported a hydraulic conductivity range of 2 x 10^{-4} -9 x 10^{-6} cm/sec for RAS. The average hydraulic conductivity measured in the current study remains outside of this range most probably due to relatively higher fines content of the RAS utilized by Soleimanbeigi et al. (3.8% versus 0.2%). Among all recycled materials tested in this research program, material hydraulic conductivity is the highest for RAP and the lowest for the FS, averaging at 1.7 x 10^{-2} cm/sec and 2.1 x 10^{-6} cm/sec, respectively. The order in material hydraulic conductivities ($k_{FS}<k_{RCA-1}<k_{RAS}<k_{RCA-2}<k_{RAP}$) do not entirely match with that in fines contents (RCA-1>FS>RCA-2>RAP>RAS), even though several researchers in the past suggested that hydraulic conductivity decreased with increasing fines content of recycled material (Abbaspour et al. 2018, Rahman et al. 2014, Alakayleh 2018 Delgado-Rodriguez 2011, NAM 2015, McCulloch 2017, Behring 2014). There may be several reasons for the behavior observed in the current study. For instance, FS can have varying bentonite contents that affect its hydraulic conductivity (Abichou et al. 2004), even though an analysis was not conducted to determine the bentonite content of the FS utilized in the current study. It can be clearly seen that FS has comparable fines content with RCA-1 whereas, its hydraulic conductivity is 100 times lower than that of RCA-1. Kenny et al. (1992) also pointed out that existence of empty voids filled with no bentonite is the most substantial factor contributing to the hydraulic conductivity of foundry sand. RAS has the lowest finest content (0.2%) although it did not yield the lowest hydraulic conductivity among all, which may be attributed to its excessive compressibility. Soleimanbeigi et al. (2013) reported that hydraulic conductivity of RAS has reduced with increasing confining pressure because of compressibility therefore, stabilization is required to be used as a substitute to natural soils. Again, a separate analysis was not conducted herein to test the influence of compressibility on RAS hydraulic conductivity.

Two clogging ratios (K_R and Ψ_R) are plotted versus permittivity of virgin geotextiles (Figure A1). Attempts were also made to relate the permeability to three characteristic pore opening sizes of a geotextile (O_{95}, O_{90} and O_{50}) in contact with the industrial by-products but no clear-cut trends were observed (Figure A4). This is somewhat consistent with the findings of Faure et al. (2000), Krug et al. (2000), Aydilek and Edil (2003), Palmeria and Trejos Galvis (2017) and Sabiri et al. (2017) that both permittivity and pore structure parameters (i.e., porosity and pore size distribution) rather than a single hydraulic property is more likely to influence the clogging performance of geotextiles.

Stabilized values of the permeability ratio are plotted versus each applied hydraulic gradient in Figure A2. K_R values seem to be affected from the increase in hydraulic gradient. There is a gradual but inconsistent increase in K_R with increasing hydraulic gradient. K_R is mostly lower than the limit of 3, indicating that the partial clogging of the geotextiles does not have a significant effect on the overall filtration performance of the system.

3.1.2. Effect of Geotextile Pore Structure on the Clogging Performance

The clogging ratios (K_R, POA_R, Ψ_R) for all recycled materials tested are plotted versus the percent open area in Figure 3.4. No clear trend can be observed, even though permeability ratio (K_R) seemed to be influenced by the virgin geotextile POA during testing with RAS.

Permittivity ratio (Ψ_R) does not clarify if the system permeability has changed or a recycled material-geotextile system is compatible, but it is an indicator of changes in the flow capacity of a geotextile. Theoretically, the permittivity ratio should be equal to 1.0 if there is no reduction in the serviceability of a geotextile (i.e. no changes in the flow capacity of a geotextile). However, in order to take physical and biological clogging into account, permittivity of a geotextile reported by the manufacturer is divided by a safety factor ranging from 2 to 10 in practice, corresponding to a flow reduction of 50 to 90%, respectively (Koerner 2012). The data in Table 3.2 indicates that the average reduction in flow, in general, remains in a range of 1-22% for the materials tested. These percent reductions correspond to a mean permittivity ratio range of 0.78-0.99, and mean hydraulic conductivity range of 3.3×10^{-3} cm/s – 5.0×10^{-3} cm/s. The calculated decreases in the permittivity would be acceptable for geotextiles filtering recycled materials, as the clogged geotextile still has about 3-5 times higher permeability than that of a clean uniform sand ($k=1\times10^{-3}$ cm/s, Coduto et al. 2010).

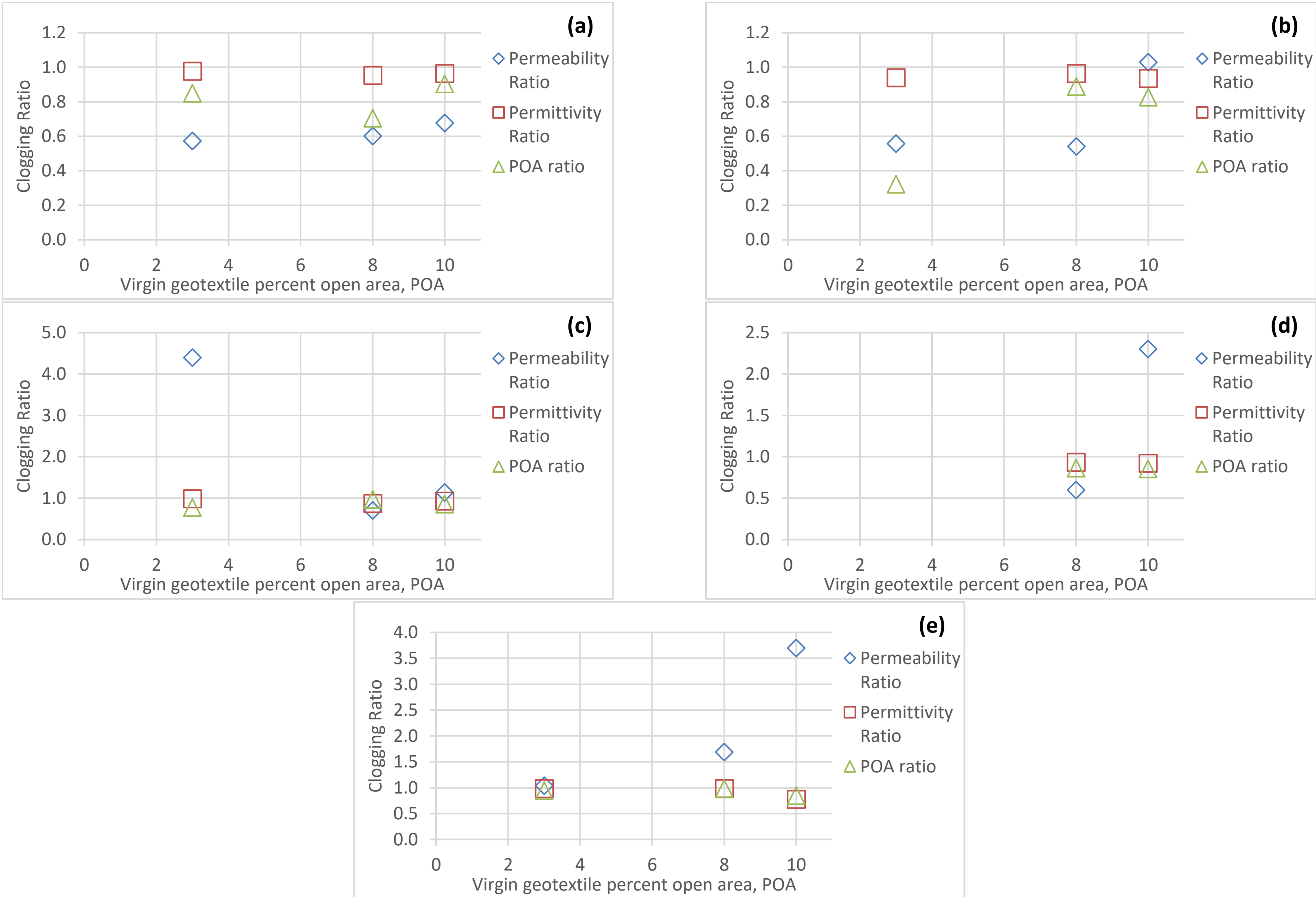

Figure 3.4 Clogging ratios versus virgin geotextile percent open area for RCA-1 (a), and for RCA-2 (b), RAP (c), FS (d), RAS (e)

3.2. _Retention Behavior_

Long-term filtration tests also presented important information about retention performance of geotextiles. Piping is a phenomenon caused by the migration of some fine fraction of soil particles that pass through the geotextile.

The amount of soil piped through the geotextiles in all soil-geotextile combinations is in a range of 12 g/m^2 to 2,280 g/m^2 (Table 3.2). Geotextile W1 piped the most; however, the piped amount (2,280 g/m^2) is still less than 2,500 g/m^2, an internal stability limit typically used for granular and geotextile filters (Lafleur et al. 1989, Bhatia et al. 1996, Aydilek and Edil 2002, Kutay and Aydilek 2005, Huang and Luo 2007, Palmeria and Tatto 2015, Fatema and Bhatia 2018,). It should be noted that geotextile W1 has considerably higher POA (%10) than the other woven geotextiles. The piping rates were found to be higher for the soils with higher fines content.

Upon termination of each filtration test, sieve analyses were performed on the samples collected from different depths in the permeameters (i.e., 0-25; upper layer of 25 mm, 25-75; middle layer of 50 mm, 75-94; lower layer of 19 mm, 94-100; bottom layer of 6 mm above the geotextile) and compared to the grain size distribution (GSD) of the virgin recycled material (Figure A6 – A8). The shifts in GSD of the recycled material-geotextile combinations were generally comparable with the measured piping rates. Figure 3.5 is given as an example to show such changes in grain size distribution curves for RCA-1 upon testing with W1 and W2. Considering the layers immediately above the geotextile filter where graded filter zone forms (i.e., 75-94 and 94-100), the shift from the virgin material grain size distribution is more clearly pronounced for W1 (POA = %10) as compared to W3 (POA=3%) due to a higher piping rate measured for W1 (1,110 g/m^2 versus 67.9 g/m^2). GSD of soil-geotextile interface (94-100 mm) shifts to the right in most cases as compared to the GSD of the virgin material for woven geotextiles, suggesting that accumulation of soil fines has occurred at the interface. However, it should be noted that since the intended layer was 6 mm as the maximum particle size of the soils was 19 mm, often, coarse particles sitting directly over geotextile had to be removed, in order to reach to the 6 mm-thick layer of soil over the geotextile. The shifts at the lower layers (i.e., 75-94 mm and 94-100 mm) are more pronounced for the woven geotextiles.

To illustrate the effect of pore structure on piping rate, piping rates are plotted versus POA and two commonly used retention ratios, O_{95}/D_{85}, O_{50}/D_{50} in Figure 3.6 and geotextile pore opening size (i.e., O_{95}, O_{90}, O_{50}) in Figure A5 Piping rate increases with the increasing POA, as percent open area is an important geotextile pore structure parameter that controls retention performance (Austin et al. 1997, Mylnarek et al. 1997). No clear-cut trends could be observed between the piping rates and the two retention rations nor the common geotextile pore opening sizes, inconsistent with the findings of Fatema and Bhatia (2018). Furthermore, Figure A3 also shows that, in general, piping rate increased with increasing permittivity for most of the materials, with the exception of RAS which has very low fines content (0.2%, Table 2.1).

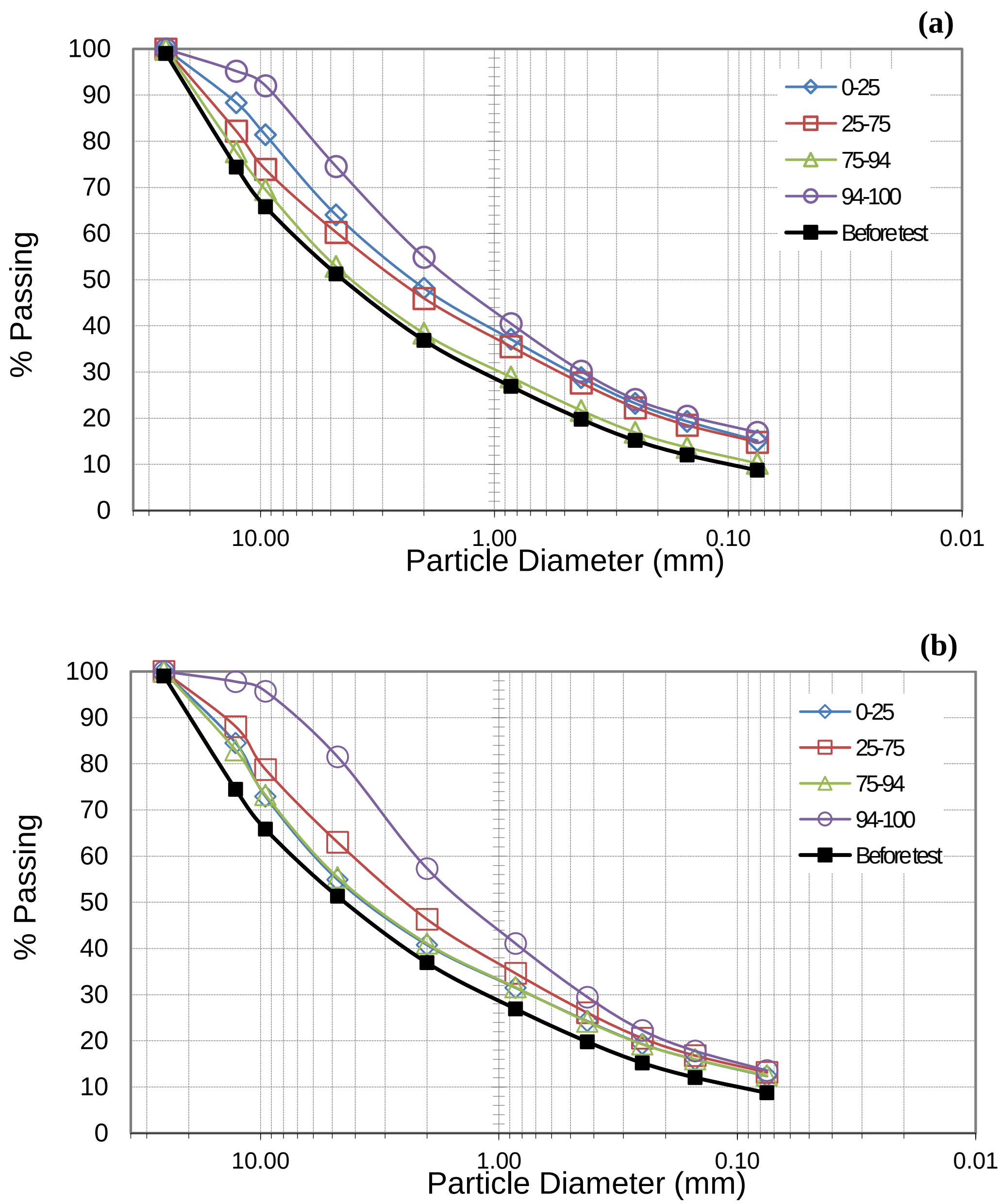

Figure 3.5 Grain size distribution of the RCA-1 samples tested with W1 (a), tested with W3 (b)

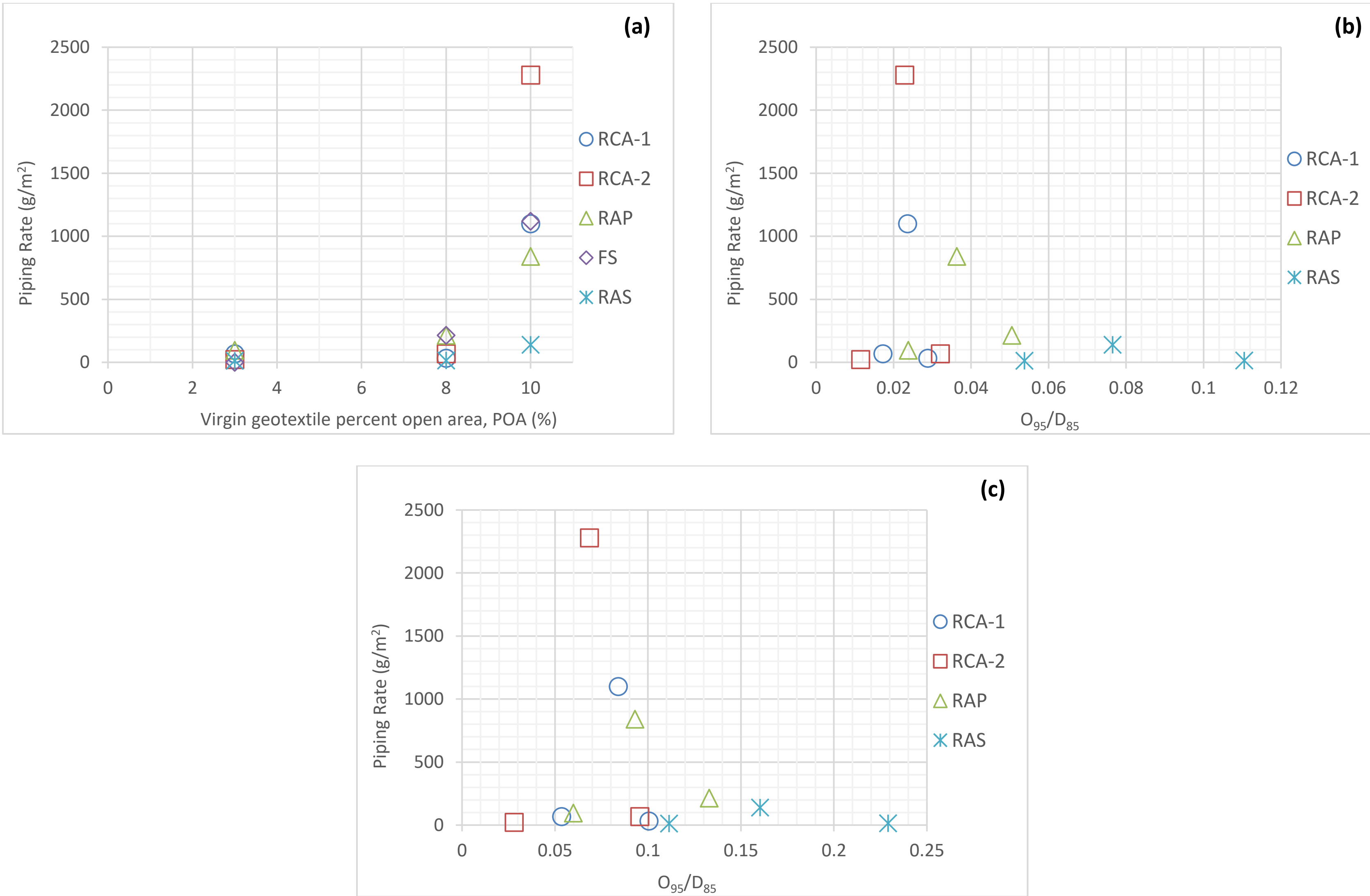

Figure 3.6 Piping rates versus virgin geotextile POA (a), Piping rates versus virgin geotextile O95/D85 (b), Piping rates versus virgin geotextile O50/D50 (c)

3.3. *Post Long-term Filtration test–Analysis of Pore Structure Change of Geotextiles*

The geotextiles subjected to long-term filtration tests were analyzed using image analysis to determine the changes in their POAs and characteristic pore opening sizes. Table 3.3 shows that POA of most of the geotextiles remained unchanged after the filtration tests were completed. The percent reduction in POA remains in a range of 0-30% for most of the combinations. The only exception is the W3-RCA-2 combination, which experienced a 70% reduction in POA, possibly due to low percent open area of the virgin geotextile (3%). The decrease in POA is generally lower for the geotextiles tested with RAP and RAS, which may be attributed to the lower fines contents of these two recycled materials (1.2% and 0.2%, respectively).

The shifts in PSDs shown in Figure 3.7 depict the differences in reduction in characteristic pore opening sizes. Characteristic pore opening sizes (e.g., O_{95}, O_{60}, O_{50}, O_{40}, O_{30}, O_{15}, and O_{10}) of the post-filtration test geotextile decrease in all cases, indicating that clogging did not affect a single parameter. Percent change in pore sizes in two characteristic sizes, O_{95} and O_{50}, upon filtration are summarized in Table 3.3. Decrease in pore sizes are insignificant, being less than 15% in most cases, except the geotextile W3 tested with RCA-2 that experienced 34.7% and 43% reduction in O_{95} and O_{50}, respectively, as evidenced by the shifts in its PSD (Figure 3.7). An example collage of planar images of post-test and virgin geotextiles W1, W2 and W3 subjected to filtration with RCA-2 are shown in Figure 3.8. The images clearly show the particle accumulation within the woven geotextiles.

Table 3.3 Change in the O_{95}, O_{50} and POA of the geotextiles subjected to filtration testing

Name of geotextile	POA (%)	Percent Reduction in POA of geotextile (%)					Characteristic pore size	Measured pore size of virgin geotextile (mm)	Percent Reduction in Measured pore size of geotextile (%)				
		RCA-1	RCA-2	RAP	FS	RAS			RCA-1	RCA-2	RAP	FS	RAS
W1	10	9.5	17.3	14.1	14.8	15.4	O_{95}	0.42	7.3	10.9	7.4	9.9	9.8
							O_{50}	0.40	4.7	8.7	7.6	7.8	7.5
W2	8	29.6	11.1	2.9	13.6	1.8	O_{95}	0.56	14.3	5.0	2.2	4.2	1.0
							O_{50}	0.54	15.6	5.7	2.4	6.3	2.1
W3	3	15.0	67.8	22.7	NA	6.0	O_{95}	0.29	1.4	34.7	11.4	NA	7.4
							O_{50}	0.26	7.4	43.0	9.3	NA	2.1

NA: Test not performed.

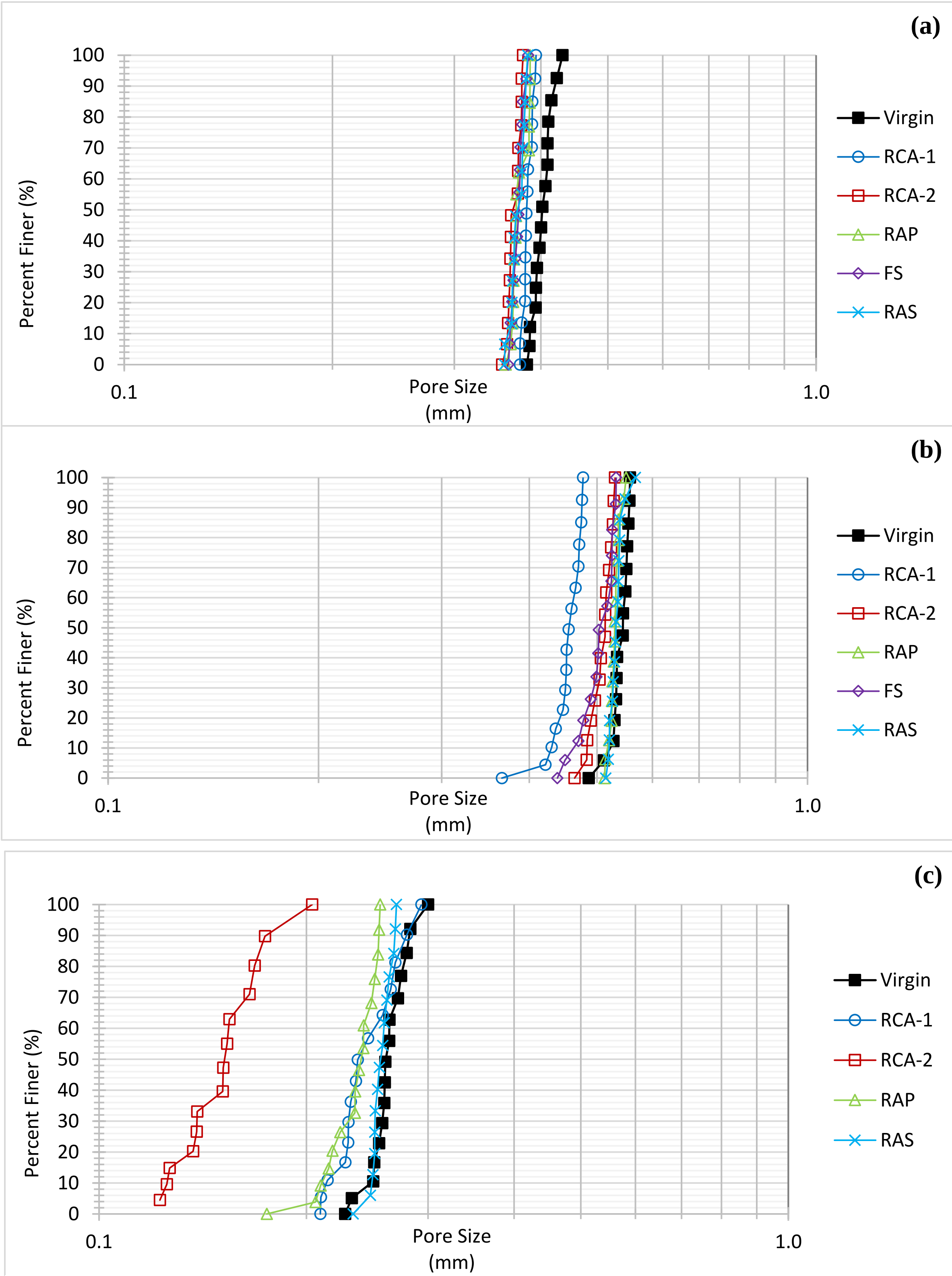

Figure 3.7 Change in PSD of geotextiles before and after filtration tests, W1 (a), W2 (b), W3 (c)

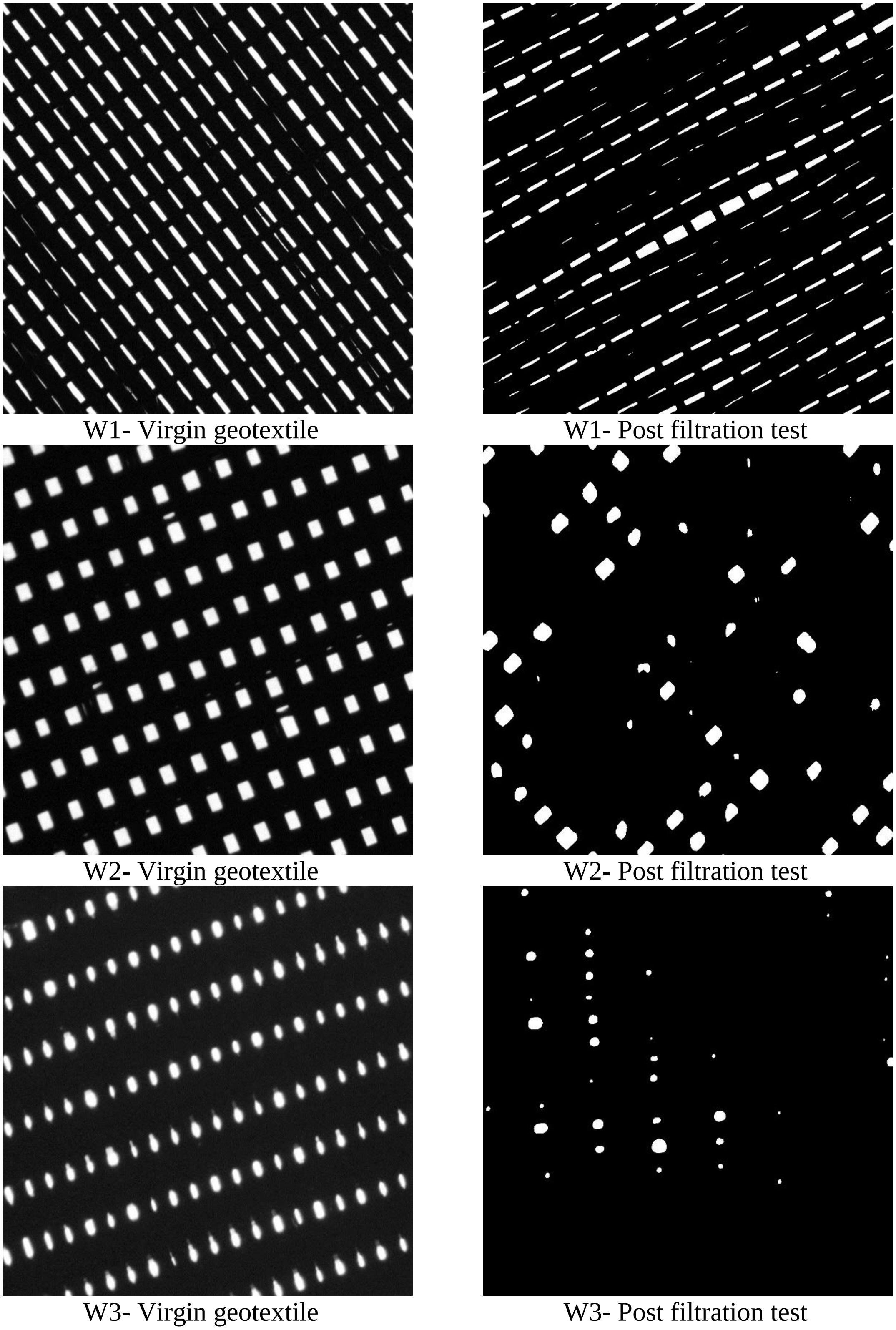

Figure 3.8 Post test and virgin images of geotextiles W1, W2 and W3 tested with RCA-2

3.4. *Applicability of Existing Filter Selection Criteria*

The results from long term filtration tests and PSDs from image analyses used in order to determine the applicability of widely utilized current geotextile filtration criteria for all the recycled materials were used in this research. Tables 3.4 and 3.5 compare the predictions of existing filter criteria to actual performance observed in the laboratory tests. Table 3.4 summarizes that existing retention criteria predicted most of the tests. All geotextile-recycled material test combinations performed well and did not experience significant piping. All of the existing criteria, except Calhoun (1972), Christopher and Holtz (1985), Ogink (1975) and Miller et al (1980) predicted results with %100 success rate. Almost all existing empirical criteria failed to predict the retention performance of the foundry sand. However, filters that fail to meet the retention criteria can still function as the particle entrapment increases the retention capacity of the geotextile (Palmeira and Gardoni 2000, Palmeria and Fannin 2002, Raut 2006, Koerner 2016 and Miszkowska et al. 2017). All geotextiles performed successfully in the laboratory tests in terms of clogging performance, except geotextile W3 tested with RAP and geotextile W1 tested with FS, considering both stabilized K_R and GR values (Table 3.2). Table 3.5 summarizes the predictions for the anti-clogging criteria. Based on the estimated reduction in pore sizes from the long-term filtration tests, it appears that the criteria based on O_{15} and O_{50} (Millar et al. 1980; Fischer et al. 1990) provide better prediction than the criterion based on O_{95}. These findings agree with the laboratory and model-based measurements of Aydilek (2006) that the controlling geotextile pore sizes for clogging are generally small and range between O_{15} and O_{50}. Figure 3.9 and Figure 3.10 summarizes these predictions.

Table 3.4 Predictions of the existing retention criteria for the recycled materials tested-geotextile systems

Recycled Material	Geotextile	Performance observed in laboratory tests	Calhoun(1972) $O_{95}/D_{85} \le 1$			Carroll (1983) $O_{95}/D_{85} \le 2\text{-}3$			Christopher and Holtz (1985) $O_{95}/D_{85} \le 1.8$			Giroud (1982) $O_{95}/D_{50} \le (9\text{-}18)/Cu$		
			W1	W2	W3	W1	W2	W3	W1	W2	W3	W1	W2	W3
RCA-1	W1	Retention	Pass	Pass	Pass	Pass	Pass	Pass	Pass	Pass	Pass	Pass	Pass	Pass
	W2	Retention												
	W3	Retention												
RCA-2	W1	Retention	Pass	Pass	Pass	Pass	Pass	Pass	Pass	Pass	Pass	Pass	Pass	Pass
	W2	Retention												
	W3	Retention												
RAP	W1	Retention	Pass	Pass	Pass	Pass	Pass	Pass	Pass	Pass	Pass	Pass	Pass	Pass
	W2	Retention												
	W3	Retention												
FS	W1	Retention	Fail	Fail	Pass	Pass	Pass	Pass	Pass	Fail	Pass	Pass	Pass	Pass
	W2	Retention												
	W3	Retention												
RAS	W1	Retention	Pass	Pass	Pass	Pass	Pass	Pass	Pass	Pass	Pass	Pass	Pass	Pass
	W2	Retention												
	W3	Retention												

Pass=Retention, Fail=Piping

Table 3.4 Predictions of the existing retention criteria for the recycled materials tested-geotextile systems (continued)

Recycled Material	Geotextile	Performance observed in laboratory tests	Ogink (1975) $O_{90} / D_{90} \leq 1$			Schoeber & Teindl (1979) $O_{90} / D_{50} \leq 2.5\text{-}4.5$			Fisher (1994) $O_{85} / D_{75} \leq 2$			Miller et al (1980) $O_{50} / D_{85} \leq 1$		
			W1	W2	W3	W1	W2	W3	W1	W2	W3	W1	W2	W3
RCA-1	W1	Retention	Pass	Pass	Pass	Pass	Pass	Pass	Pass	Pass	Pass	Pass	Pass	Pass
	W2	Retention												
	W3	Retention												
RCA-2	W1	Retention	Pass	Pass	Pass	Pass	Pass	Pass	Pass	Pass	Pass	Pass	Pass	Pass
	W2	Retention												
	W3	Retention												
RAP	W1	Retention	Pass	Pass	Pass	Pass	Pass	Pass	Pass	Pass	Pass	Pass	Pass	Pass
	W2	Retention												
	W3	Retention												
FS	W1	Retention	Fail	Fail	Pass	Pass	Pass	Pass	Pass	Pass	Pass	Fail	Fail	Pass
	W2	Retention												
	W3	Retention												
RAS	W1	Retention	Pass	Pass	Pass	Pass	Pass	Pass	Pass	Pass	Pass	Pass	Pass	Pass
	W2	Retention												
	W3	Retention												

Pass=Retention, Fail=Piping

Table 3.5 Predictions of the existing anti-clogging criteria for the recycled materials tested-geotextile systems

Recycled Material	Geotextile	Performance observed in laboratory tests	Christopher and Holtz (1985) $O_{95}/D_{15} > 3$			French Committee on Geotextiles and Geomembranes (1986) $O_{90}/D_{15} > 4$			Millar et al (1980) $O_{50}/D_{15} > 1$			Fischer et al (1990) $O_{15}/D_{15} > 0.8\text{-}1$		
			W1	W2	W3	W1	W2	W3	W1	W2	W3	W1	W2	W3
RCA-1	W1	Not Clogged	Fail	Fail	Fail	Fail	Fail	Fail	Pass	Pass	Pass	Pass	Pass	Pass
	W2	Not Clogged												
	W3	Not Clogged												
RCA-2	W1	Not Clogged	Fail	Fail	Fail	Fail	Fail	Fail	Fail	Pass	Fail	Pass	Pass	Fail
	W2	Not Clogged												
	W3	Not Clogged												
RAP	W1	Not Clogged	Fail	Fail	Fail	Fail	Fail	Fail	Fail	Fail	Fail	Fail	Fail	Fail
	W2	Not Clogged												
	W3	Clogged												
FS	W1	Clogged	Fail	Pass	Fail	Fail	Fail	Fail	Pass	Pass	Pass	Pass	Pass	Pass
	W2	Not Clogged												
	W3	Not Clogged												
RAS	W1	Not Clogged	Fail	Fail	Fail	Fail	Fail	Fail	Fail	Fail	Fail	Fail	Pass	Fail
	W2	Not Clogged												
	W3	Not Clogged												

Pass=Retention, Fail=Piping

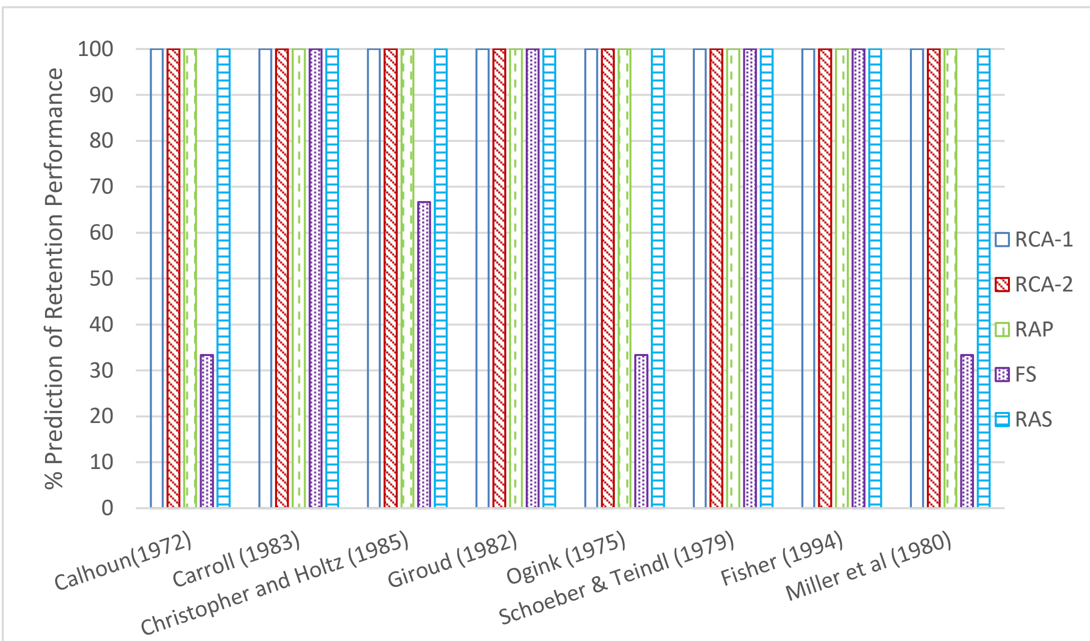

Figure 3.9 Predictions of existing retention criteria

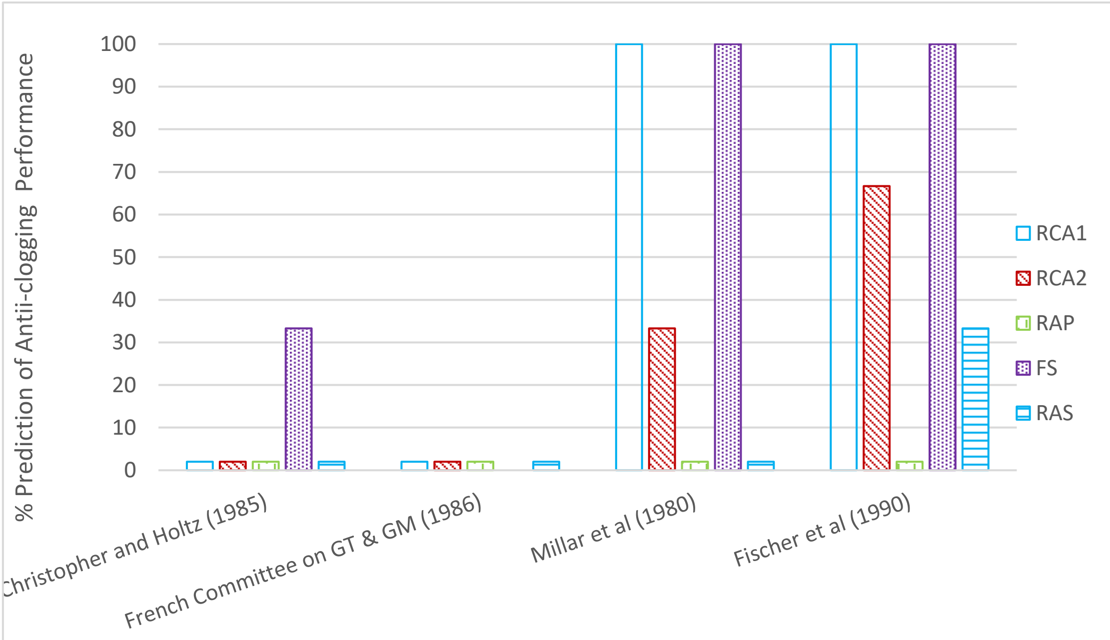

Figure 3.10 Predictions of existing anti-clogging criteria

Chapter 4

Results of Laboratory Study of Filtration by Nonwoven Geotextiles

4.1. *Clogging Behavior*

4.1.1. Long-Term Filtration Test Results

The results of the long-term filtration tests performed using nonwoven geotextiles (NW1, NW2, and NW3) are presented in Tables 4.1 and 4.2. Review of the data shows that RAP tested with all nonwoven textiles and RAS tested with NW3 would be considered clogged based on the criterion that sets G_R of 3 as the limit. A similar analysis in order to compare two commonly used clogging ratios, as conducted for woven geotextiles in Chapter 3, can be performed here as well. For example, stabilized soil and system permeabilities of 3.4 x 10^{-5} cm/sec and 3.3 x 10^{-5} cm/sec, respectively, were measured for geotextile NW3 tested with RCA-1 under a hydraulic gradient of 1.0. The ratio of those two permeabilities (K_R) is 1.0, which is below the limit set for clogging (i.e., K_R of 3) and indicates minimal impedance of flow through system. However, the gradient ratio is 2.1, which clearly indicates clogging according to the ASTM D5101 criterion. Similarly, geotextile NW1 tested with RAP had a stabilized soil permeability of 5.3 x 10^{-3} cm/sec under a hydraulic gradient of 1.0 with a corresponding system permeability of 2.1 x 10^{-3} cm/sec.

Table 4.1 Results of the long-term filtration tests with nonwoven geotextiles

Recycled Material	Geotextile	Piping Rate (g/m^2)	K_{system} (cm/sec)	K_{soil} (cm/sec)	$K_R = k_{soil}/k_{system}$	Gradient Ratio (G_R)
RCA-1	NW1	57				
	i=1.0		1.5×10^{-5}	9.3×10^{-6}	0.6	0.4
	i=2.5		1.3×10^{-5}	8.2×10^{-6}	0.6	0.5
	i=5.0		2.3×10^{-5}	1.4×10^{-5}	0.6	0.4
	NW2	22				
	i=1.0		3.3×10^{-5}	3.4×10^{-5}	1.0	2.1
	i=2.5		4.2×10^{-5}	4.3×10^{-5}	1.0	2.0
	i=5.0		3.5×10^{-5}	3.6×10^{-5}	1.0	2.1
	NW3	209				
	i=1.0		2.2×10^{-5}	1.1×10^{-5}	0.5	0.1
	i=2.5		5.1×10^{-5}	2.7×10^{-5}	0.5	0.1
	i=5.0		4.8×10^{-5}	2.9×10^{-5}	0.6	0.4
RCA-2	NW1	96				
	i=1.0		1.8×10^{-4}	1.1×10^{-4}	0.6	0.2
	i=2.5		1.5×10^{-4}	8.9×10^{-5}	0.6	0.2
	i=5.0		1.1×10^{-4}	6.5×10^{-5}	0.6	0.2
	NW2	19				
	i=1.0		7.5×10^{-4}	4.9×10^{-4}	0.7	0.2
	i=2.5		7.9×10^{-4}	4.9×10^{-4}	0.6	0.2
	i=5.0		3.6×10^{-4}	1.9×10^{-4}	0.5	0.1
	NW3	57				
	i=1.0		2.3×10^{-4}	1.5×10^{-4}	0.6	0.5
	i=2.5		1.4×10^{-4}	8.4×10^{-5}	0.6	0.5
	i=5.0		9.9×10^{-5}	6.1×10^{-5}	0.6	0.4
RAP	NW1	119				
	i=1.0		2.1×10^{-3}	5.3×10^{-3}	2.5	44.2
	i=2.5		2.3×10^{-3}	6.0×10^{-3}	2.6	46.8
	i=5.0		7.8×10^{-4}	2.0×10^{-3}	2.6	49.9
	NW2	19				
	i=1.0		8.5×10^{-3}	5.0×10^{-2}	5.8	20.2
	i=2.5		4.4×10^{-3}	4.0×10^{-2}	9.0	32.6
	i=5.0		2.9×10^{-3}	3.3×10^{-2}	11.4	42.5
	NW3	35				
	i=1.0		1.5×10^{-3}	8.4×10^{-3}	5.4	14.8
	i=2.5		3.4×10^{-4}	6.6×10^{-3}	19.5	70.8
	i=5.0		3.2×10^{-4}	3.1×10^{-3}	10.0	35.3

Table 4.1. Results of the long-term filtration tests with nonwoven geotextiles (continued)

Recycled Material	Geotextile	Piping Rate (g/m^2)	K_{system} (cm/sec)	K_{soil} (cm/sec)	$K_R = k_{soil}/k_{system}$	Gradient Ratio (G_R)
FS	NW1	17				
	i=1.0		4.4×10^{-7}	2.3×10^{-7}	0.5	0.02
	i=2.5		5.3×10^{-7}	2.7×10^{-7}	0.5	0.01
	i=5.0		1.1×10^{-5}	8.2×10^{-6}	0.8	0.64
	NW2	NA				
	i=1.0		NA	NA	NA	NA
	i=2.5		NA	NA	NA	NA
	i=5.0		NA	NA	NA	NA
	NW3	NA				
	i=1.0		NA	NA	NA	NA
	i=2.5		NA	NA	NA	NA
	i=5.0		NA	NA	NA	NA
RAS	NW1	10				
	i=1.0		4.4×10^{-3}	8.0×10^{-3}	1.8	0.4
	i=2.5		1.8×10^{-3}	3.6×10^{-3}	2.0	0.2
	i=5.0		3.4×10^{-4}	9.2×10^{-4}	2.7	0.3
	NW2	3				
	i=1.0		3.1×10^{-3}	5.08×10^{-3}	1.7	0.8
	i=2.5		1.6×10^{-3}	2.91×10^{-3}	1.8	0.5
	i=5.0		3.2×10^{-4}	4.25×10^{-4}	1.3	0.4
	NW3	5				
	i=1.0		1.2×10^{-3}	1.63×10^{-3}	1.4	1.0
	i=2.5		7.7×10^{-4}	1.78×10^{-3}	2.3	0.7
	i=5.0		4.1×10^{-4}	1.38×10^{-3}	3.4	0.5

NA: Test not performed.

The ratio of those two permeabilities (K_R) is 2.5, which is below the limit set for clogging; however, the gradient ratio is 44.2, which again indicates severe clogging.

All geotextile-soil combinations indicated acceptable performance based on their K_R ratios except NW2 and NW3 tested with RAP where K_R ratios were 11.4 and 10, respectively. Furthermore, NW3 tested with RAS started clogging after 1000 hours with a stabilized K_R of 3.4.

The clogging performance of the recycled material-geotextile combinations were also verified by permittivity ratios (Ψ_R) summarized in Table 4.2. Review of data indicates that average reduction in flow is in a range of 2% to 27%. Majority of Ψ_R is measured around 1.0, which indicates geotextiles remained unclogged.

The only exception is the performance observed during testing with RAP. A 21-27% reduction in flow is observed for these combinations, corresponding to Ψ_R of 0.73-0.79, slightly below the limit of 0.8 set as the permittivity ratio criterion for clogging. Also, this reduction for RAP corresponds to mean hydraulic conductivity of 1.3×10^{-2} cm/sec which is still higher than the hydraulic conductivity of clean uniform sand ($k=1 \times 10^{-3}$ cm/sec, Coduto et al. 2010) and within one order of magnitude of the range for fine to medium coarse sands ($k=10^{-3}$ cm/sec to 10^{-1} cm/sec, Holtz et al. 2011). Thus, such drop-in permittivity would be acceptable for filtering RAP providing that clogged geotextile still allows sufficient flow.

Temporal characteristics of system permeabilities and K_R are given in Figure 4.1, Figure 4.2 and Figure 4.3. Three different hydraulic gradients (i=1.0, i=2.5, i=5.0) were applied and FS was only tested with NW1 due to the difficulties in

Table 4.2 Summary of long term filtration tests

Recycled Materials	Permittivity Ratio, Ψ_R			Permeability Ratio*, K_R			Gradient Ratio* G_R			Piping Rate (g/m^2)		
	NW1	**NW2**	**NW3**	**NW1**	**NW2**	**NW3**	**NW1**	**NW2**	**NW3**	**NW1**	**NW2**	**NW3**
RCA-1	0.91	0.98	0.93	0.6	1.0	0.6	0.4	2.1	0.4	57	22	209
RCA-2	0.93	0.97	0.92	0.6	0.5	0.6	0.2	0.1	0.4	96	19	57
RAP	0.74	0.79	0.73	2.6	11.4	10.0	49.9	42.5	35.3	119	19	35
FS	NA	NA	NA	0.8	NA	NA	0.8	NA	NA	17	NA	NA
RAS	0.92	0.97	0.95	2.7	1.3	3.4	2.7	1.3	3.4	10	3	5

*Reported clogging values are the stabilized values at the end of testing. NA: Test not performed.

measuring its low hydraulic conductivity. The data in Figures 4.1-4.3 show that K_R ratios for RCA-1, RCA-2 and FS stay in a range of 0.5 to 1.0 which is an indicator of a good compatibility. On the other hand, poor hydraulic compatibility can be observed between the geotextiles and RAP-NW2-NW3 and RAS-NW3.

An analysis, similar to the one performed for woven geotextiles in Chapter 3, was conducted in order to identify the flow patterns for the nonwoven geotextiles. Three distinct flow patterns can be observed in Figures 4.1- 4.3, similar to the behavior described by Gabr and Akram (1996). A review of data shows that both RCAs exhibit normal behavior when tested with all three nonwoven geotextiles.

RAP tested with NW1 and NW2 experienced blocking/blinding pattern starting from the beginning of the test. The system permeabilities for these tests decrease from 1.0 x 10^{-2} cm/sec to 7.5 x 10^{-3} cm/sec and 1.8 x 10^{-2} cm/sec to 2.7 x 10^{-3} cm/sec, for NW1 and NW2, respectively. The corresponding increase in K_R is from 2.3 to 2.7 and from 2.95 to 11.9. Similar behavior is observed with RAS when tested with NW1 and NW3. The system permeabilities decrease from 1.5 x 10^{-2} to 3.2 x 10^{-4} cm/sec and from 5.1 x 10^{-3} to 3.5 x 10^{-4} cm/sec, for NW1 and NW3, respectively. Also, the corresponding increase in K_R is from 1.0 to 2.9 and from 0.9 to 3.9. A mixed behavior can be observed for RAP when tested with NW3 where system permeability slightly decreases in first 400 hours then increases where a possible filter cake starts to form then it stabilizes at 3.2 x 10^{-4} cm/sec. A piping behavior is observed with NW1 when tested with FS. The system permeability increases from 4.4 x 10^{-7} to 8.2 x 10^{-6} cm/sec.

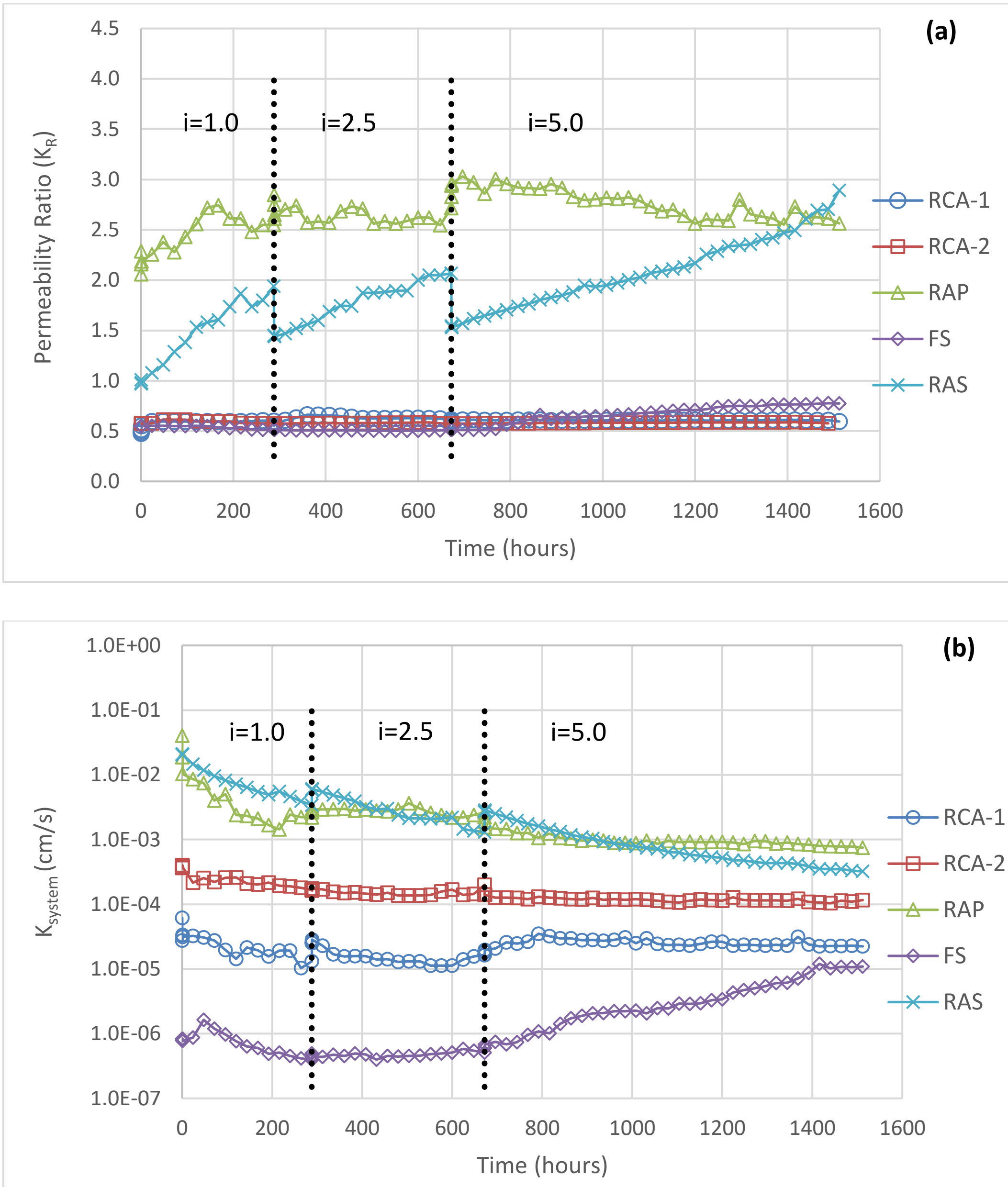

Figure 4.1 Permeability ratio versus time relationship for NW1 (a), System Permeability versus time relationship for NW1 (b)

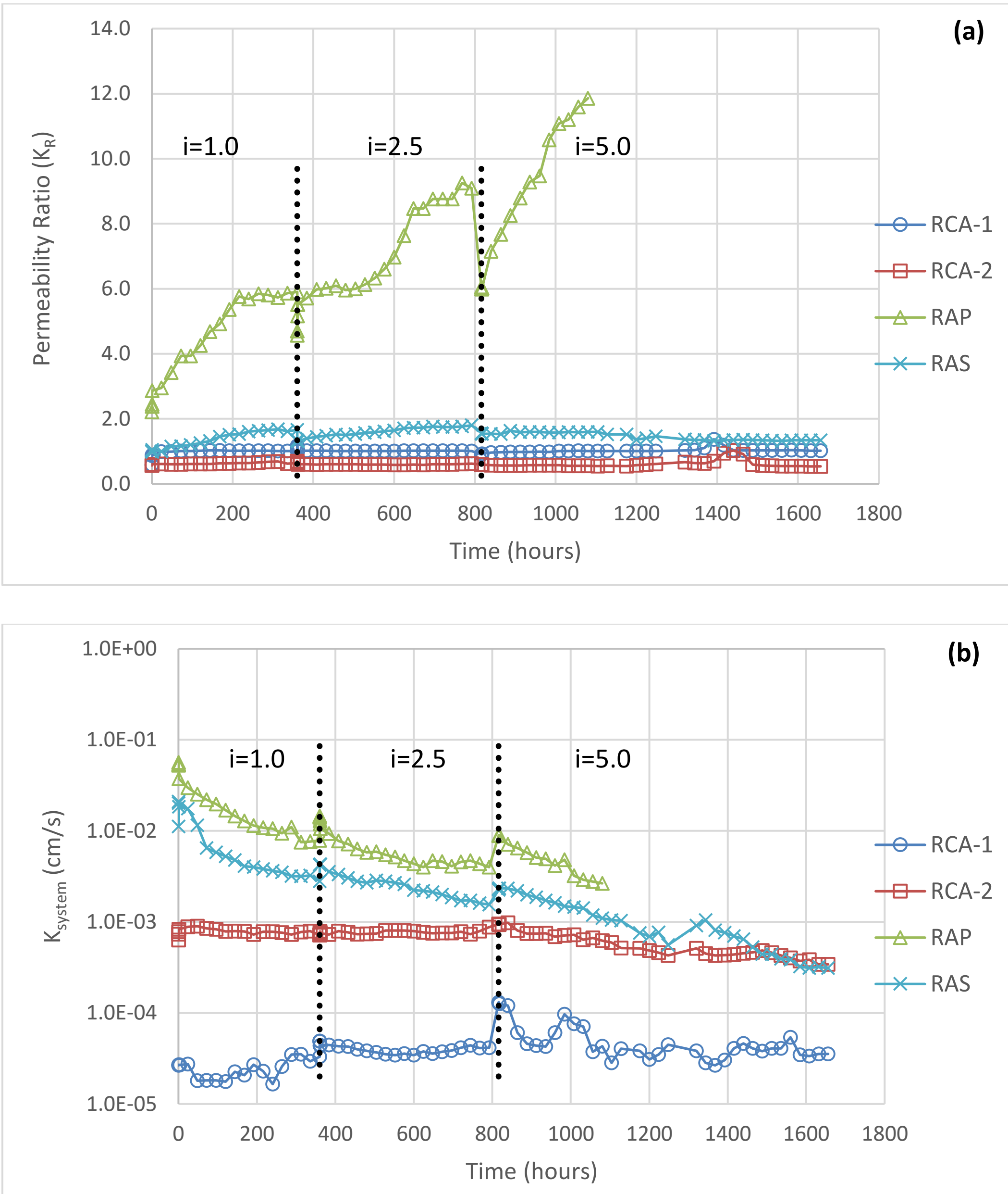

Figure 4.2 Permeability ratio versus time relationship for NW2 (a), System Permeability versus time relationship for NW2 (b)

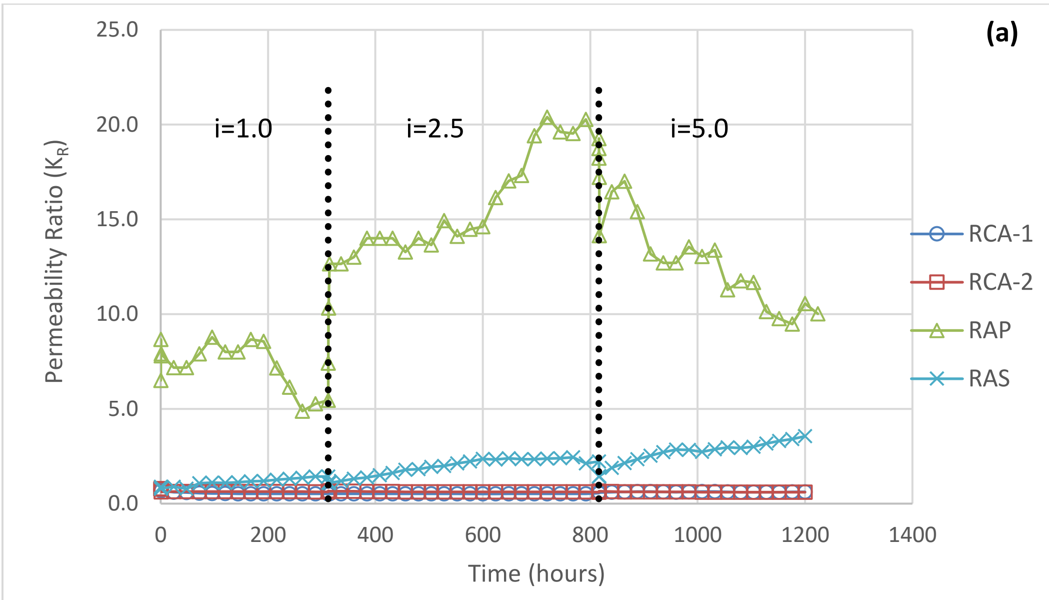

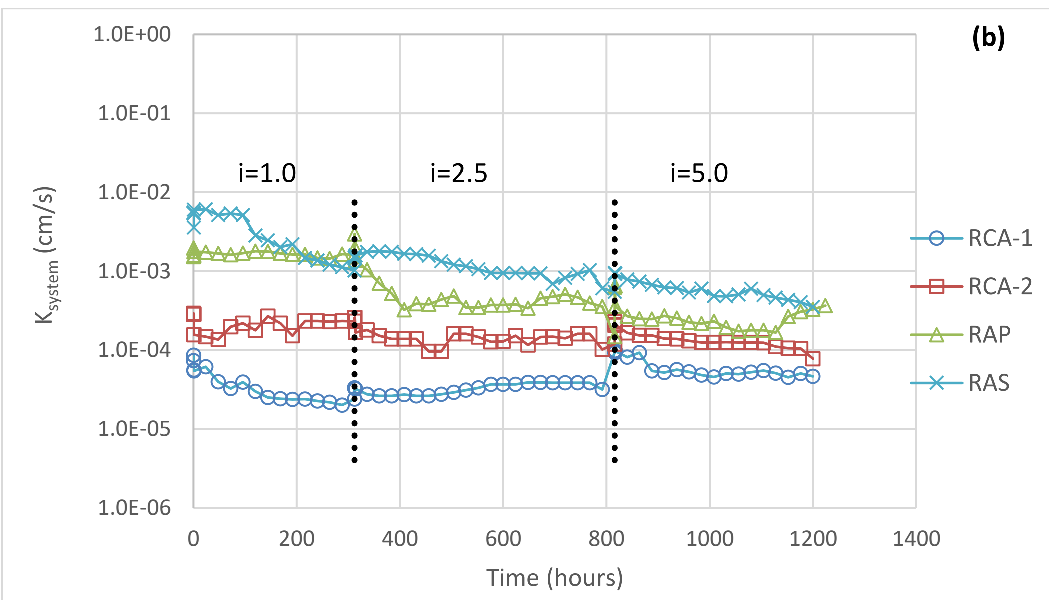

Figure 4.3 Permeability ratio versus time relationship for NW3 (a), System Permeability versus time relationship for NW3 (b)

Stabilized values of the permeability ratio are plotted versus each applied hydraulic gradient in Figure B1. K_R values for RAP and RAS seem to be affected from the increase in applied hydraulic gradient. There is a gradual but inconsistent increase in K_R with increasing hydraulic gradient for these two materials; however, a clear-cut trend cannot be observed for others. K_R is generally lower than the limit of 3, except two cases with RAP, indicating that the partial clogging of the geotextiles does not have a significant effect on the overall filtration performance of the systems evaluated.

4.1.2. Effect of Geotextile Pore Structure on the Clogging Performance

Two clogging ratios (K_R and Ψ_R) are plotted versus permittivity of virgin geotextiles in Figure 4.4. Both K_R and Ψ_R seem to be minimally affected from the increase in permittivity of virgin geotextile. The rate of change in Ψ_R is even smaller compared to K_R and the observed changes in both cases are inconsistent. Attempts made to relate the permeability to three characteristic pore opening sizes of a geotextile (O_{95}, O_{90} and O_{50}) in contact with the industrial by-products yielded no clear-cut trends (Figure B2).

4.2. *Retention Behavior*

The amount of soil piped through the geotextiles in all soil-geotextile combinations is in a range of 3 to 209 g/m^2 (Table 4.2). Geotextile NW1 piped the most; however, the piped amount (209 g/m^2) is still less than 2,500 g/m^2, an internal stability limit typically used for granular and geotextile filters (Lafleur et al. 1989, Bhatia et al.

1996, Aydilek and Edil 2002, Kutay and Aydilek 2005). It should be noted that geotextile NW1 has considerably higher permittivity (2.1 sec^{-1}) than the other woven geotextiles. The piping rates tend to be higher for the soils with higher fines content.

Upon termination of each filtration test, post testing sieve analyses were performed on the samples collected from different depths in the permeameters (i.e., 0-25; upper layer of 25 mm, 25-75; middle layer of 50 mm, 75-94; lower layer of 19 mm, 94-100; bottom layer of 6 mm above the geotextile) and compared to the grain size distribution (GSD) of the virgin recycled material.

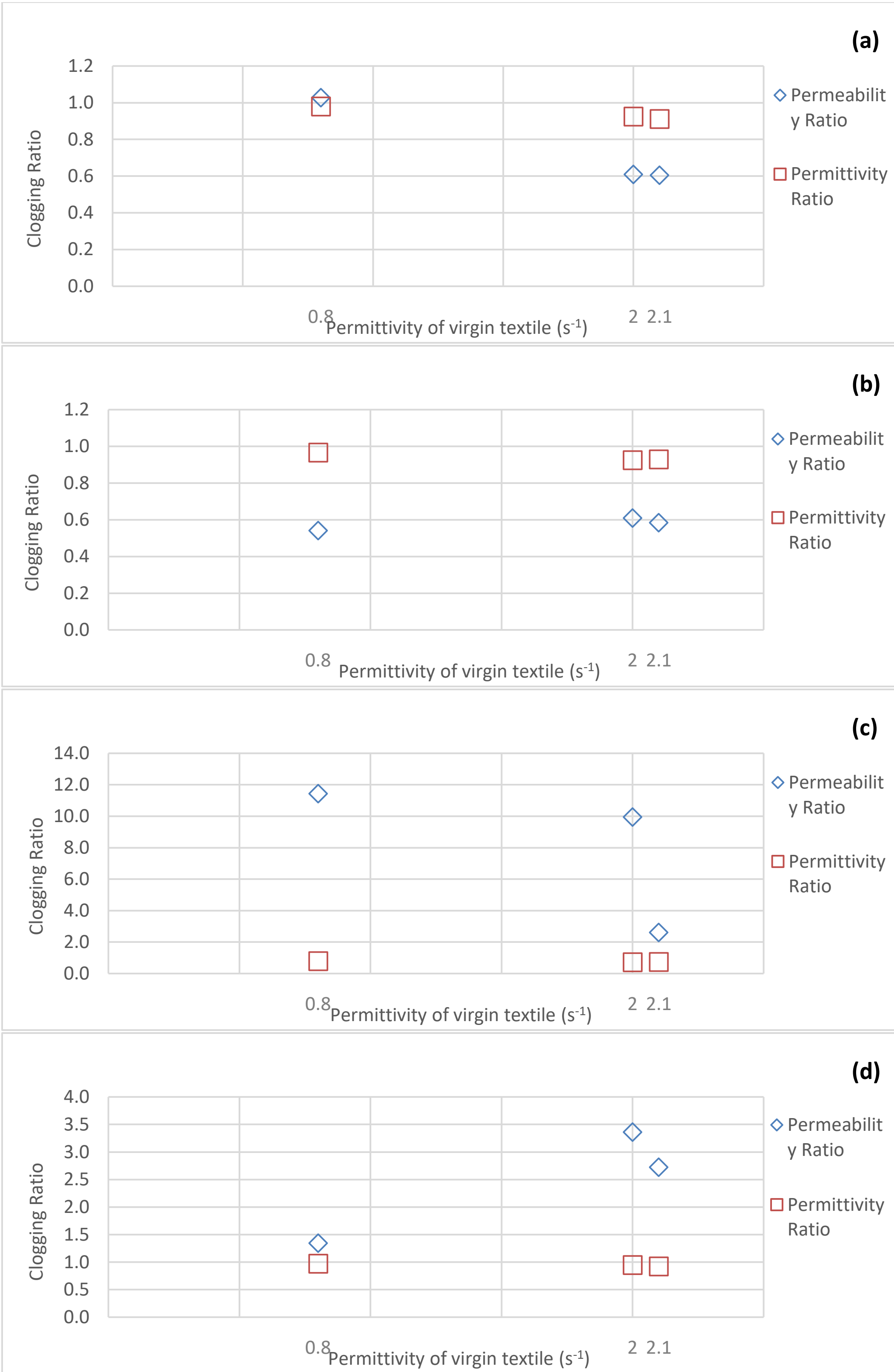

Figure 4.4 Clogging ratios versus virgin geotextile permittivity RCA-1 (a), and for RCA-2 (b), RAP (c), RAS (d)

The shifts in GSD of the recycled material-geotextile combinations are generally comparable with the measured piping rates. Figure 4.5 is given as an example to show such changes in grain size distribution curves for RCA-2 upon testing with NW1 and NW2. Considering the layers immediately above the geotextile filter where graded filter zone forms (i.e., 75-94 mm and 94-100 mm), the shift from the virgin material grain size distribution is more clearly pronounced for NW1 (Ψ= 2.1 s^{-1}) as compared to NW2 (Ψ=0.8 s^{-1}) due to higher a piping rate measured for NW1 (96 g/m^2 versus 19 g/m^2). GSD of soil-geotextile interface (94-100 mm) shifts to the right in most cases as compared to the GSD of the virgin material for woven geotextiles, suggesting that accumulation of soil fines has occurred at this interface (Figure B4 and Figure B5).

To illustrate the effect of pore structure on piping rate, piping rates are plotted versus permittivity and two commonly used retention ratios, O_{95}/D_{85}, O_{50}/D_{50} in Figure 4.6. Piping rate generally increases with the increasing permittivity, as permittivity is an important geotextile pore structure parameter that controls retention performance (Kutay and Aydilek 2004, Fatema and Bhatia 2018). Krug et al. (2000) also reported increased piping rate when tested with needle-punched geotextiles. A review of data in Figure 4.6 shows that piping ratio increases with increasing O_{50}/D_{50} and O_{95}/D_{85} for the materials tested, except RAS. This is somewhat consistent with the findings of Aydilek and Edil (2008) where they also reported that for nonwoven geotextiles, piping rate increased with the increasing $O_{50}/D_{50;}$ however, they have reported a lack of trend between piping and $O_{95}/D_{85.}$

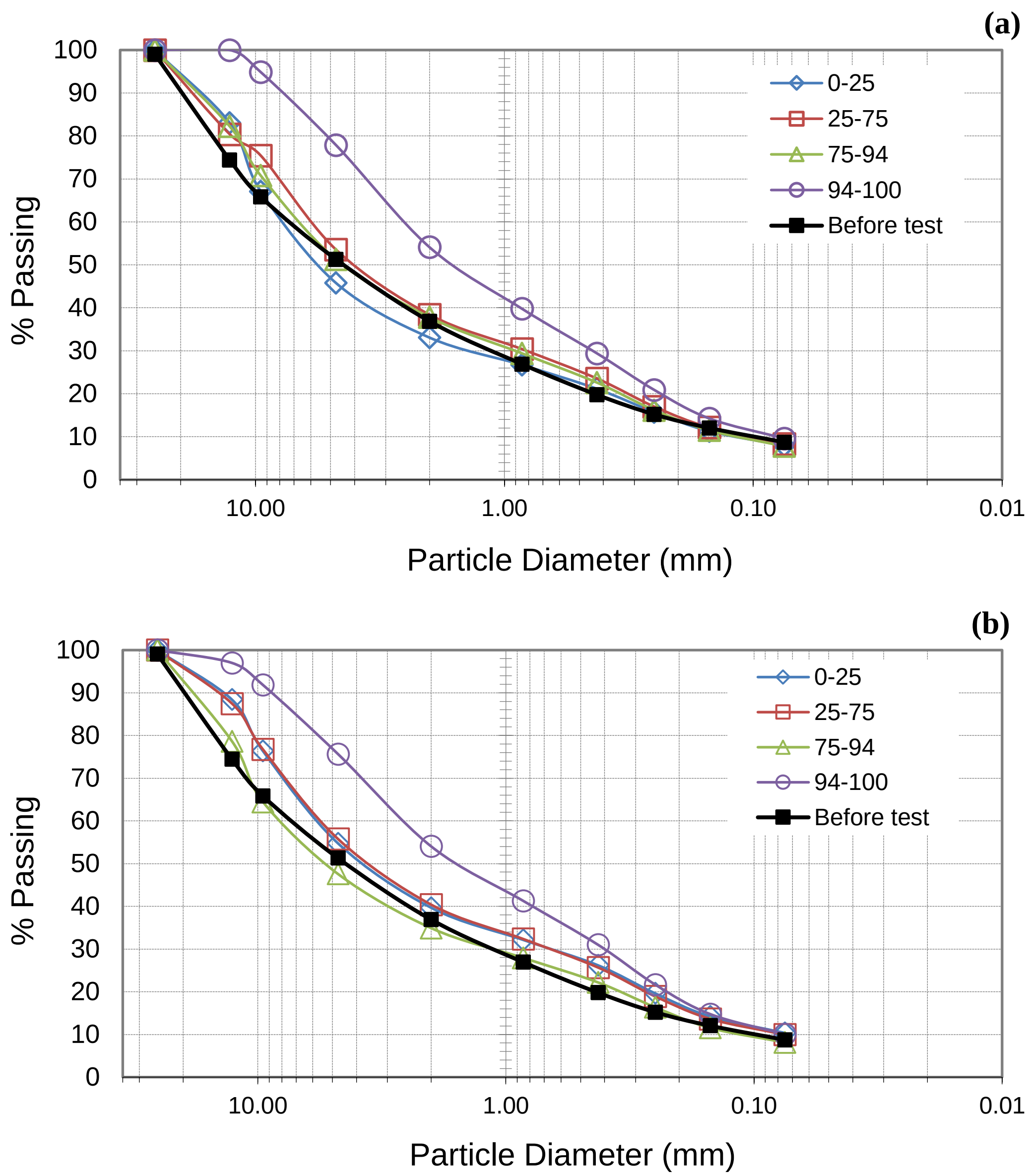

Figure 4.5 Grain size distribution of the RCA-2 samples tested with NW1 (a), tested with NW2 (b)

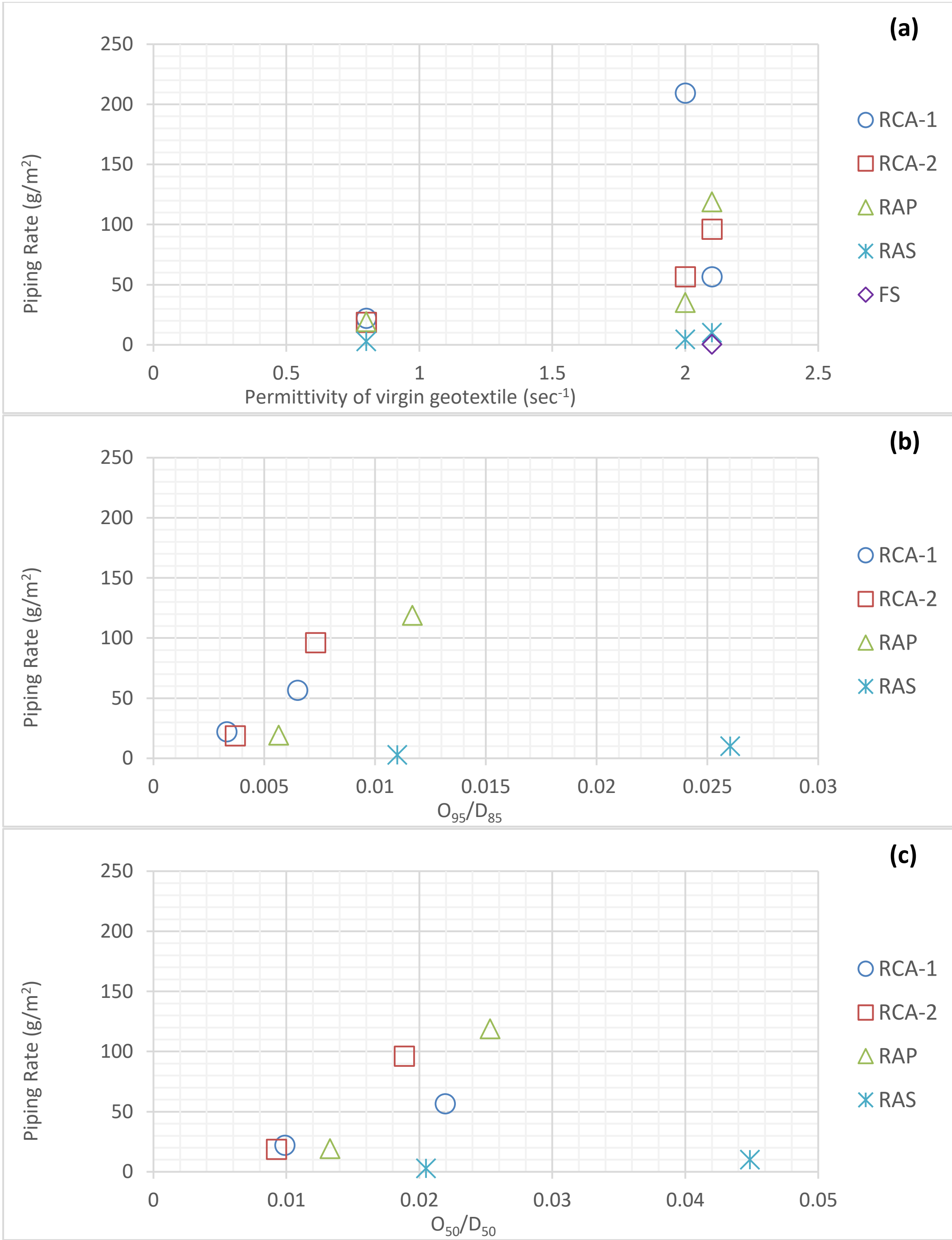

Figure 4.6 Piping rates versus virgin geotextile permittivity of virgin geotextile (a), Piping rates versus virgin geotextile O_{95}/D_{85} (b), Piping rates versus virgin geotextile O_{50}/D_{50} (c)

Piping rates are also plotted versus commonly used geotextile characteristic pore opening sizes (i.e., O_{95}, O_{90}, O_{50}) in Figure B3. The data clusters around two data points; however, higher piping seems to be present with an increase in O_{95}, O_{90} or O_{50}, again consistent with the findings of Aydilek and Edil (2008).

4.3. *Post Long-term Filtration test – Analysis of Pore Structure Change of Geotextiles*

The nonwoven geotextiles subjected to long-term filtration tests were analyzed using image analysis to determine the changes in their characteristic pore opening sizes (i.e., O_{90}, O_{50}). The shifts in PSDs are shown in Figure 4.7. Characteristic pore opening sizes (e.g., O_{95}, O_{60}, O_{50}, O_{40}, O_{30}, O_{15}, and O_{10}) of the post-filtration test geotextile decrease in all cases, indicating that clogging did not affect a single parameter. Percent reduction in pore sizes in two characteristic sizes, O_{95} and O_{50}, after laboratory tests also summarized in Table 4.3. Two characteristic pore sizes of the nonwoven geotextile (NW3 is not tested), O_{95} and O_{50}, decrease by 33-46%, 9-23%, respectively. An example collage of planar images of NW2 before and after subjected to filtration tests with RCA-2 are shown in Figure 4.8. The images clearly show the particle accumulation within the nonwoven geotextiles. Similar particle accumulations were observed for other recycled materials tested but not shown herein brevity.

4.4. *Applicability of Existing Filter Selection Criteria*

The clogging ratios obtained from the long-term filtration tests and PSDs from image analyses were used in order to determine the applicability of widely utilized

Table 4.3 Change in the O_{95} and O_{50} of the geotextiles subjected to filtration testing

Name of geotextile	Characteristic pore size	Measured pore size of virgin geotextile (mm)	Percent Reduction in Measured pore size of geotextile (%)				
			RCA-1	**RCA-2**	**RAP**	**FS**	**RAS**
NW1	O_{95}	0.19	44	37	35	35	33
	O_{50}	0.12	18	18	18	12	15
NW2	O_{95}	0.10	46	40	40	NA	46
	O_{50}	0.06	23	15	9	NA	19
NW3	O_{95}	NA	NA	NA	NA	NA	NA
	O_{50}	NA	NA	NA	NA	NA	NA

NA: Test not performed.

current geotextile filtration criteria to the recycled materials tested. Tables 4.4 and 4.5 compare the predictions of the existing filter criteria and the actual performance observed in the laboratory tests.

Table 4.4 summarizes that existing retention criteria predicted all of the tests correctly. All geotextile-recycled material test combinations performed well and did not experience significant piping. It should be noted that geotextile NW3 was not tested because it is commonly used as a part of geocomposites and subjected to filtration tests by placing double layer of the geotextile to simulate the vertical flow through the geocomposite. All geotextiles performed successfully in the laboratory tests in terms of clogging performance, except geotextile NW2 tested with RAP. Table 4.5 summarizes the predictions for the anti-clogging criteria. However, existing criteria for anti-clogging of a geotextile failed to predict observed performance for almost all cases except NW2 tested with RAP. The recycled materials tested have different nature than earthen materials, therefore existing geotextile selection criteria may not be directly applicable to these materials and, in most cases, their filtration or drainage performance with geotextiles should be investigated by conducting laboratory tests (Aydilek and Edil 2008).

Table 4.4 Predictions of the existing retention criteria for the recycled materials tested-geotextile systems

Recycled Material	Geotextile	Performance observed in laboratory tests	Calhoun (1972) O95/D85 ≤ 1		Carroll (1983) O95/D85 ≤ 2-3		Christopher and Holtz (1985) O95/D85 ≤ 1.8		Giroud (1982) O95/D50 ≤ (9-18)/Cu	
			NW1	NW2	NW1	NW2	NW1	NW2	NW1	NW2
RCA1	NW1	Retention	Pass	Pass	Pass	Pass	Pass	Pass	Pass	Pass
	NW2	Retention								
RCA2	NW1	Retention	Pass	Pass	Pass	Pass	Pass	Pass	Pass	Pass
	NW2	Retention								
RAP	NW1	Retention	Pass	Pass	Pass	Pass	Pass	Pass	Pass	Pass
	NW2	Retention								
FS	NW1	Retention	Pass	Pass	Pass	Pass	Pass	Pass	Pass	Pass
	NW2	Retention								
RAS	NW1	Retention	Pass	Pass	Pass	Pass	Pass	Pass	Pass	Pass
	NW2	Retention								

Pass=Retention, Fail=Piping

Table 4.4 Predictions of the existing retention criteria for the recycled materials tested-geotextile systems (continued)

Recycled Material	Geotextile	Performance observed in laboratory tests	Ogink (1975) O90/D90 ≤ 1		Schoeber & Teindl (1979) O90/D50 ≤ 2.5-4.5		Fisher (1994) O85/D75 ≤ 2		Miller et al (1980) O50/D85 ≤ 1	
			NW1	NW2	NW1	NW2	NW1	NW2	NW1	NW2
RCA1	NW1	Retention	Pass	Pass	Pass	Pass	Pass	Pass	Pass	Pass
	NW2	Retention								
RCA2	NW1	Retention	Pass	Pass	Pass	Pass	Pass	Pass	Pass	Pass
	NW2	Retention								
RAP	NW1	Retention	Pass	Pass	Pass	Pass	Pass	Pass	Pass	Pass
	NW2	Retention								
FS	NW1	Retention	Pass	Pass	Pass	Pass	Pass	Pass	Pass	Pass
	NW2	Retention								
RAS	NW1	Retention	Pass	Pass	Pass	Pass	Pass	Pass	Pass	Pass
	NW2	Retention								

Pass=Retention, Fail=Piping

Table 4.5 Predictions of the existing anti-clogging criteria for the recycled materials tested-geotextile systems

Recycled Material	Geotextile	Performance observed in laboratory tests	Christopher and Holtz (1985) O95/D15 > 3		French Committee on Geotextiles and Geomembranes (1986) O90/D15 >4		Millar et al (1980) O50/D15 > 1		Fischer et al (1990) O15/D15 > 0.8-1	
			NW1	NW2	NW1	NW2	NW1	NW2	NW1	NW2
RCA1	NW1	Not Clogged	Fail	Fail	Fail	Fail	Fail	Fail	Fail	Fail
	NW2	Not Clogged								
RCA2	NW1	Not Clogged	Fail	Fail	Fail	Fail	Fail	Fail	Fail	Fail
	NW2	Not Clogged								
RAP	NW1	Not Clogged	Fail	Fail	Fail	Fail	Fail	Fail	Fail	Fail
	NW2	Clogged								
FS	NW1	Not Clogged	Fail	Fail	Fail	Fail	Fail	Fail	Fail	Fail
	NW2	Not Clogged								
RAS	NW1	Not Clogged	Fail	Fail	Fail	Fail	Fail	Fail	Fail	Fail
	NW2	Not Clogged								

Pass=Not Clogged, Fail= Clogged

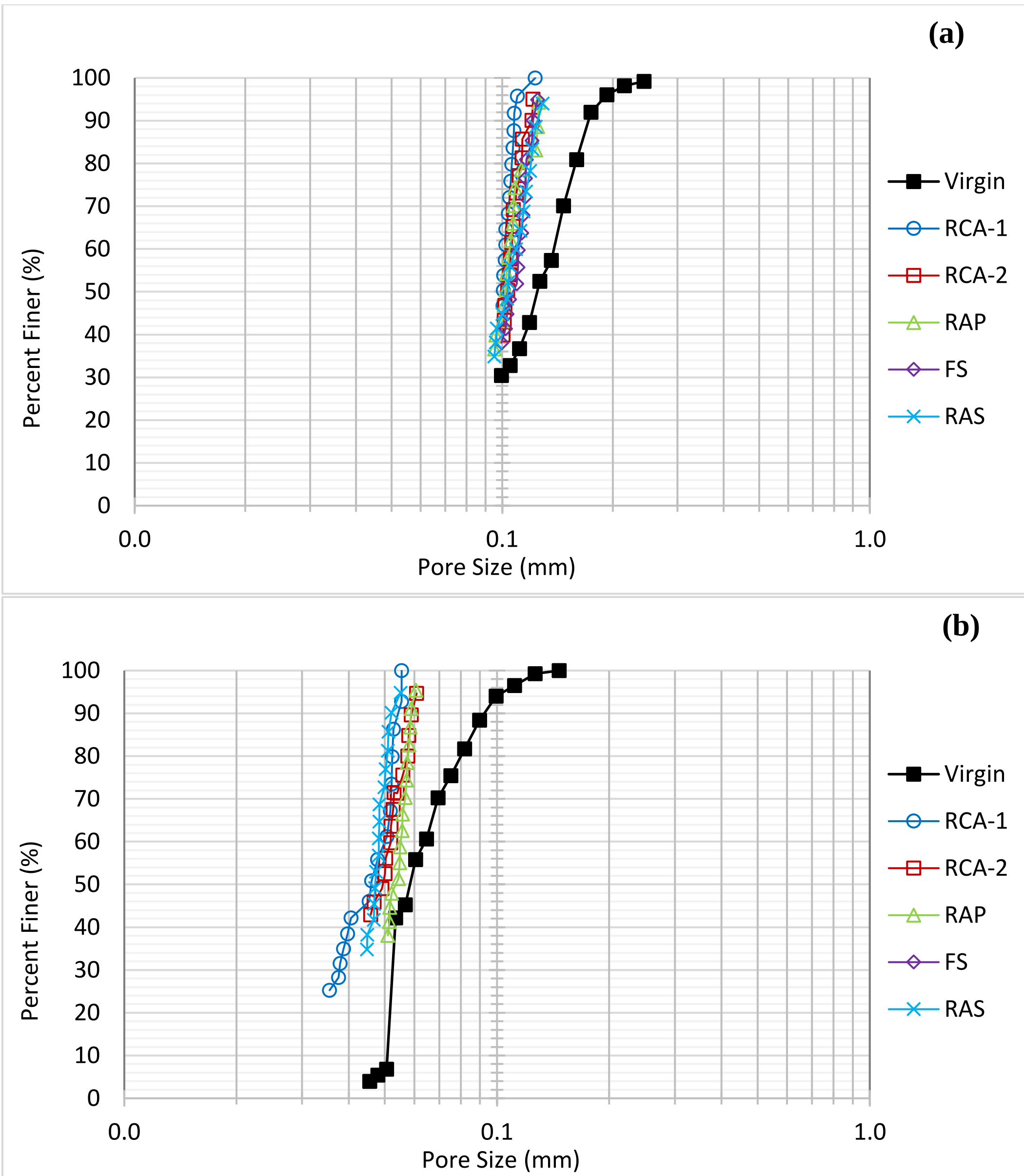

Figure 4.7 Change in PSD of geotextiles before and after filtration tests; NW1 (a), NW2 (b)

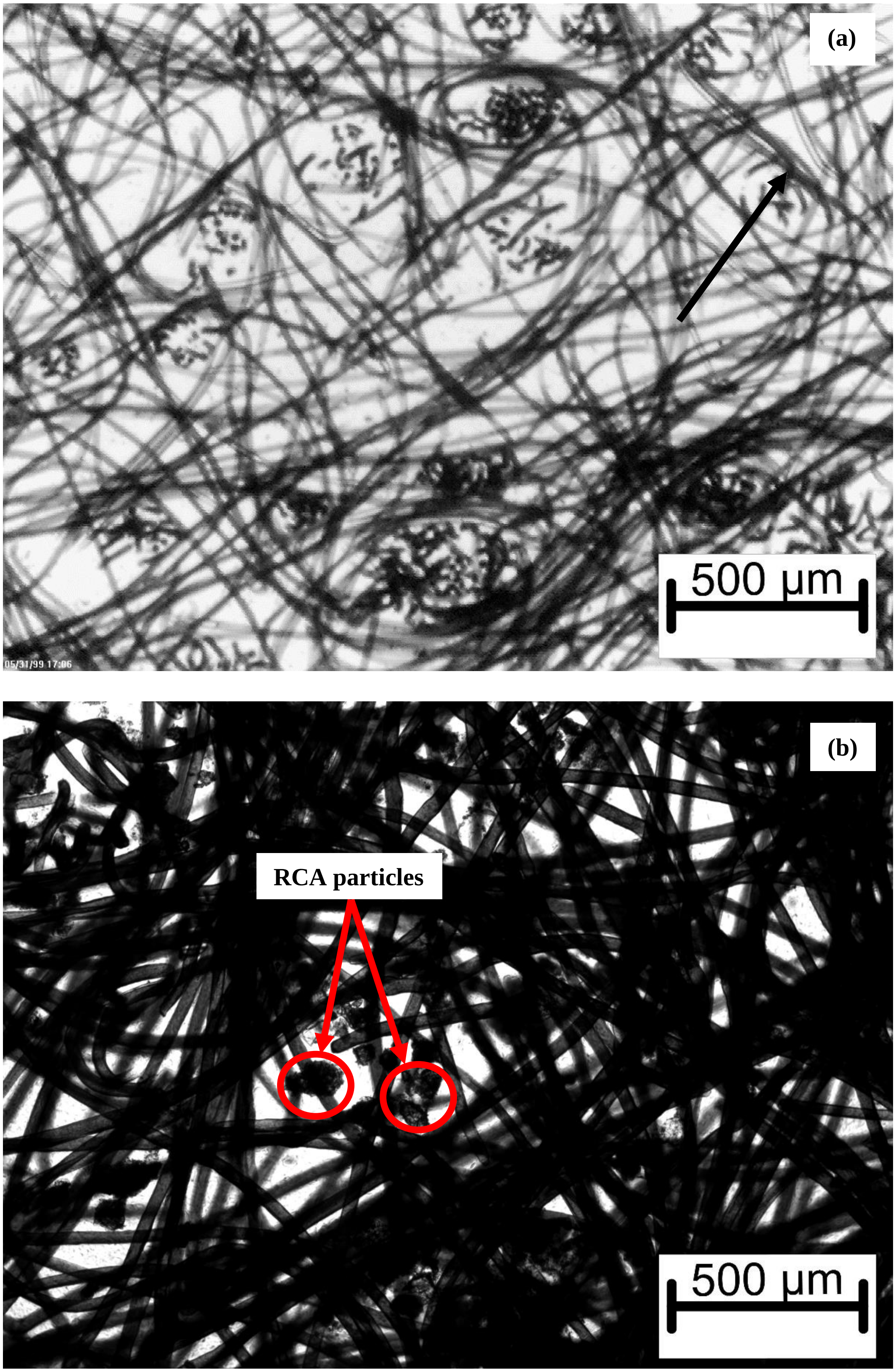

Figure 4.8 Before and post-test images of NW2 subjected to filtration with RCA-1

Chapter 5

Summary and Conclusions

The current research study evaluated the filtration performance of four different recycled materials, i.e., recycled concrete aggregate (RCA-1 and RCA-2), recycled asphalt pavement (RAP), foundry sand (FS), and recycled asphalt shingle (RAS), by using three woven geotextiles (W1, W2 and W3) and three nonwoven geotextiles (NW1, NW2 and NW3). A series of long-term filtration tests (LFT) were conducted to assess the hydraulic compatibility of these recycled materials with the geotextiles. Upon completion of the LTF tests, grain size analyses, permittivity tests, image analyses, and piping measurements were conducted to investigate the clogging and retention behavior. The following conclusions are made as a result of this laboratory study:

5.1. *Woven Geotextiles*

1) GR_{ASTM} is insufficient in defining the clogging performance of geotextiles tested with recycled materials, and permeability ratio (K_R) is considered as a better indicator of clogging. Two additional ratios, permittivity ratio (Ψ_R) and percent open area ratio (POA_R), can also be used to verify the clogging behavior.
2) 24-hour testing procedure recommended in the ASTM D5101 was usually not enough to achieve a steady-state hydraulic conductivity during testing of

the recycled materials. Therefore, tests need to be continued for at least 200 hours under imposed hydraulic gradient and, preferably, until the steady-state conditions are met.

3) All woven geotextiles tested with the recycled materials, except W1-RAS and W3-RAP, yielded acceptable anti-clogging performance based on their K_R ratios. The observed performance was also verified by the Ψ_R and POA_R values. The clogging ratio obtained for W1-RAS was K_R 3.7; however, the permittivity tests conducted after the LTF test revealed a 22% reduction in flow capacity, suggesting that W1-RAS cannot be considered clogged.

4) Percent open area (POA) of a woven geotextile was the most important pore structure parameter controlling the retention performance. More piping was observed with increasing POA; however, no clear-cut trend was found between K_R and POA.

5) The highest amount of piped soil through woven geotextiles was 2,280 g/m^2 (W1-RCA-1) where W1 had the highest POA (10%) of tested geotextiles. However, the piped amount was still less than 2,500 g/m^2, a limit set for internal stability of filters, and, therefore, all recycled material tested with woven geotextiles indicated satisfactory retention performance.

6) Existing geotextile filter criteria were not able to predict the clogging behavior observed in the laboratory long-term filtration tests. The predictive capability of the criteria was generally poor (0-33%), except the criteria described by Millar et al. (1980) and Fischer et al. (1990) were able to predict 60% of the tests, suggesting that small pore opening sizes (e.g., O_{15} and O_{50})

are more likely to control clogging. The existing criteria were generally successful in predicting the retention performance observed in the laboratory.

5.2. *Nonwoven Geotextiles*

1) All nonwoven geotextiles tested with recycled materials, NW2 and NW3 tested with RAP, and NW3 tested with RAS yielded acceptable anti-clogging performance based on their K_R ratios. The observed performance was also verified by the Ψ_R and POA_R values. The highest reduction in permittivity was 26% for NW1-RAP, with a corresponding K_R ratio of 2.6; however, this clogging ratio did not accompany a noticeable drop in the flow.
2) Permittivity (Ψ) was the most important pore structure defining the filtration performance of nonwoven geotextiles. More piping and less clogging was observed with increasing permittivity.
3) Piping rate increased with increasing commonly used pore sizes O_{95}, O_{90}, O_{50} and the retention ratio O_{50}/ D_{50}.
4) The highest amount of piped soil through woven geotextiles was 209 g/m^2 (NW3-RCA-1), significantly less than 2,500 g/m^2, a limit set for internal stability of filters, thus the nonwoven geotextiles had satisfactory retention performance for the recycled materials tested.
5) The existing retention criteria successfully predicted the performance observed in the laboratory tests. The existing clogging criteria predicted the laboratory performance of NW2-RAP; however, was not successful in predicting the performance for the other combinations.

6) The decrease in O_{50} was less than 23% for all of the nonwoven geotextiles employed in testing. However, O_{95} decreased up to 46%. The thickest nonwoven geotextile (NW2) had the highest reduction in O_{95}, possibly due to entrapment of higher amount of materials in this fabric.

Overall results showed that nonwoven geotextiles performed better in terms of retention, and woven geotextiles functioned better in terms of clogging resistance. Recycled concrete aggregates (RCA-1 and RCA-2) presented better compatibility when tested with both types of geotextiles (i.e., woven and nonwoven) compared to other recycled materials tested. Clogging seemed to be more pronounced for the geotextiles interacting with recycled asphalt pavement (RAP). Permittivity and POA were the main parameters that influenced the clogging and retention performance of nonwoven and woven geotextiles, respectively. The success of existing criteria in predicting the filtration performance was inconsistent, suggesting that a parametric study is required to find the best characteristic pore opening size-to- soil grain size ratios that discriminate the clogging performance. Such a study would require additional tests on recycled materials with varying coefficients of uniformity and fines content and geotextiles with varying pore structure parameters (i.e., characteristic pore opening sizes and permittivities).

5.3. *Limitations of the study*

This study focused on assessing the hydraulic compatibility between a group of recycled materials and geotextiles when used in highway bases and landfill covers.

The findings of this research were limited to only evaluating physical clogging potential of the geotextile pores. Chemical and biological clogging can be equally important, especially when these filters are used within the landfill systems where leachate flow through the geotextile exists. Furthermore, three types of nonwoven and three types of woven geotextile were subjected to long-term filtration tests with four different recycled materials. Therefore, in its current status, the findings of the laboratory study are only applicable to these geotextile-recycled material combinations.

5.4. *Recommendations for future work*

1) A numerical model can be developed to simulate the filtration process through geotextile filters to better understand the mechanism of geotextile filtration and particle entrapment in geotextiles. The model can be applied to various conditions including different geotextiles, different soil types etc.
2) The current testing methodology handles one-dimensional flow. It is necessary to develop a new testing technique for soil-geotextile combinations that experience multidimensional flows (i.e., conical filters).

Appendices

Appendix A: Tests with Woven Geotextiles

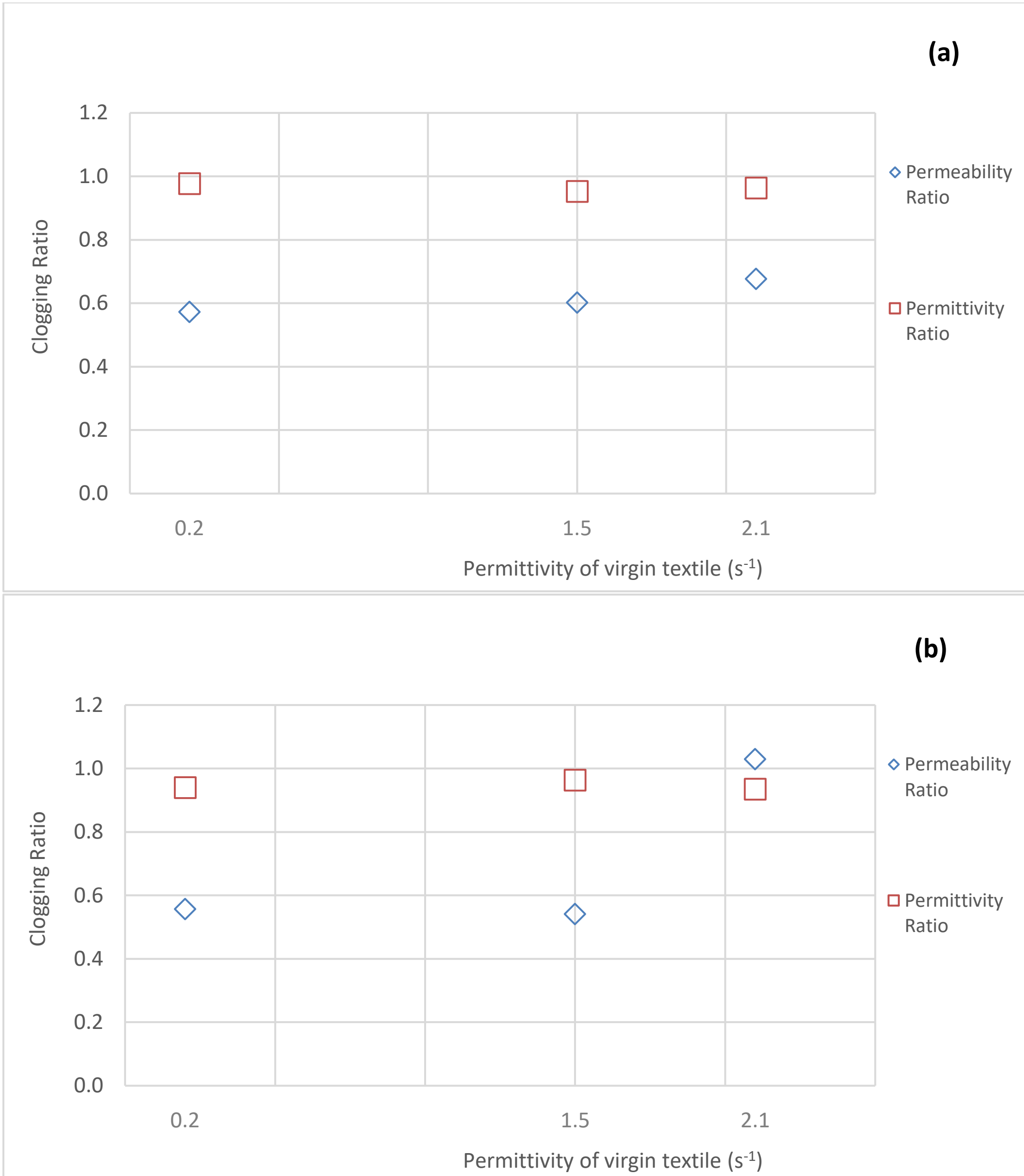

Figure A1. Relationship between clogging ratios and permittivity of virgin geotextiles, RCA-1 (a), RCA-2 (b)

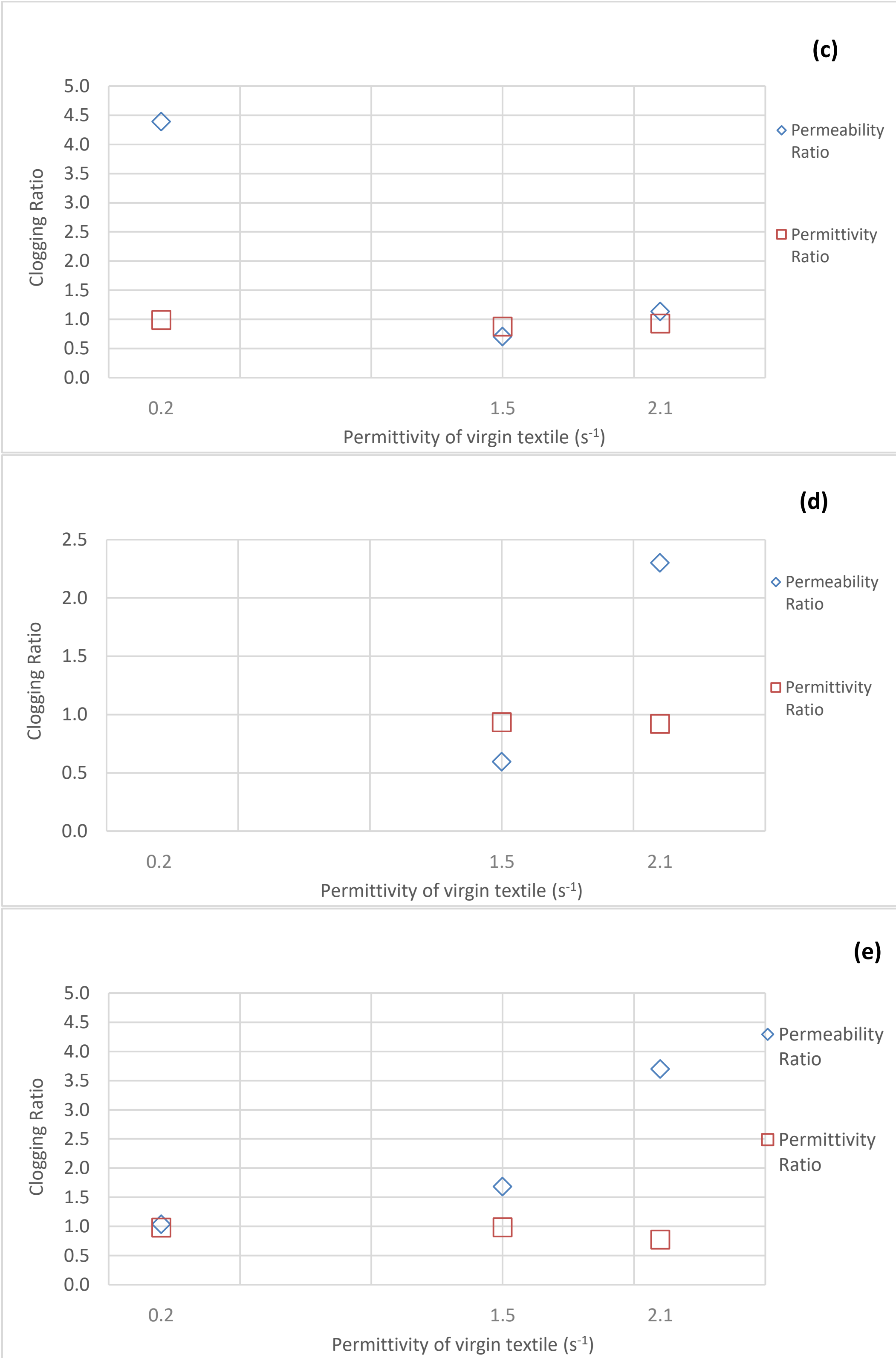

Figure A1. Relationship between clogging ratios and permittivity of virgin geotextiles, RAP (c), FS (d), RAS (e) (continued)

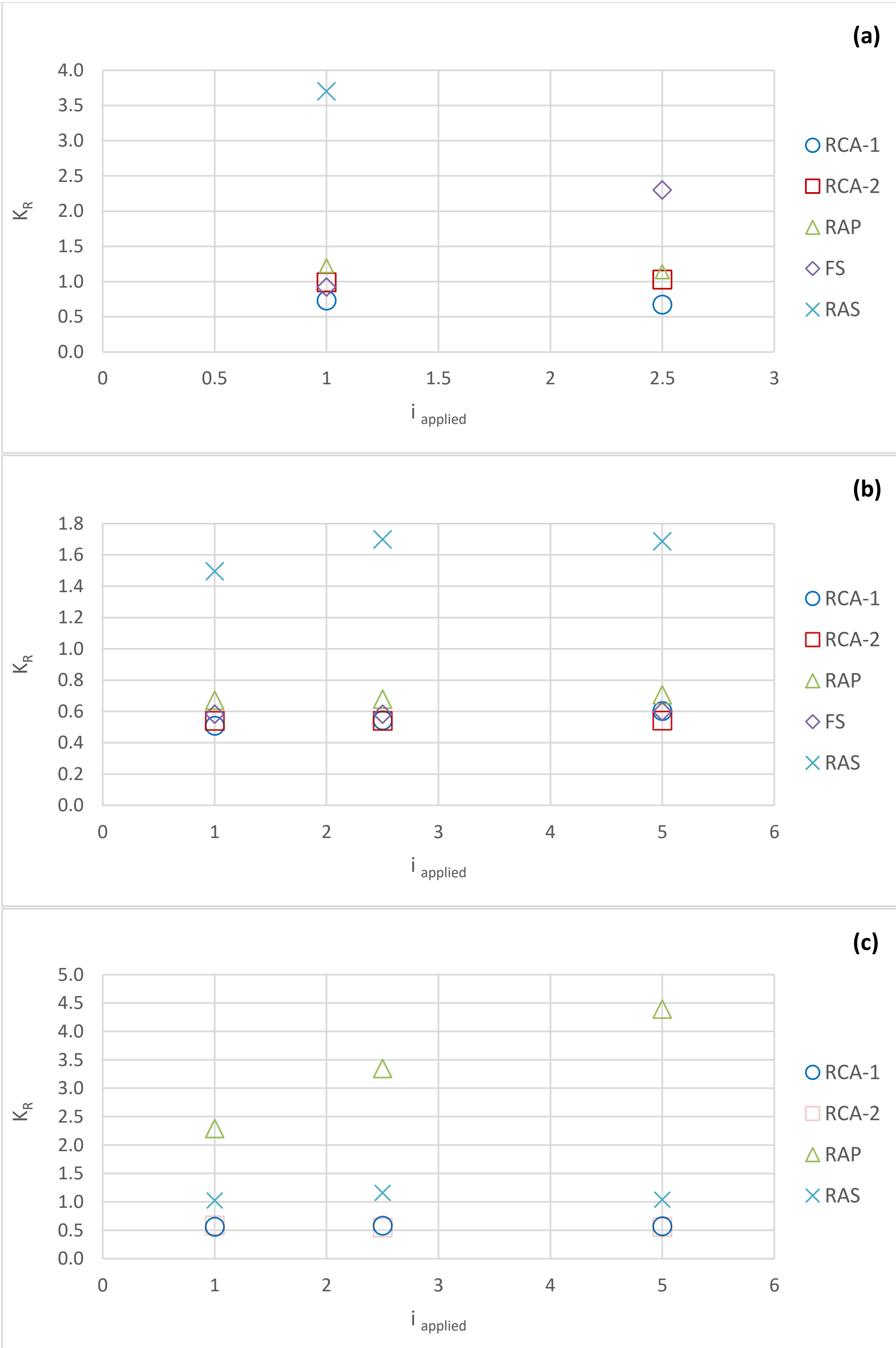

Figure A2. Relationship between permeability ratio and applied hydraulic gradient, W1 (a), W2 (b), W3 (c)

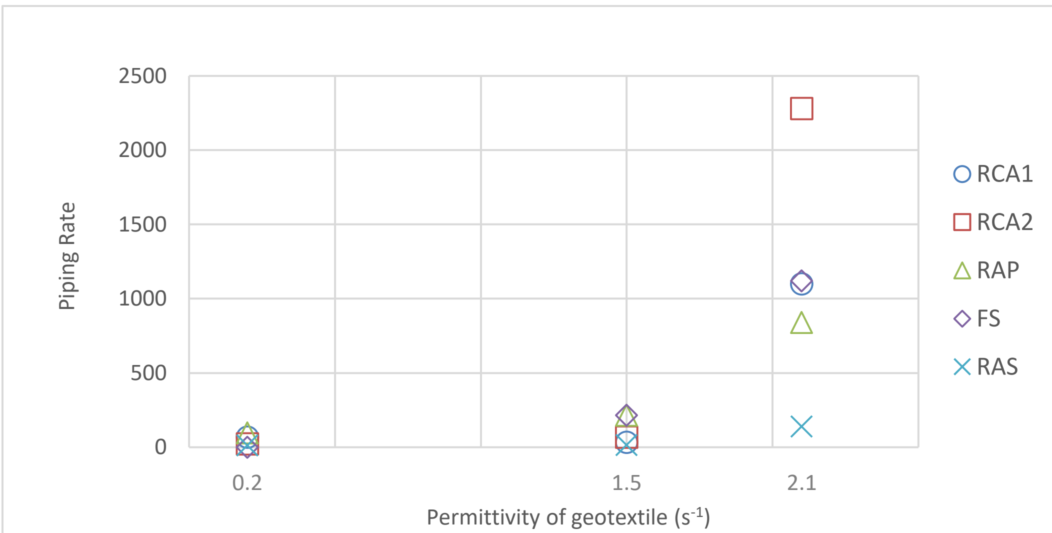

Figure A3. Relationship between piping rate and permittivity of virgin geotextiles

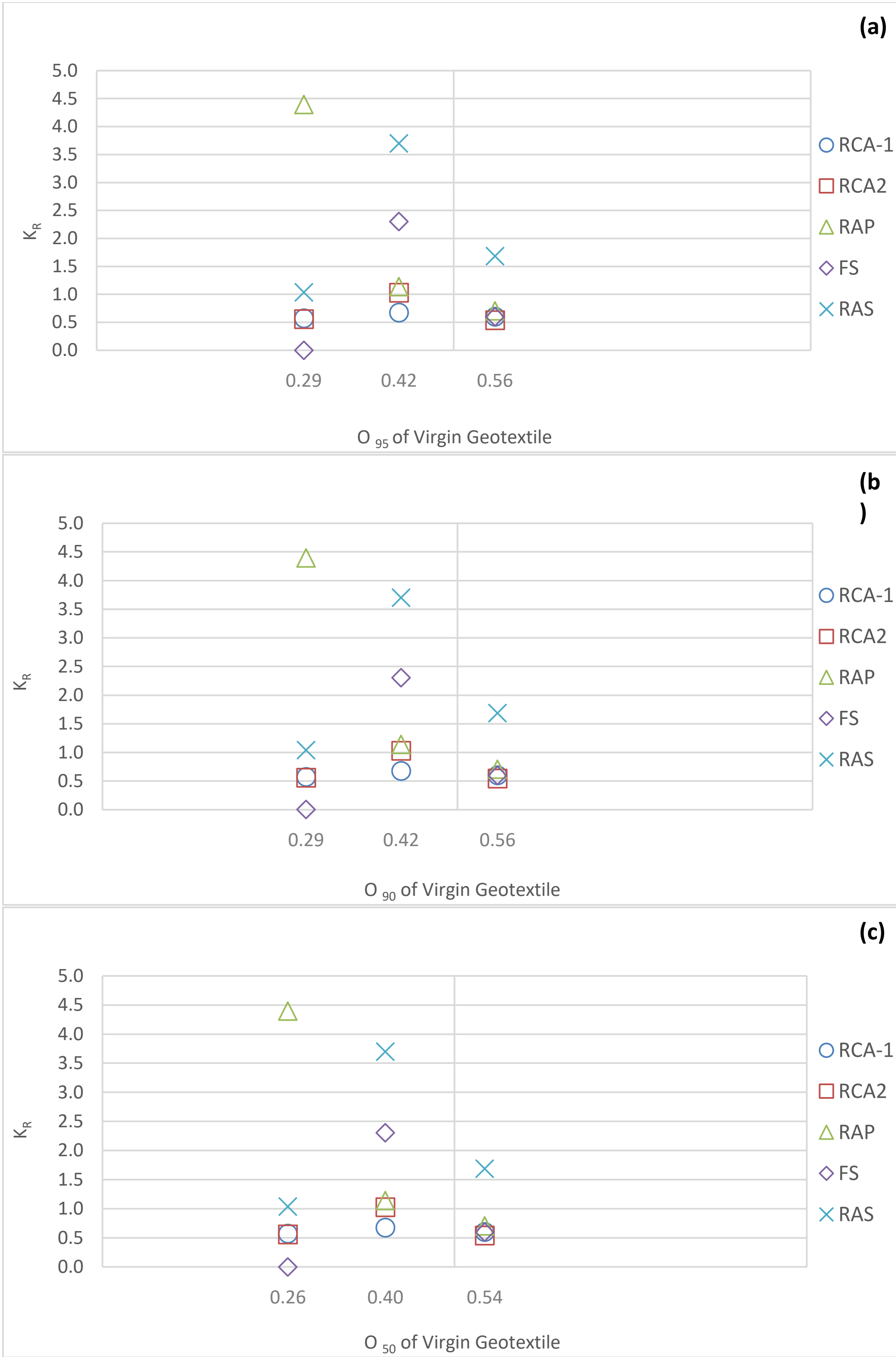

Figure A4. Relationship between permeability ratio characteristic pore opening size of geotextiles W1 (a), W2 (b), W3 (c)

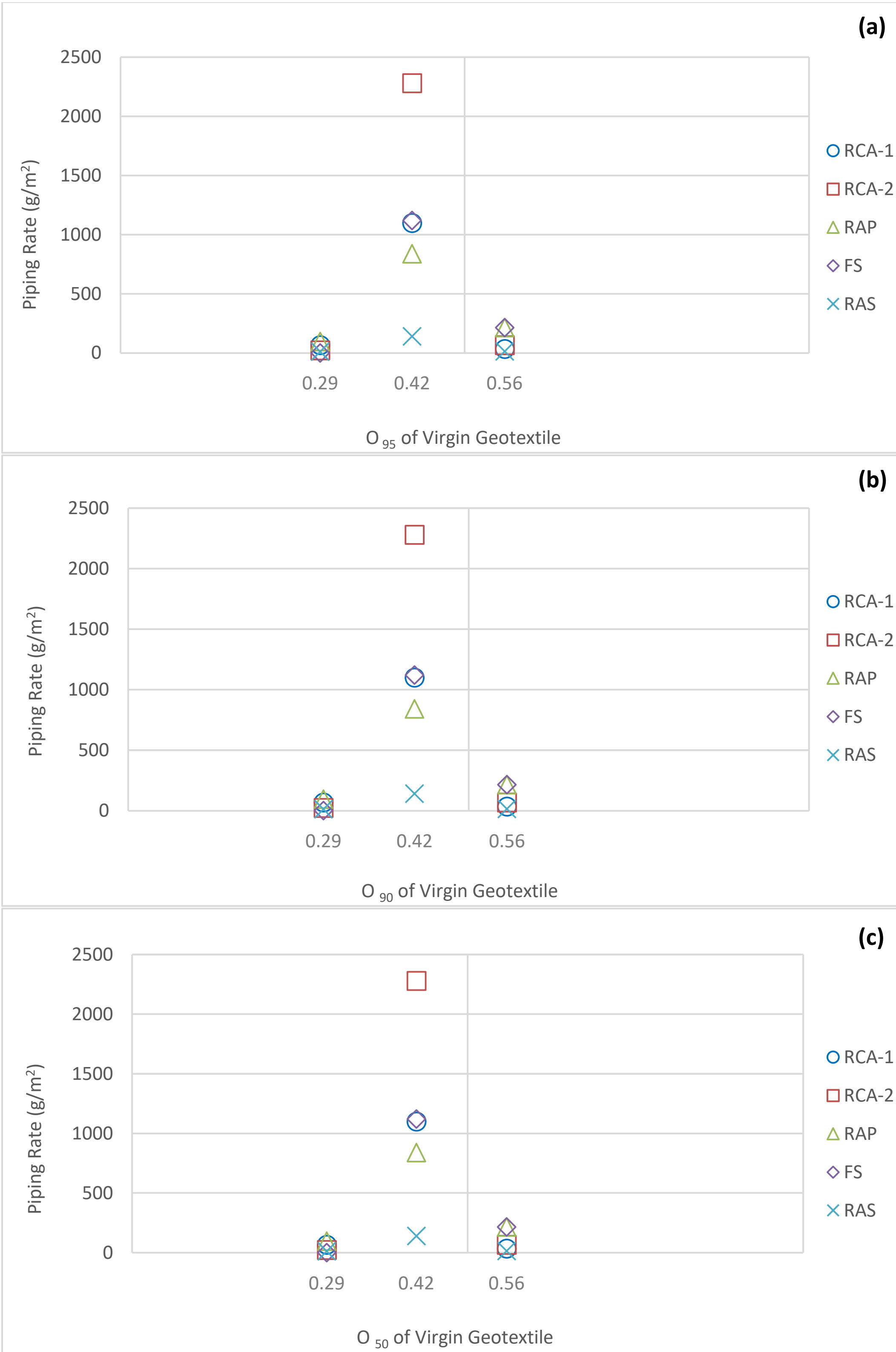

Figure A5. Relationship between piping rate and characteristic pore opening size of geotextiles O_{95} (a), O_{90} (b), O_{50} (c)

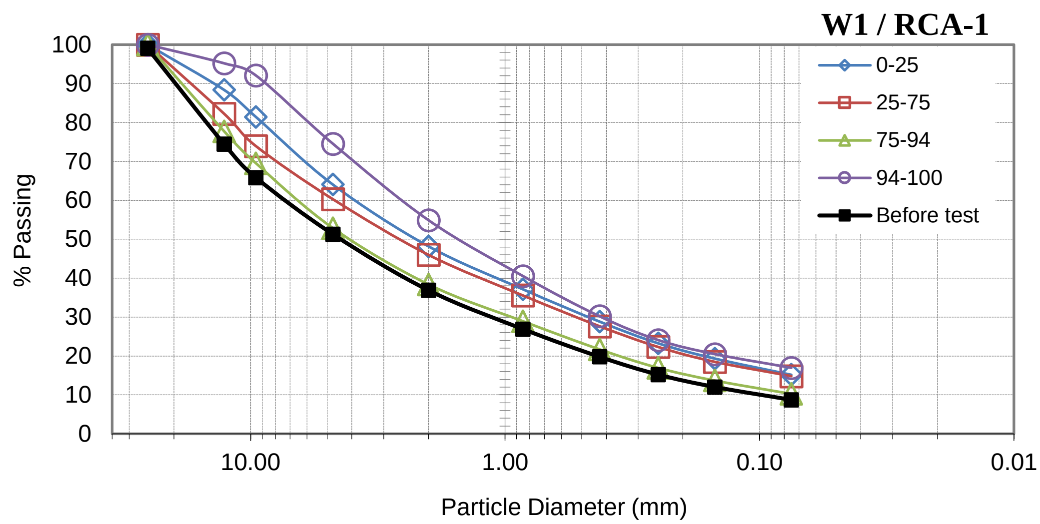

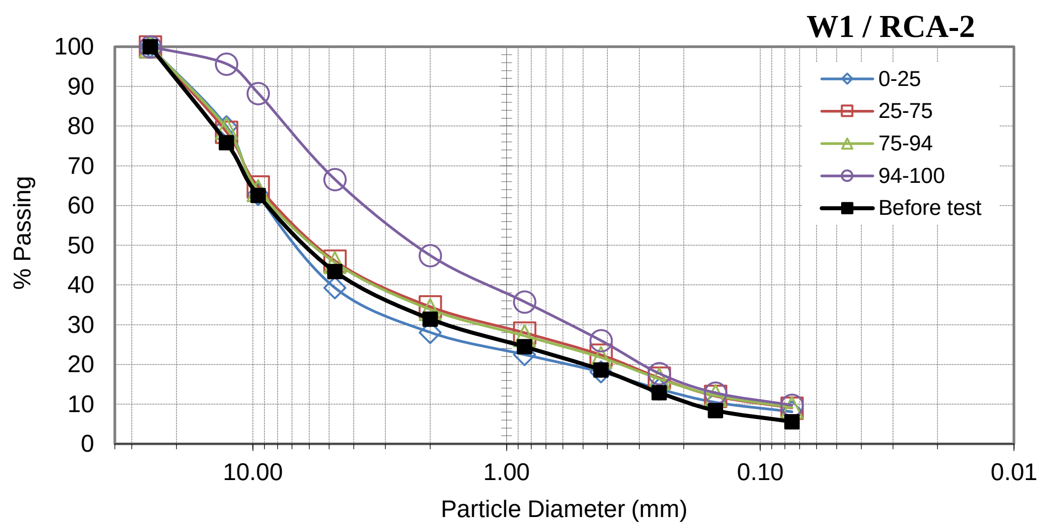

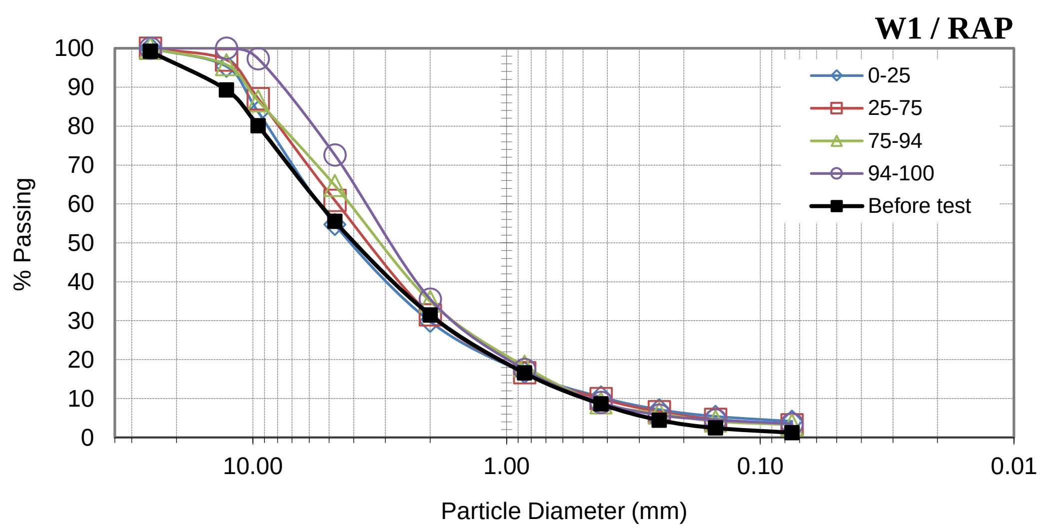

Figure A6. Grain size distributions of specimens taken from various depths after testing with geotextile W1 (continued)

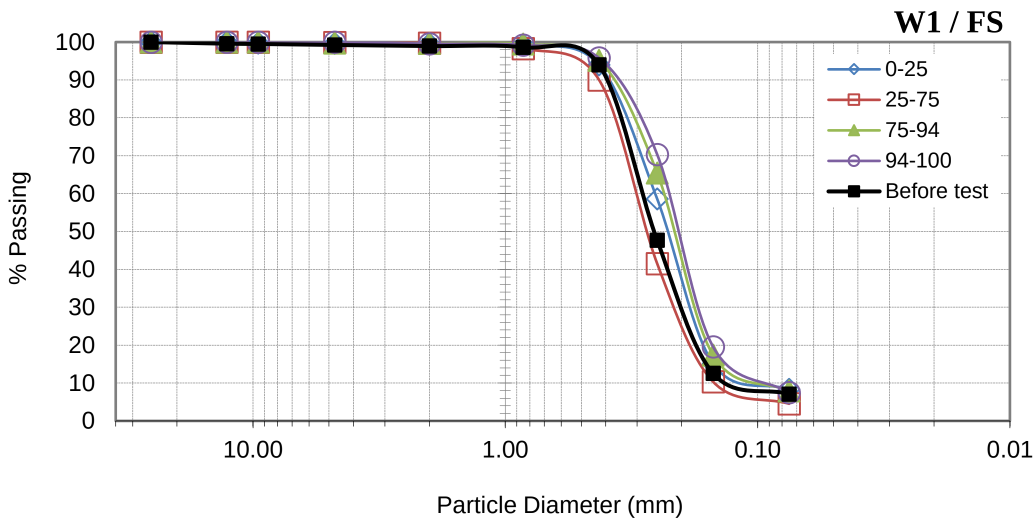

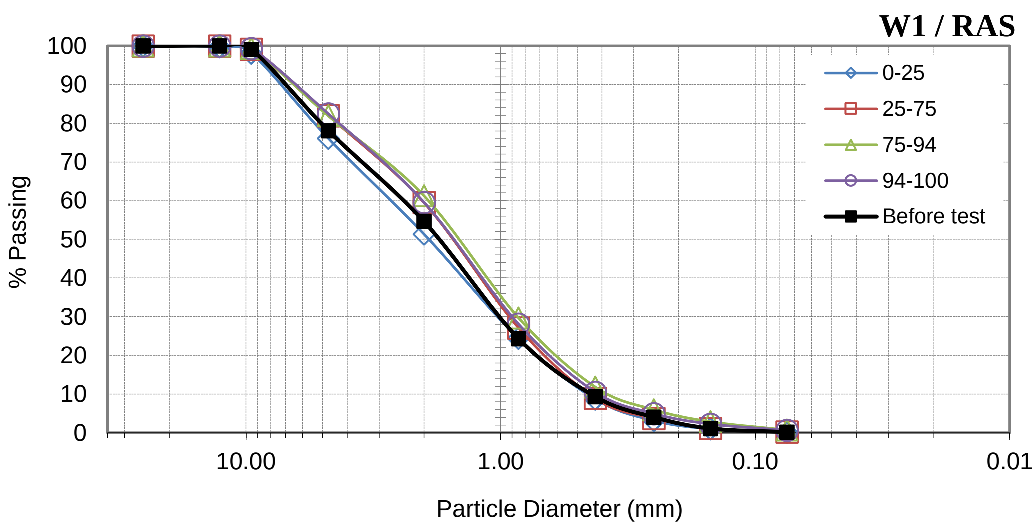

Figure A6. Grain size distributions of specimens taken from various depths after testing with geotextile W1

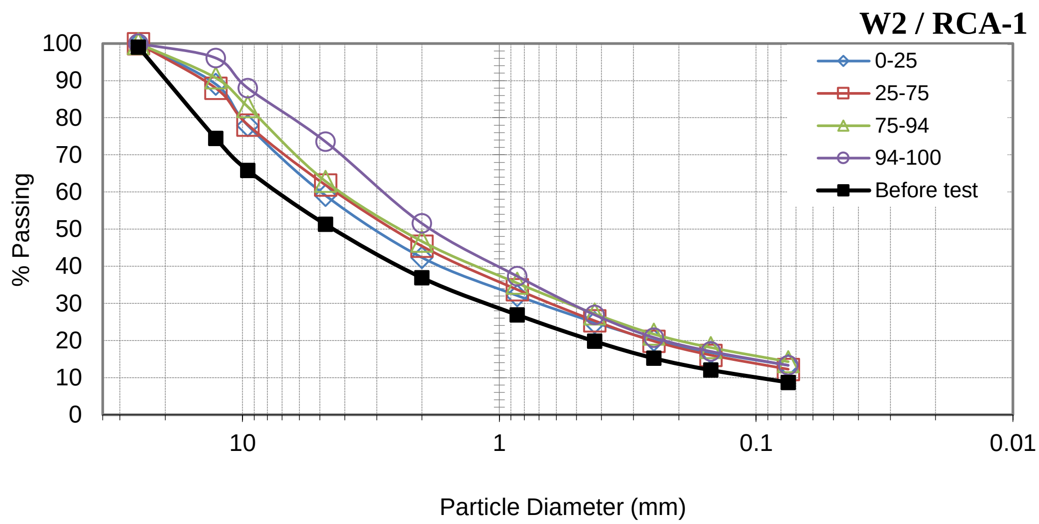

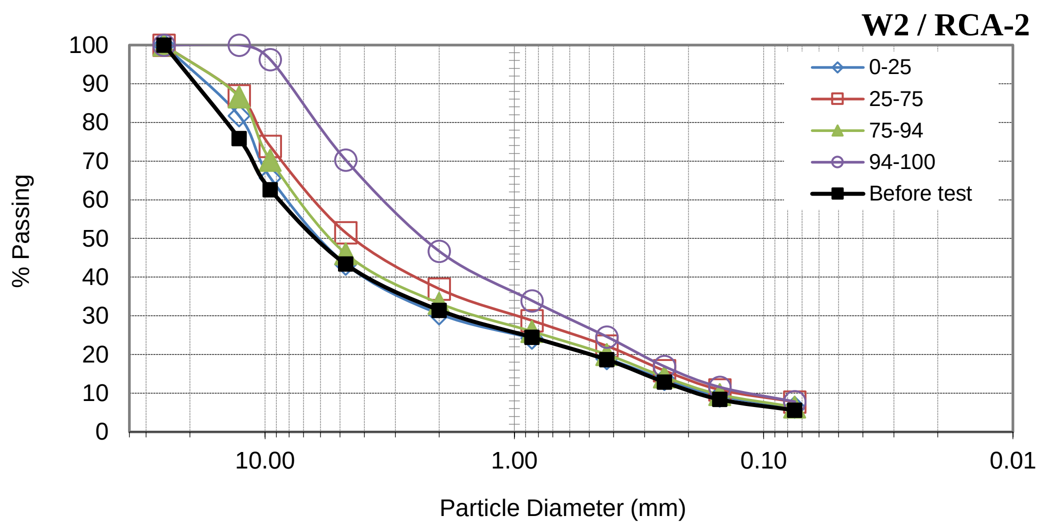

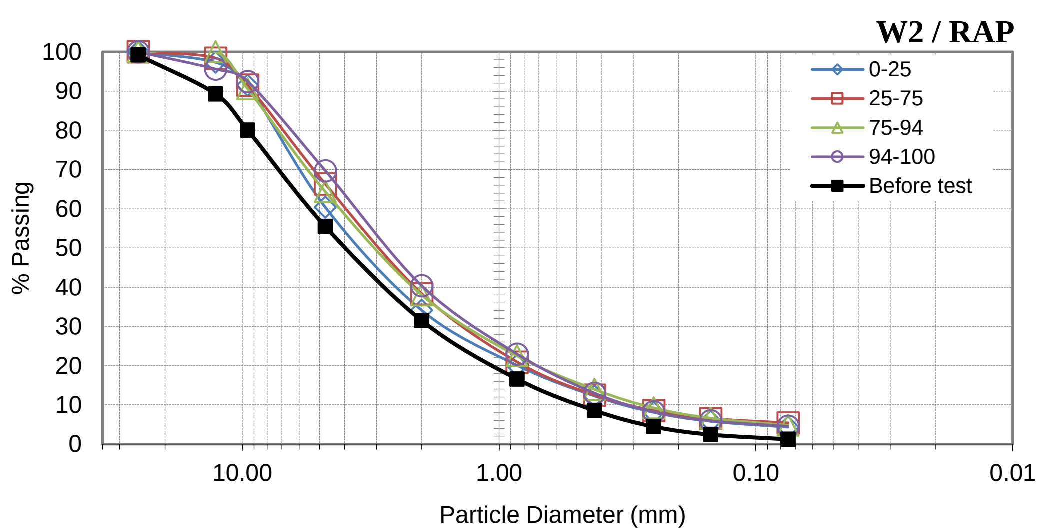

Figure A7. Grain size distributions of specimens taken from various depths after testing with W2 (continued)

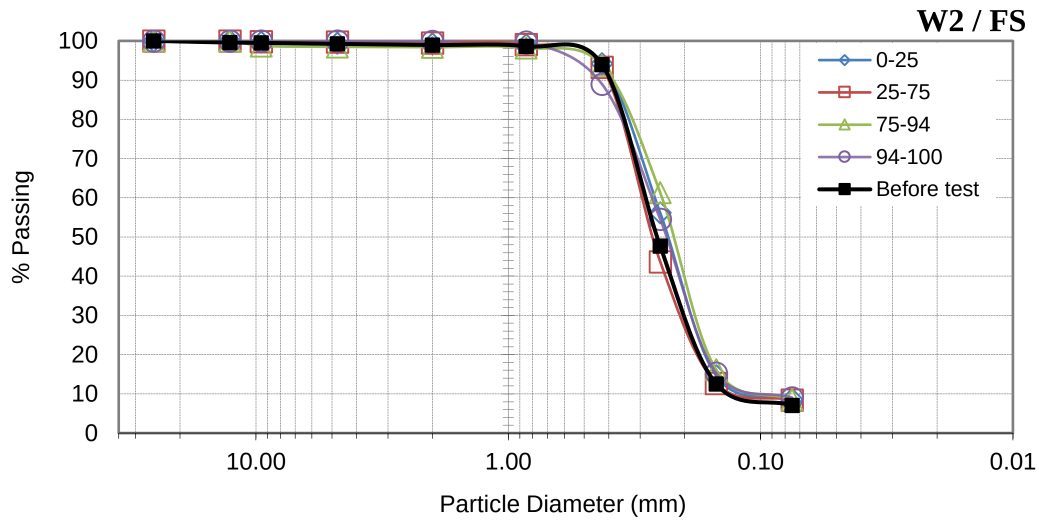

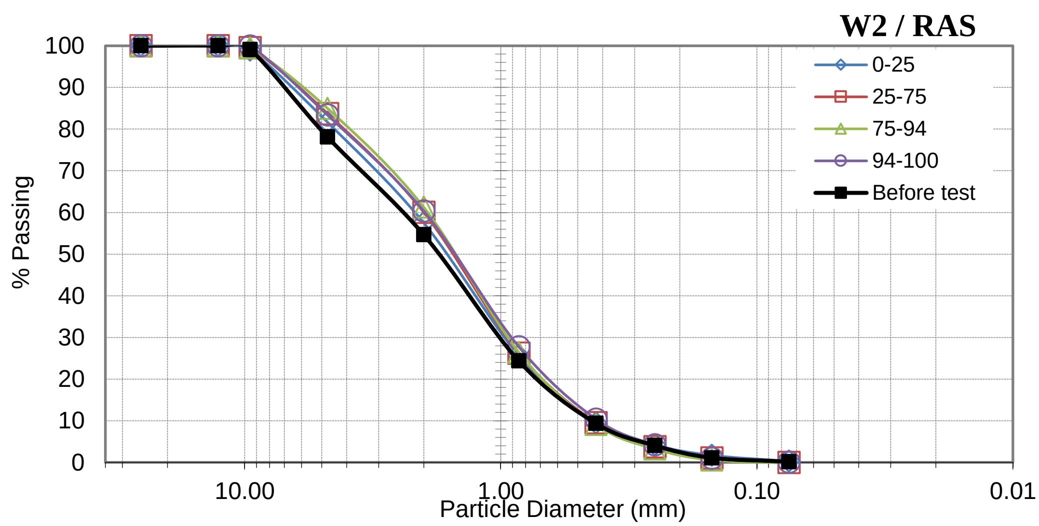

Figure A7. Grain size distributions of specimens taken from various depths after testing with W2

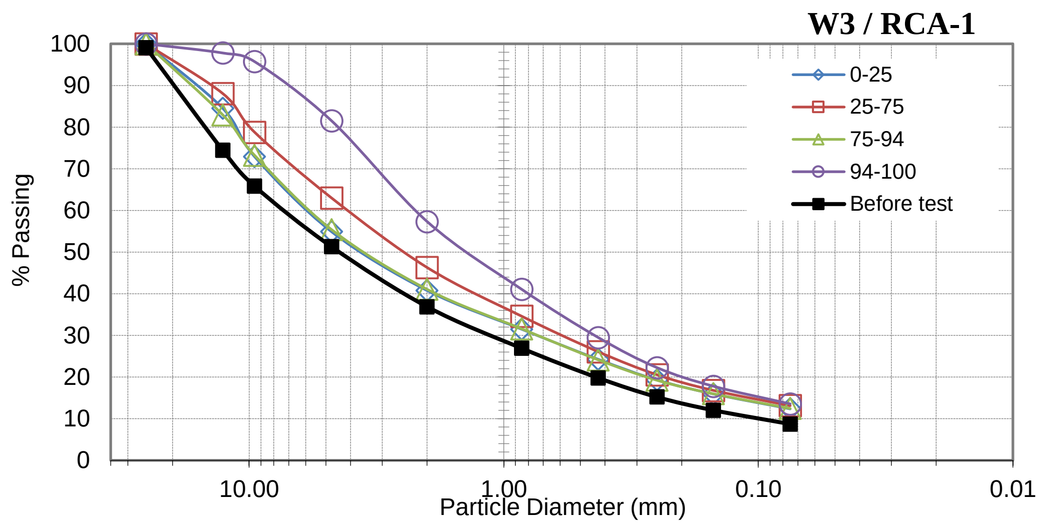

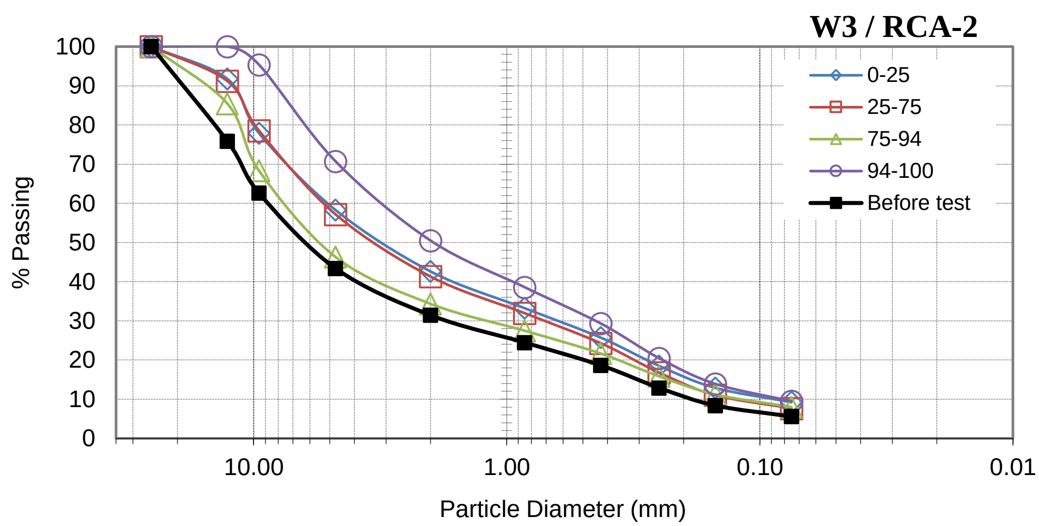

Figure A8. Grain size distributions of specimens taken from various depths after testing with W3 (continued)

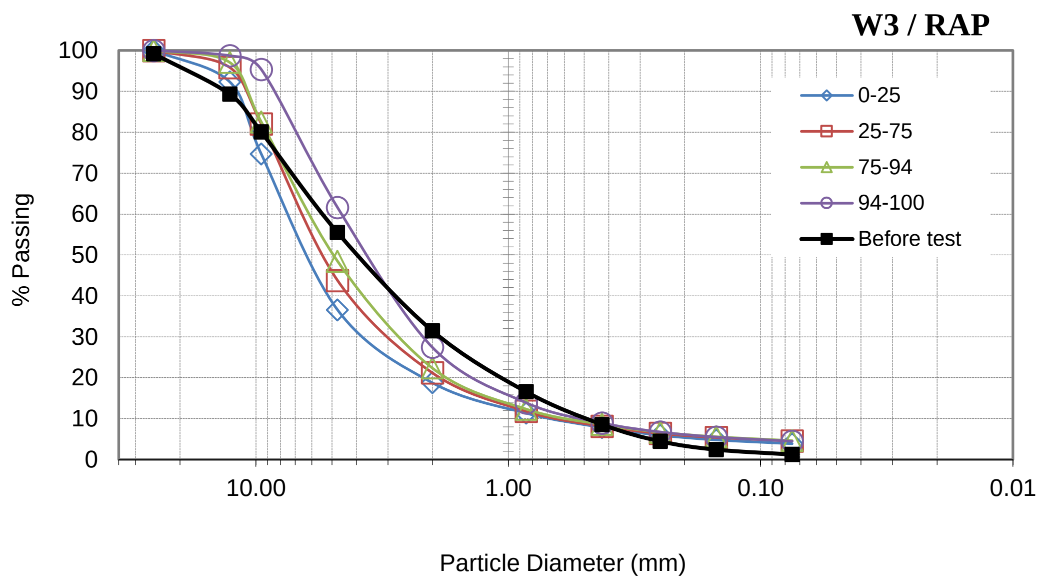

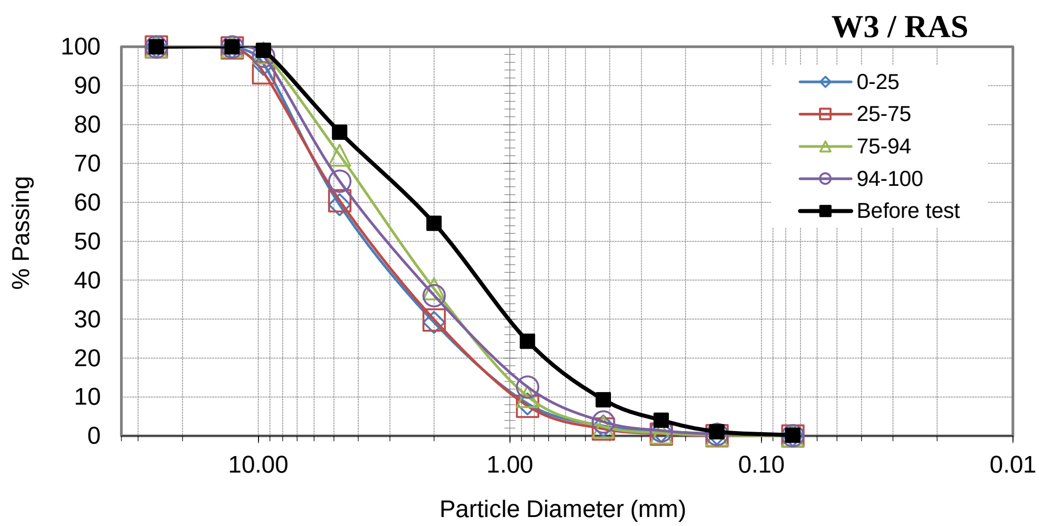

Figure A8. Grain size distributions of specimens taken from various depths after testing with W3

Appendix B: Tests with Nonwoven Geotextiles

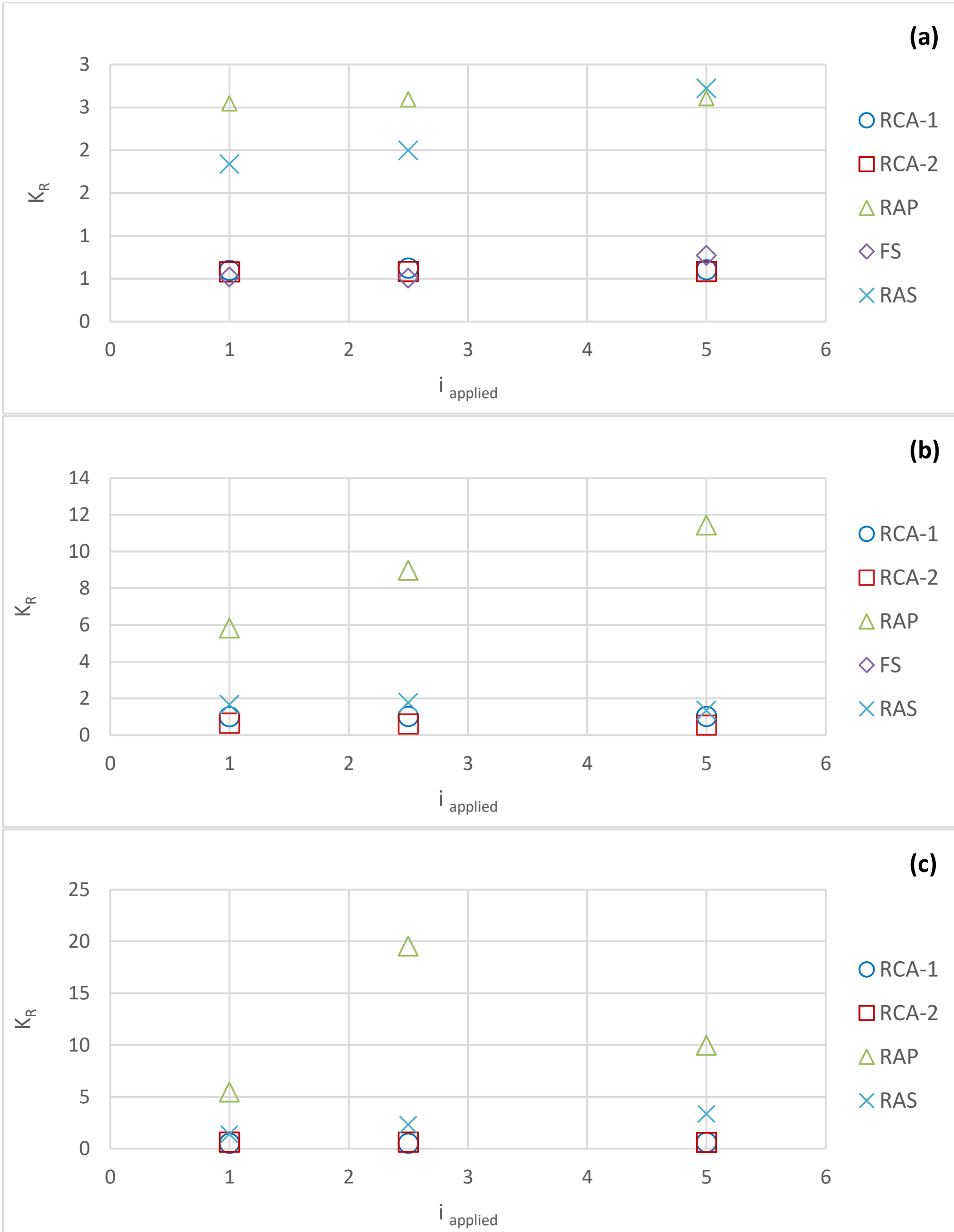

Figure B1. Relationship between permeability ratio and applied hydraulic gradient, NW1 (a), NW2 (b), NW3 (c)

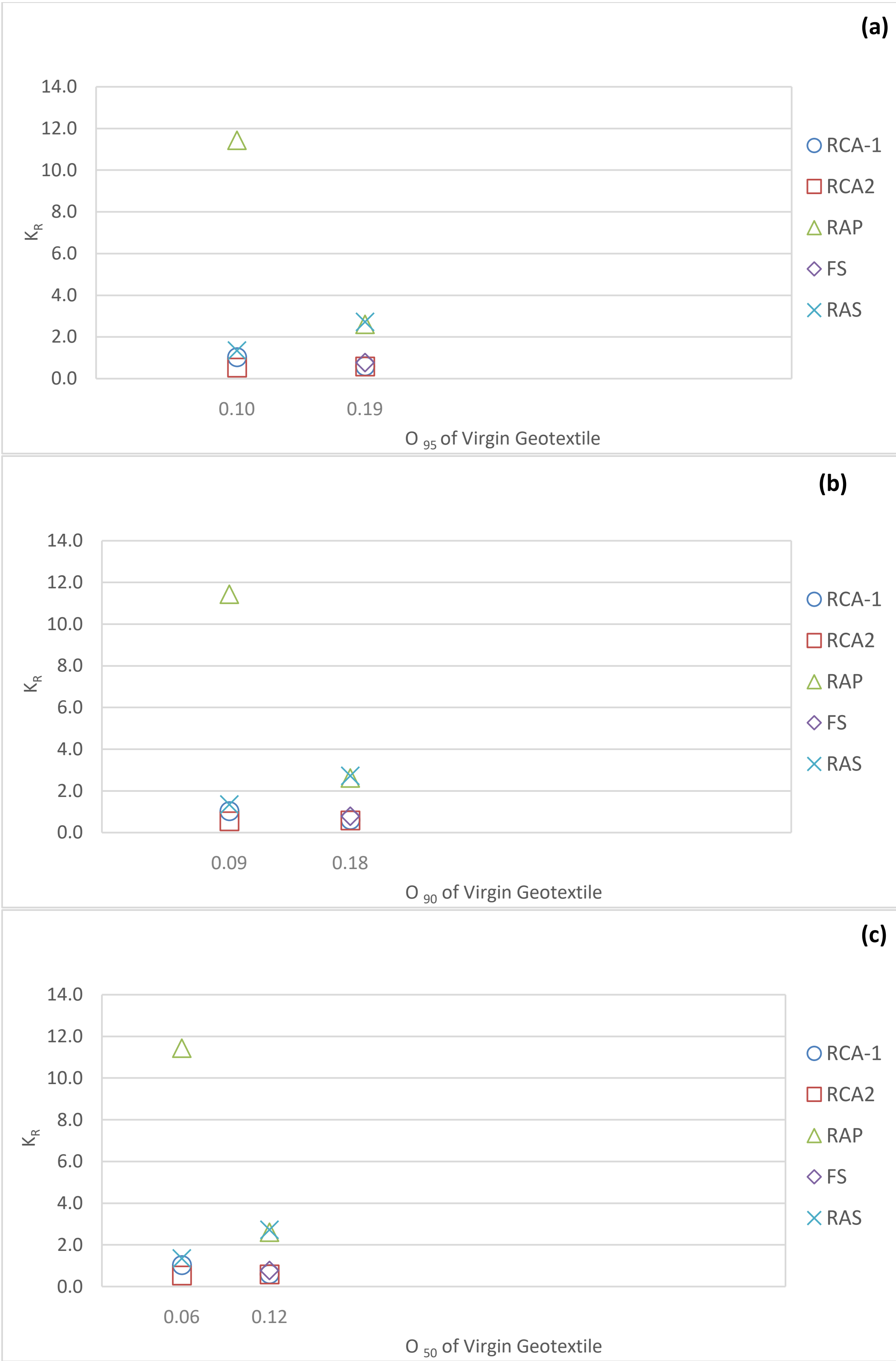

Figure B2. Relationship between permeability ratio characteristic pore opening size of geotextiles NW1 (a), NW2 (b), NW3 (c)

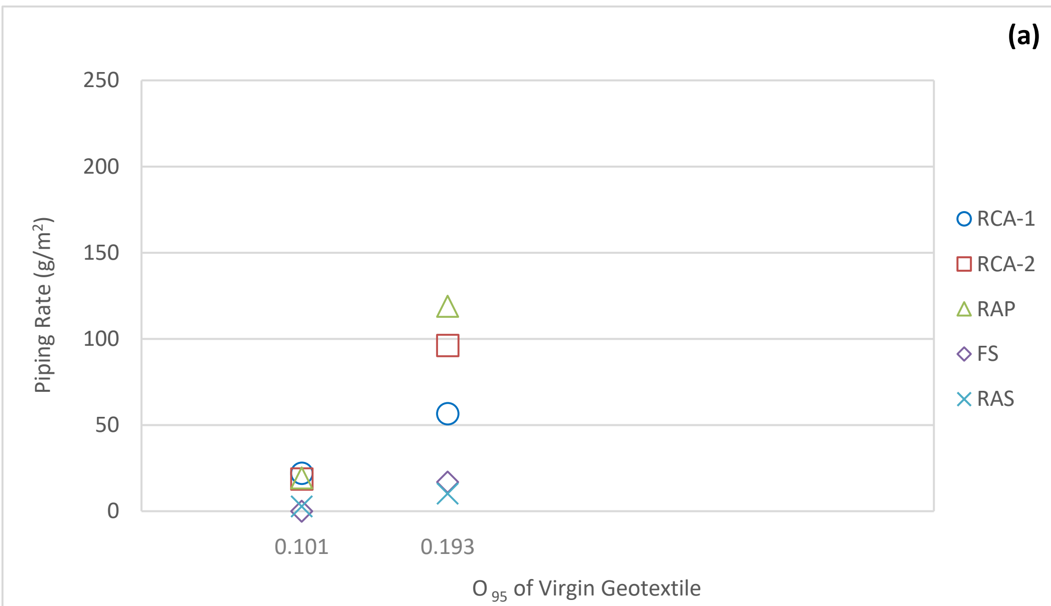

Figure B3. Relationship between piping rate and characteristic pore opening size of geotextiles O_{95} (a), O_{90} (b), O_{50} (c)

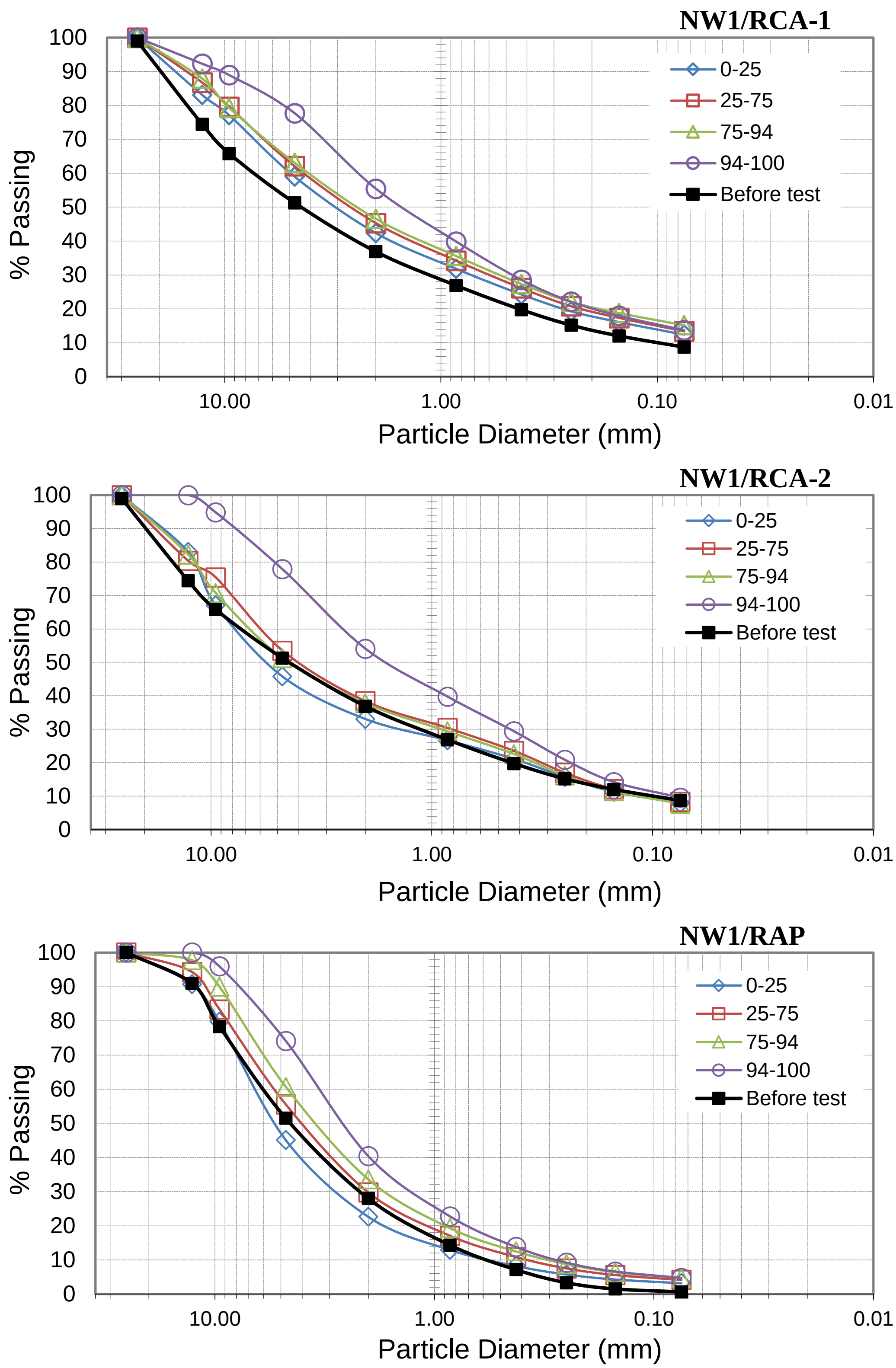

Figure B4. Grain size distributions of specimens taken from various depths after testing with NW1

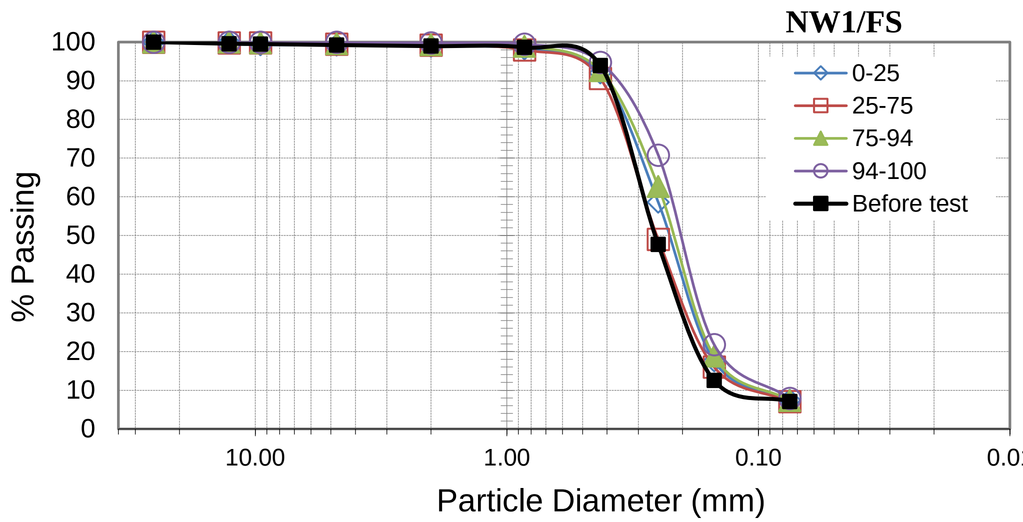

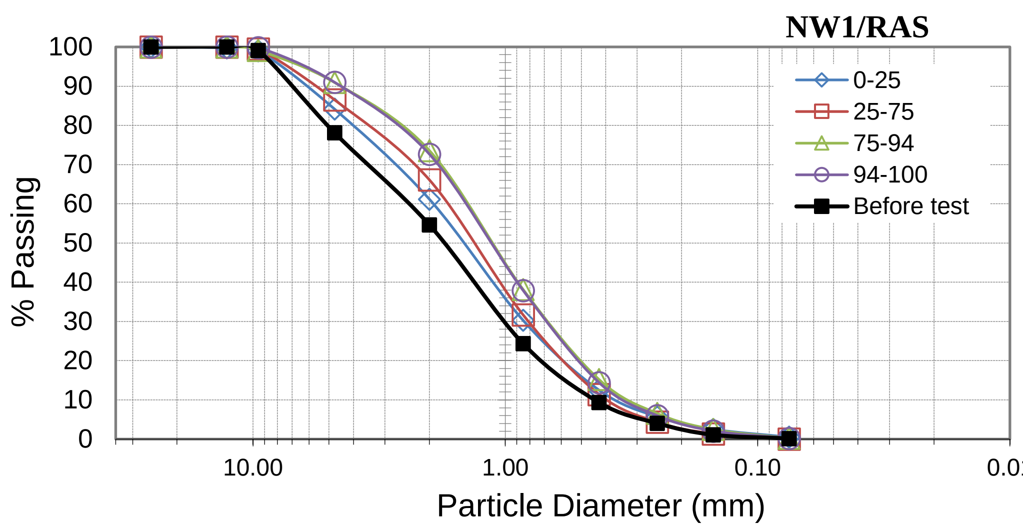

Figure B4. Grain size distributions of specimens taken from various depths after testing with NW1 (continued)

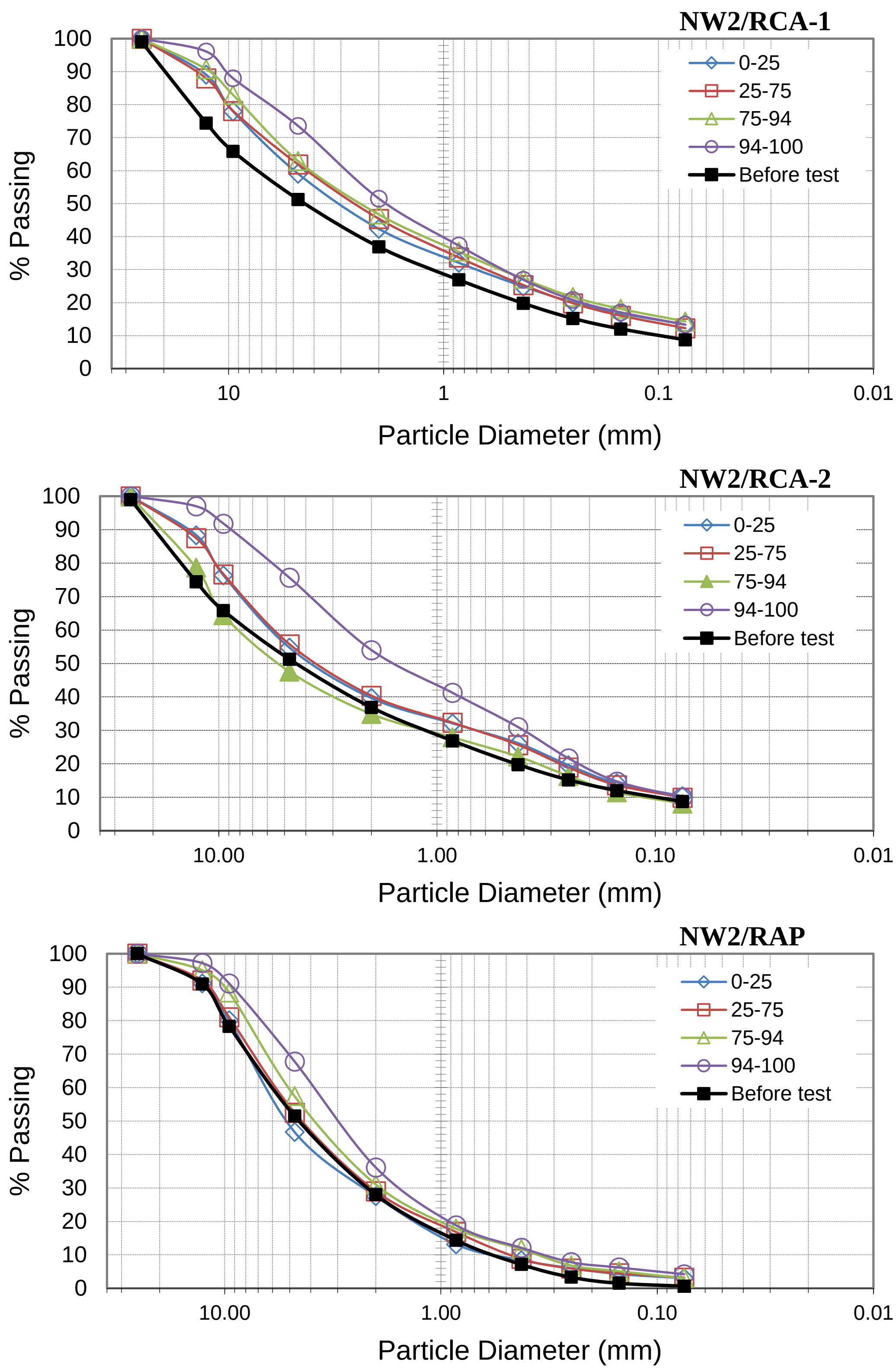

Figure B5. Grain size distributions of specimens taken from various depths after testing with NW2

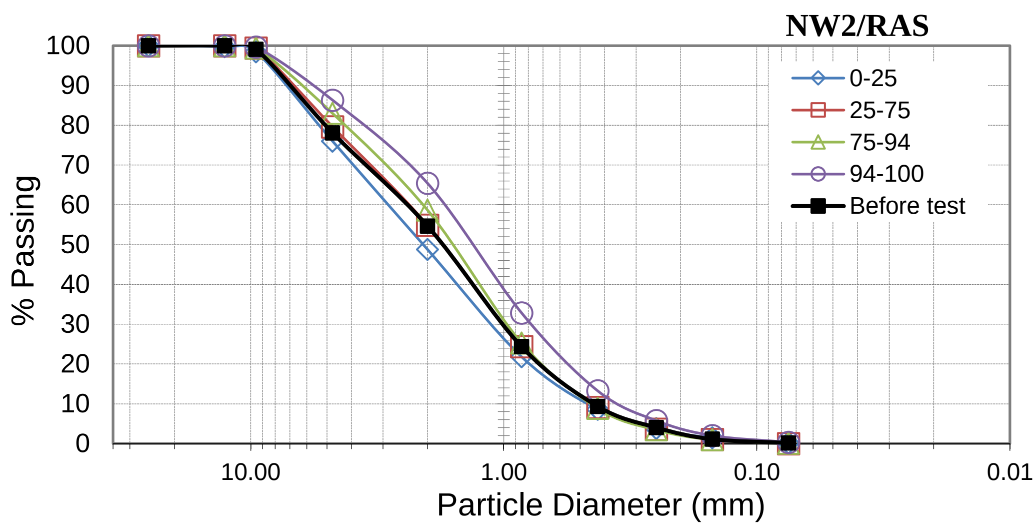

Figure B5. Grain size distributions of specimens taken from various depths after testing with NW2 (continued)

REFERENCES

Alakayleh, Z., Clement, T. P., & Fang, X. (2018). "Understanding the Changes in Hydraulic Conductivity Values of Coarse-and Fine-Grained Porous Media Mixtures". *Water*, *10*(3), 313.

American Associaton of State Highway and Transportation Officials (1982). *AASHTO Materials, Part 1, Specifications,* Washington, D.C.

Abbaspour, A., Tanyu B. F., and Aydilek A. H. (2018). "Methodology To Evaluate Hydraulic Compatibility Of Geotextile And Rca İn Underdrain Systems." *Geosynthetics International,* 25(1): 67–84.

Abichou, T., Benson, C., and Edil, T. (1998a). "Beneficial Reuse Of Foundry Sands In Construction Of Hydraulic Barrier Layers.'' *Environmental Geotechnics Rep. No. 98–14*, Dept. of Civil and Environmental Engineering, Univ. of Wisconsin-Madison, Madison.

Abichou, T., Benson, C., and Edil, T. (2000). ''Foundry Green Sands As Hydraulic Barriers: Laboratory Study.'' *Journal of Geotechnical and Geoenvironmental Engineering*, 126(12), 1174–1183

Abichou, T., Edil, T., Benson, C.H., and Tawfiq, K. (2004). "Hydraulic Conductivity of Foundry Sands and Their Use as Hydraulic Barriers." *Recycled Materials in Geotechnics*: 186–200.

ASTM C702-11. *Standard Practice for Reducing Samples of Aggregate to Testing Size,* ASTM International, West Conshohocken, PA, 2011, https://doi.org/10.1520/C0702_C0702M-11

ASTM D698-12. *Standard Test Methods for Laboratory Compaction Characteristics of Soil Using Standard Effort (12 400 ft-lbf/ft3 (600 kN-m/m3)),* ASTM International, West Conshohocken, PA, 2012, https://doi.org/10.1520/D0698-12E02

ASTM D2434-68. *Standard Test Method for Permeability of Granular Soils (Constant Head),* ASTM International, West Conshohocken, PA, 2000, https://doi.org/10.1520/D2434-68R00

ASTM D4318-17. *Standard Test Methods for Liquid Limit, Plastic Limit, and Plasticity Index of Soils,* ASTM International, West Conshohocken, PA, 2017, https://doi.org/10.1520/D4318-17

ASTM D4491-14. *Standard Test Methods for Water Permeability of Geotextiles by Permittivity*. ASTM International, West Conshohocken, PA.

ASTM D4751-16. *Standard Test Methods for Determining Apparent Opening Size of a Geotextile*. ASTM International, West Conshohocken, PA.

ASTM D5101-12. *Standard Test Method for Measuring the Filtration Compatibility of Soil-Geotextile Systems.*" ASTM International, West Conshohocken, PA, 2017, https://doi.org/10.1520/D5101-12R17

ASTM D5856-15. *Standard Test Method for Measurement of Hydraulic Conductivity of Porous Material Using a Rigid-Wall*, Compaction-Mold Permeameter, ASTM International, West Conshohocken, PA, 2015, https://doi.org/10.1520/D5856-15

Austin, D., Mlynarek, J., and Blond, E. (1997). "Expanded Anti-Clogging Criteria for Woven Filtration Geotextiles." *Proceedings of Geosynthetics' 97*, Long Beach, California, USA, 1123–1144.

Aydilek, A. H., & Edil, T. B. (2008). "Remediation of High Water Content Geomaterials: A Review of Geotextile Filter Performance". In *First Panamerican Conference on Geosynthetics, GeoAmericas*, 902-910

Aydilek, A. H. (2006). "A Semi-Analytical Methodology for Development of Woven Geotextile Filter Selection Criteria." *Geosynthetics International*, 13(2), 59–72.

Aydilek, A. H., and Edil, T. B. (2003). "Long-Term Filtration Performance of Nonwoven Geotextile-Sludge Systems." *Geosynthetics International*, 10(4), 110–123.

Aydilek, A.H., and Edil, T. B. (2002). "Filtration Performance of Woven Geotextiles with Wastewater Treatment Sludge." *Geosynthetic International* 9(1): 41–69.

Aydilek, A. H., Oguz, S. H., and Edil, T. B. (2002). "Digital Image Analysis to Determine Pore Opening Size Distribution of Nonwoven Geotextiles." *Journal of Computing in Civil Engineering*, 16(4), 280–290.

Behring, Z., Kim, J., Nam, B., Chopra, M., & Shoucair, J. (2014). "Drainage performance evaluation of reclaimed concrete aggregate". In *Innovative and sustainable use of geomaterials and geosystems* (pp. 33-40).

Bell, A. L., McCullough, L. M., & Gregory, B. J. (1981). Clay contamination in crushed rock highway sub-bases. In *The Second Australian Conference on Engineering Materials, held at Sydney July 6-8, 1981.*

Bell, A. L., McCullough, L. M., & Snaith, M. S. (1982, August). An experimental investigation of sub-base protection using geotextiles. In *Proceedings of the 2nd International Conference on Geotextiles* (Vol. 2, 435-440).

Bhatia, S. K., Moraille, J., and Smith, J. L. (1998). "Performance of Granular versus Geotextile Filters in Protecting Cohesionless Soils," Filtration and Drainage in Geotechnical and Geoenvironmental Engineering, ASCE, Geotechnical Special Publication 78, L. N. Reddi and M. V. S. Bonala, Eds., 1–29

Bilodeau, J.-P., and Doré, G. (2012). "Resilient modulus water sensitivity of compacted unbound granular materials used as pavement base." *International Journal of Pavement Engineering*, 13(5): 459–471. doi:10.1080/10298436.2011. 573556.

Bonaparte, R., Ah-Line, C., Charron, R., & Tisinger, L. (1988). Survivability and durability of a nonwoven geotextile. In *Geosynthetics for Soil Improvement* (68-91). ASCE.

Bourgès-Gastaud, S., Stoltz, G., Sidjui, F., & Touze-Foltz, N. (2014). Nonwoven geotextiles to filter clayey sludge: An experimental study. *Geotextiles and Geomembranes*, *42*(3), 214-223.

Brorsson, I., & Eriksson, L. (1986). Long-term properties of geotextiles and their function as a separator in road construction. In *Proceedings of Third International Conference on Geotextiles* (93-98).

Calhoun, C. C. (1972). "Development Of Design Criteria and Acceptance Specifications for Plastic Filter Cloths". Technical Report, S-72-7, U.S. Army Waterways Experiment Station, Vicksburg, Mississippi, USA, 107. Carroll, R. G. (1983). "Geotextile filter criteria." *Transportation Research Record*, (916), 46–53.

Christopher, B.R. (1983) "Evaluation of Two Geotextile Installations in Excess of a Decade Old," *Transportation Research Record 916,* Transportation Research Board, 79-88.

Christopher, B. R., & Holtz, R. D. (1985). "Geotextile Engineering Manual". US Federal Highway Administration, Report FHWA-TS86/203, 1044

Christopher, B. R., Schwartz, C., and Boudreau, R. (2006). "*Geotechnical Aspects of Pavements*." Report No. FHWA NHI-05-037, Washington, D.C., US Department of Transportation, Federal Highway Administration.

Christopher, B. R., & Valero, S. N. (1999). Thirty-year performance evaluation of a geotextile filter. In *Geosynthetics' 99 Conference Proceedings* (977-990).

Coduto, D. P., Yeung, M. R., and Kitch, W. A. (2010). *Geotechnical Engineering: Principles & Practices (2nd Edition)*, Pearson.

Das, B. M., & Shin, E. C. (1998). Strip foundation on geogrid-reinforced clay: Behaviorunder cyclic loading. Geotextiles and Geomembranes, 13(10), 657–666.

Delgado-Rodriguez, O., Peinado-Guevara, H. J., Green-Ruiz, C. R., Herrera-Barrientos, J., & Shevnin, V. (2011). "Determination of hydraulic conductivity and fines content in soils near an unlined irrigation canal in Guasave, Sinaloa, Mexico". *Journal of Soil Science and Plant Nutrition*, *11*(3), 13-31.

Edil, T. B., Tinjum, J. M., and Benson, C. H. (2012). *Recycled Unbound Materials*. Final Report, 763 MN/RC 2012-35, Minnesota Department of Transportation, Saint Paul, Minnesota, 340.

Fannin, R. J. (2010, May). On the clogging of geotextile filters. In *Proceedings of the 9th International Conference on Geosynthetics, Guarujá, Brazil* (23-27).

Fatahi, B., Khabbaz, H., & Liem Ho, H. (2011). Effects of geotextiles on drainage performance of ballasted rail tracks. *Australian Geomechanics*, *46*(4), 91.

Fatema, N., & Bhatia, S. K. (2018). Sediment Retention and Clogging of Geotextile with High Water Content Slurries. *International Journal of Geosynthetics and Ground Engineering*, *4*(2), 13.

Faure, Y. H., Kehila, Y., Olivier, F., and Paillez, S. (2000), "Behavior of Nonwoven Geotextiles for Filtrating Particles in Suspension," *Filters and Drainage in Geotechnical and Geoenvironmental Engineering*, W. Wolski and J. Mlynarek, Eds., Balkema, Rotterdam, The Netherlands, 59–66.

Fischer, g. R. (1994). "The Influence of Fabric Pore Structure on the Behavior of Geotextile Filters." PhD dissertation, University of Washington, Seattle, Washington, USA.

Fischer, G. R., Holtz, R. D. & Christopher, B. R. (1990). "Filter Criteria Based on Pore Size Distribution". Proceedings of the 4th International Conference on Geotextiles, The Hague, Netherlands, Vol.1, 289–294.

Floss, R., Laier, H., & Brau, G. (1990, May). Dynamic loading of geotextile/soil-systems. In *Proceedings of the Fourth International Conference on Geotextiles, Geomembranes and Related Products* (183-188).

Franks, C. A., Davis, A. P., & Aydilek, A. H. (2013). Effects of runoff characteristics and filter type on geotextile storm water treatment. *Journal of Irrigation and Drainage Engineering*, *140*(2), 04013014.

Franks, C., Davis, A. P., and Aydilek A.H. (2014). “Effects of Runoff Characteristics and Filter Type on Geotextile Stormwater Treatment”, *Journal of Irrigation and Drainage Engineering*, ASCE, Vol. 140, No. 2, pp.04013014-1-9

Franks, C., Koebler, J., Myers, R., Hatipoglu, M., Davis, A. P., and Aydilek A.H. (2015). “Field Evaluation of a Geotextile Filter for Stormwater Runoff Control”, *Geosynthetics International*, Vol. 22, No. 4, pp. 288-300.

French Committee on Geotextiles and Geomembranes (1986). “Recommendations for the Use of Geotextiles in Drainage and Filtration Systems”. Geotextile Manual, Institut Textile de France, BoulogneBillincourt, France, 43–54.

Germaine, John T., and Amy V. Germaine. (2009). Geotechnical Laboratory Measurements for Engineers. *Geotechnical Laboratory Measurements for Engineers*. John Wiley & Sons.

Giroud, J. P. (1982). “Filter criteria for geotextiles”. *Proceedings of the 2nd International Conference on Geotextiles*, Las Vegas, NV, Vol. 1, 103–108.

Giroud, J. P. (1988). Review of geotextile filter criteria. *Proceedings of the 1st Indian Geotextiles Conference on Reinforced Soil and Geotextiles*, Bombay, 1–6.

Giroud, J., 1996. Granular filters and geotextile filters. In: Geo-filters', vol. 96, pp. 565-680.

Glynn, D. T., & Cochrane, S. R. (1987). The behavior of geotextiles as separating membranes on glacial till subgrades. *Proceedings of Geosynthetics' 87*, *1*, 26-37.

Grand View Research, (2016). Geotextile market projected to reach $8.18 billion by 2024. Retrieved from. https://www.grandviewresearch.com/press-release/globalgeotextiles-market.

Goulias, D., Aydilek, A.H., and Zhang, Y. (2016). *Recycled Material Availability in Maryland – A Synthesis Study*. Final Report, MD-16-SHA-UM-4-03, University of Maryland and Maryland State Highway Administration, College Park, MD, 275.

Haider, I., Cetin, B., Kaya, Z., Hatipoglu, M., Cetin, A., & Aydilek, A. H. (2014). “Evaluation of the Mechanical Performance of Recycled Concrete Aggregates Used in Highway Base Layers”. In *Geo-Congress 2014: Geo-characterization and Modeling for Sustainability*, 3686-3694.

Haliburton, T. A., and Wood, P. D. (1982). “Evaluation of US Army Corps Of Engineers Gradient Ratio Test for Geotextile Performance.” *Proceedings of the*

Second International Conference on Geotextiles, International Fabrics Association International St Paul, MN, 97–101.

Holtz, R.D., Christopher, B.R. and Berg, R.R. (1998) “Geosynthetic Design and Construction Guidelines,” National Highway Institute, Federal Highway Administration, Washington DC, Report No. FHWA HI-95-038, 460.

Holtz, R. D., Kovacs, W. D., and Sheahan, T. C. (2011). *An Introduction to Geotechnical Engineering* (2nd ed.). Upper Saddle River, NJ: Pearson.

Huang, C. C., & Luo, S. Y. (2007). “Dewatering of reservoir sediment slurry using woven geotextiles”. Part I: Experimental results. *Geosynthetics International*, *14*(5), 253-263.

Jang, D.-J., Frost, J. D., and Park, J.-Y. (1999). “Preparation of Epoxy Impregnated Sand Coupons for Image Analysis.” *Geotechnical Testing Journal*, 22(2), 153–164.

Kenney T.C., Van Veen, W.A., Swallow M.A. and Sungaila M.A. (1992). “Hydraulic Conductivity of Sand Bentonite Mixtures.” *Canadian Geotechnical Journal*, 29(3), 364-374

Koerner, R. (2012). *Designing with Geosynthetics* (6th edition, Vol 1). XLibris Corporation, Bloomington, IN.

Koerner, R. (2016). *Geotextiles: From Design to Applications*. Woodhead Publishing.

Koerner, R., Lord Jr., A., Halse, Y., (1988). Long-term durability and aging of geotextiles. Geotext. Geomembr. 7 (1-2), 147-158.

Krivit, D. & Associates (2007). “Recycling of Tear-off Shingles: Best Practices Guide.”

Krug, M., Heyer, D., and Floss, R., (2000), “Filtration Effectiveness of Geotextiles in Cover Sealing Systems of Landfills,” Filters and Drainage in Geotechnical and Geoenvironmental Engineering, W. Wolski and J. Mlynarek, Eds., Balkema, Rotterdam, The Netherlands, 271–278.

Kutay, M. E., & Aydilek, A. H. (2005). “Filtration Performance of Two-Layer Geotextile Systems”. *Geotechnical Testing Journal*, *28*(1), 79-91.

Kutay, M. E., & Aydilek, A. H. (2004). “Retention Performance of Geotextile Containers Confining Geomaterials”. *Geosynthetics International*, *11*(2), 100-113.

Kutay, M. E., & Aydilek, A. H. (2003). "Hydraulic Compatibility of Geotextile Drains with Fly Ash in Pavement Structures". In *Proc. 82nd Annual Meeting of the Transportation Research Board*, Washington, DC

Lafleur, J., Mlynarek, J., and Rollin, A.L. (1989). "Filtration of Broadly Graded Cohesionless Soils", Journal of Geotechnical Engineering, ASCE, Vol. 115,(12), 1747-1768.

Locander, R. (2009). *Analysis of Using Reclaimed Asphalt Pavement (Rap) As a Base Course Material* (Rep. No. CDOT-2009-5). Denver, CO: Colorado Department of Transportation.

McCulloch, T., Kang, D., Shamet, R., Lee, S. J., & Nam, B. H. (2017). "Long-Term Performance of Recycled Concrete Aggregate for Subsurface Drainage". *Journal of Performance of Constructed Facilities*, *31*(4), 04017015.

Meshram, K., Mittal, S. K., Jain, P. K., & Agarwal, P. K. (2013). Application of Coir Geotextile in Rural Roads Construction on BC Soil Subgrade. *International journal of engineering and innovative technology*, *3*(4), 264-268.

Metcalfe, R.C., Holtz, R.D., and Allen (1995) "Field Investigations to Evaluate the Long-Term Separation and Drainage Performance of Geotextile Separators," Geosynthetics '95 Conference Proceedings, Nashville, USA, Vol. 3, 951-962.

Millar, P. J., Ho, K. W. & Turnbull, H. R. (1980). "A Study of Filter Fabrics for Geotechnical Applications in New Zealand. Ministry of Works and Development", Central Laboratories Report No. 2-80/5, New Zealand.

Miszkowska, A., Lenart, S., & Koda, E. (2017). "Changes of permeability of nonwoven geotextiles due to clogging and cyclic water flow in laboratory conditions". *Water*, *9*(9), 660.

Mlynarek, J. and Lombard, G. (1997). "Significance of Percent Open Area in the Design of Woven Geotextile Filters," *Proceedings of Geosynthetics '97*, IFAI, Long Beach, CA, March 1997, pp. 1093–1107.

Nam, B. H., Behring, Z., Chopra, M., Shoucair, J., & Nam, S. (2015). "Investigation on clogging potential of recycled concrete aggregate in French drain systems". In *IFCEE 2015*(pp. 2787-2796).

Narejo, D., Li, M., Zimmel, E., and Wu, Y. (2013). "A Monolithic Layered Nonwoven–Woven Geotextile for Use with Drainage Geocomposites in Coal Combustion Residual Projects" Geotextiles and Geomembranes, 37, 16-22.

Nishida, K., & Nishigata, T. (1994). The evaluation of separation function for geotextiles. In *Proceedings of the 5th International Conference on Geotextiles, Geomembranes and Related Products* (Vol. 1, 139-142).

Nokkaew, K., Tinjum, J. M., & Benson, C. H. (2012). "Hydraulic Properties of Recycled Asphalt Pavement and Recycled Concrete Aggregate". In *GeoCongress 2012: State of the Art and Practice in Geotechnical Engineering*, 1476-1485.

Ogink, H. J. M. (1975). "Investigations on the Hydraulic Characteristics of Synthetic Fabrics". Delft Hydraulics Laboratory, Publication No. 146

Palmeira, E. M., & Cunha, M. G. (1993). A study of the mechanics of unpaved roads with reference to the effects of surface maintenance. *Geotextiles and Geomembranes*, *12*(2), 109-131.

Palmeira, E. M., & Gardoni, M. G. (2000). "Influence of Partial Clogging and Pressure on the Behavior of Geotextiles in Drainage System". *Geosynthetics International*, *7*(4-6).

Palmeira, E. M., & Fannin, R. J. (2002). "Soil-geotextile compatibility in filtration". In *Geosynthetics: state of the art-recent developments. Proceedings of the seventh international conference on Geosynthetics, 7-icg, held 22-27 September 2002, Nice, France.* (Vol. 3).

Palmeira, E. M., Remigio, A. F., Ramos, M. L., & Bernardes, R. S. (2008). A study on biological clogging of nonwoven geotextiles under leachate flow. *Geotextiles and Geomembranes*, *26*(3), 205-219.

Palmeira, E. M., & Tatto, J. (2015). "Behaviour of geotextile filters in armoured slopes subjected to the action of waves". *Geotextiles and Geomembranes*, *43*(1), 46-55.

Palmeira E. M., & Trejos Galvis, H. L. (2017). "Opening Sizes and Filtration Behaviour of Nonwoven Geotextiles Under Confined and Partial Clogging Conditions." Geosynthetics International, 24(2), 125-138.

Rahman, M. A., Imteaz, M. A., Arulrajah, A., Piratheepan, J., and Disfani, M. M. (2015). "Recycled Construction and Demolition Materials in Permeable Pavement Systems": geotechnical and hydraulic characteristics. *Journal of Cleaner Production*, 90, 183-194. doi:10.1016/j.jclepro.2014.11.042

Raut, A. K. (2006). "Mathematical modelling of granular filters and constriction-based filter design criteria".

Richter, C.A. (2006). "Seasonal variations in the moduli of unbound pavement layers." Federal Highway Administration, Report FHWA-HRT-04-079, 283.

Rollin, A., Lombard, G., (1988). Mechanisms affecting long-term filtration behaviour of geotextiles. Geotext. Geomembr. 7, 119-145.

Saathoff, F. (1988) “Examinations of Long-Term Filtering Behaviour of Geotextiles,” *Proceedings of Durability of Geotextiles Seminar,* Saint-Rémy-lès-Chevreuse, France, 86-114.

Sabiri, N. E., Caylet, A., Montillet, A., Le Coq, L., and Durkheim, Y. (2017). “Performance of Nonwoven Geotextiles on Soil Drainage and Filtration”. *European Journal of Environmental and Civil Engineering*, doi: 10.1080/19648189.2017.1415982

Sañudo-Fontaneda, L. A., Coupe, S. J., Charlesworth, S. M., & Rowlands, E. G. (2018). Exploring the effects of geotextiles in the performance of highway filter drains. *Geotextiles and Geomembranes*, *46*(5), 559-565.

Schneider, C.A., Rasband, W.S., and Eliceiri, K.W.(2012). “NIH Image to ImageJ: 25 years of image analysis”. *Nature Methods*, 9, 671-675

Schober, W., and Teindl, H. (1979). “Filter Criteria for Geotextiles.” *Proceedings of the 7 th Europian Conference on Soil Mechanics and Fundation Engineerings, British Geotechnical Society*, 121–129.

Shedivy, R.F., Meier, A., Edil, T.B., Tinjum, J.M., and Benson, C.H. (2012). *Leaching Characteristics of Recycled Asphalt Pavement Used as Unbound Road Base*. University of Wisconsin-Madison, WI.

Soleimanbeigi, A., Edil, T. B., and Benson, C. H. (2013). “Evaluation of Fly Ash Stabilization of Recycled Asphalt Shingles for Use in Structural Fills.” *Journal of Materials in Civil Engineering*, *25*(1), 94-104.

Townsend, T., Powell, J., & Xu, C. (2007). “Environmental Issues Associated with Asphalt Shingle Recycling”. *Construction Materials Recycling Association, US EPA Innovations Workgroup*.

Trani, L. D. O., and Indraratna, B. (2010). “Assessment of subballast filtration under cyclic loading.” *Journal of Geotechnical and Geoenvironmental Engineering*, 136(11), 1519-1528.

Tsai, W.S. and Holtz, R.D. (1998) “Rut Prediction for Roadways with Geosynthetic Separators,” *Proceedings of Sixth International Conference on Geosynthetics*, Atlanta, USA, Vol. 3, 939-944.

US Army Corps of Engineers (1986). “Geotextiles Used as Filters. Civil Works Construction Guide Specification”, CW-02215.

US Environmental Protection Agency. (1989). Technical guidance document: final covers on hazardous waste landfills and surface impoundments.

Veylon, G., Stoltz, G., Mériaux, P., Faure, Y. H., & Touze-Foltz, N. (2016). Performance of geotextile filters after 18 years' service in drainage trenches. *Geotextiles and Geomembranes*, *44*(4), 515-533.

Vieira, J. L., Abramento, M., & Campos, M. V. W. (2010). Experimental study of clogging in drainage systems. In *Proceedings of the 9th International Conference on Geosynthetics, Guarujá, Brazil* (23-27).